University of Nevada, Reno

Perceptual responses to color in the human cortex

A dissertation submitted in partial fulfillment of the requirements for the degree of Doctor of Philosophy

in Neuroscience

by

Talia L. Retter

Drs. Fang Jiang, Bruno Rossion & Michael A. Webster / Dissertation Advisors

August, 2019

THE GRADUATE SCHOOL

We recommend that the dissertation
prepared under our supervision by

Entitled

be accepted in partial fulfillment of the
requirements for the degree of

_____, Advisor

_____, Co-advisor

_____, Committee Member

_____, Committee Member

_____, Committee Member

_____, Graduate School Representative

David W. Zeh, Ph.D., Dean, Graduate School

Abstract

_____

Electrophysiological responses to color, as recorded on the scalp (electroencephalogram; EEG), were originally seen as distinctive from retinal responses, in that they related more to the perceptual experience of color. However, EEG has only been used extensively to probe high-level color responses, e.g., relating to color categories or implicit color associations, within the last couple decades. It still remains poorly understood to what extent cortical responses to color reflect activity from the first few visual areas, and to what extent they may be influenced by more anterior visual areas. Here, we explore the high-level (perceptual) _vs._ low-level (sensory) organization of cortical response to color with EEG in three studies, with a frequency-tagging approach. In Study 1, we test for neural correlates of perceptual blue-yellow asymmetries, and of individual differences in high-level color inferences. In Study 2, we investigate the extent to which cone-opponent mechanisms or categorical perception may explain the variance in the spatiotemporal dynamics of EEG responses to twelve different colors. Finally, in Study 3 we compare actual _vs._ implicit color responses to color-diagnostic grayscale objects. Overall, the results provide evidence that cortical responses to color are reflective of high-level perception, from their earliest selective onset. Throughout, I interpret these results in a theoretical framework in which the purpose of color perception may be to categorize objects within the environment.

Acknowledgments

_____

Table of Contents

List of Tables

List of Figures

_____

Chapter 1

Introduction

_____

_____

1.1 General introduction

As gradients of luminance enrich a black-and-white image, the perception of color adds multidimensional shading to a grayscale world. Unsurprisingly, there are many advantages conferred by color for visual perception, both at early and later stages of visual processing. During early visual processing, color contributes to image segmentation and grouping (e.g., Allen, 1879; Buck, & Boynton, 1979; Shapley & Hawken, 2011). In an extreme example, color enables the detection of chromatic edges or patterns with equal luminance levels. In natural scenes, color is typically not the only cue available, but it interacts with luminance to greatly assist in these early visual processes, e.g., in grouping the grass despite the superimposed shadows from tree branches. During relatively later visual processing, color contributes to more sophisticated interpretations of scenes, such as object recognition (e.g., Gegenfurtner & Kiper, 2003; Jonson & Mullen, 2016). For example, the associated color of citrus fruit facilitates its recognition, or the color of a traffic light signal may be more readily interpreted than its spatial position. The vast utility of color perception in modern visual perception awakes the question of what its utility is, both in terms of modern times (e.g., the impact that color deficiencies may have on people) and in evolutionary terms.

Different views on the potential purpose of color perception have provided the foundation for at least two strong research foci in the field of color perception. At one level, the purpose of color perception is thought to be for decoding the objective physical properties of wavelength spectra. Research in this vein thus focuses on the visual system's ability to decode the sometimes limited information afforded by a scene, in terms of the spectral discrimination

of object surface *vs.* illuminant reflectance (e.g., Land, 1977; Marr, 1982; Brainard & Maloney, 2011). At another level, the purpose of color perception is thought to be for enriching perceptual (object) categorizations that may have supported functionally relevant behaviors (e.g., Hardin, 1992; Hatfield, 1992; Thompson, 1995). Research in this vein thus focuses on the subjective interpretations of color, with a particular emphasis on the broad universality and specific differences in the perception of color categories. These views are largely complementary in practice (see Brainard & Maloney, 2011), given that spectral information is necessary for perceptual categorization by color. However, these views put different emphases on the importance of physical and early-stage (retino-thalamic) biological response properties (the former), and more abstract, psychological and sociological properties (the latter). Indeed, the view of that objective physical properties of wavelength spectra are important has been extensively investigated with biological means, leaving the opinion that color is important for perceptual categorization relatively under supported.

Here, I will attempt to unite biological, neural research with (categorical) perceptual phenomena by investigating cortical responses to color. Specifically, I will report three studies probing the subjective nature of human color perception and its potential cortical correlates. I expect that these experiments will show novel biological evidence for the subjective view of color perception, deviating from the measurable physical properties of the stimuli. In Study 1 (Chapter 2), I will use the image of #thedress to search for 1) neural correlates of perceptual blue-yellow asymmetries, in which blues of nominally equal physical contrast to yellows appear less saturated, and 2) neural correlates of individual differences in perception of the original dress images as blue-black or white-gold. In Study 2 (Chapter 3), I will map the neural responses to color in parametric steps around a cone-opponent color space, investigating the impact of

subjective interpretations of the difference between colors. In Study 3 (Chapter 4), I will

quantify the contribution of color to color-diagnostic grayscale object recognition, and show the

potentially early timecourse of this effect. Throughout, I will interpret the results in a

framework of subjective, categorical color perception, which I postulate correlates with such

stimuli's wavelength to a limited extent for physical and biochemical reasons (see Discussion).

This view is organic, based on the limited and imperfect neurophysiology and evolution of

human color sensation and perception. I will accordingly take a step back, and begin with a brief

review of these aspects of human color vision in the following sections.

1.2. The bases of vision: photoreceptors

At the beginning, sensory receptors, in conjunction with nervous and motor systems, enabled

emergent living organisms to interact with their environment. This is substantiated by

biophysical processes: as a photon of light hits a photoreceptor, it may be absorbed by opsin

protein containing retinal pigments. Upon absorption, the retinal molecule changes shape (from

a cis- to trans-structure), triggering a molecular cascade which ultimately inhibits glutamate

neurotransmitter release from the synaptic terminal of the photoreceptor to complete

transduction. Through this process, a physical signal from the environment activates neural

activity within an organism, laying the foundations of vision.

Even prior to the emergence of color perception, there were incentives and constraints

on the range of wavelengths to which a photoreceptor might be sensitive. Coarse limits are

imposed by the range of wavelengths of light in our environment, i.e., those reaching Earth from

the sun (approximately 290 to over 3,200 nm): indeed, the sensitivity of photoreceptors across

organisms, spanning from approximately 300 to 800 nm (Menzel & Backhaus, 1991; Bowmaker,

Thorpe & Douglas, 1991), appears well-matched to capture the sun's radiant energy, and the

optical properties of the environment (see Nassau, 1983; Smith & Baker, 1981). This range may be further constrained given that shorter wavelengths with higher energy may be damaging to biological tissue (but see Cronin & Bok, 2016), and longer wavelengths may begin to overlap with thermal radiations produced by an observers' own body heat. Beyond constraints, the range of wavelength sensitivities largely conserved across modern organisms may have been specifically selected, as it is related to the emission spectra of objects that are functionally relevant in the environment (e.g., Gouras & Zrenner, 1981; Jacobs, 2013). Fitting neatly within these constraints, the human retina is receptive to wavelengths from roughly 400 to 700 nm (**Figure 1.1B**): this also defines the range of wavelengths that may contribute to our color perception.
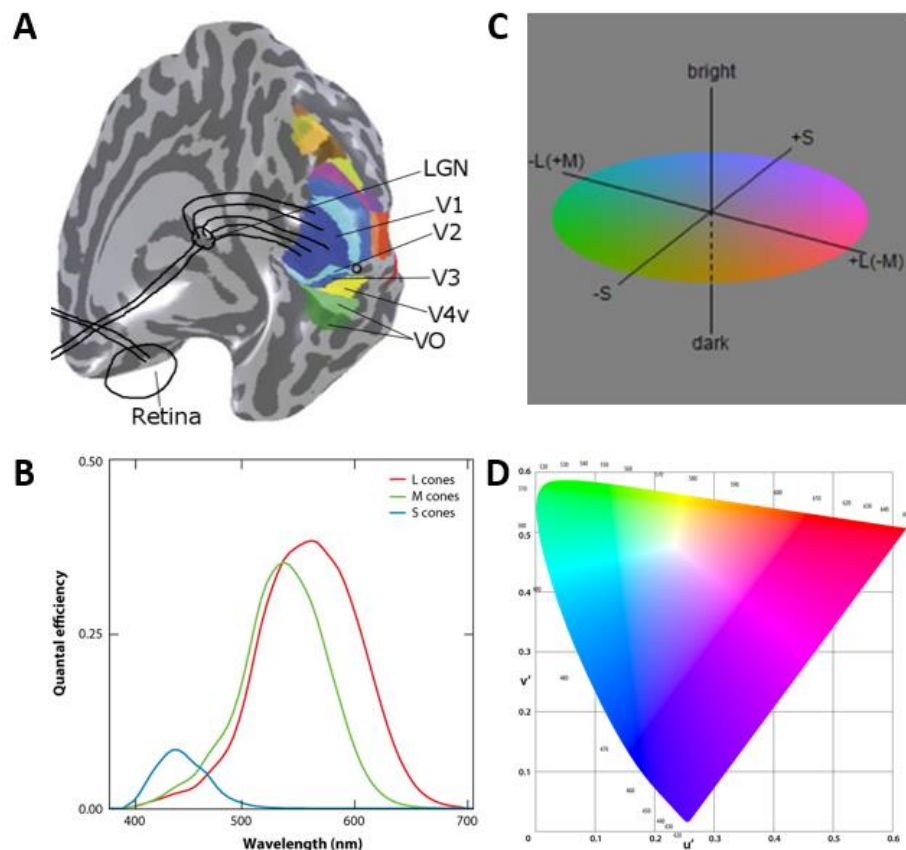
Figure 1.1. ***A)*** *Color-responsive regions of the human brain are labeled on retinotopically-defined areas (adapted from Fig. 2. of Wandell, Dumoulin, & Brewer, 2007).* ***B)*** *Spectral sensitivities of the typical three human cone types (from Fig. 1. of Brainard, 2015, which was derived from Stockman & Sharpe, 2000).* ***C)*** *A cone-opponent color space, representing the dimensionality of color responses that reach the visual cortex, i.e., departing from the retina and present in the LGN (from Webster, 2015, which was adapted from Webster et al., 2000).* ***D)*** *A perceptually-scaled and monitor-friendly color space, in which uniform distances correspond to human perceptual difference judgements (CIE, 1976).*

1.3. The bases of color vision: multiple photoreceptor types (and their origins)

In humans, there are typically three different cone types in the retina, termed short-, medium-, and long-wavelength sensitive (S, M, and L, respectively). These cone types are differentiated by their *spectral sensitivities*, i.e., different probabilities of absorbing different wavelengths of light (**Figure 1.1B**). For example, the S cone sensitivity begins at the shortest wavelengths to which we are sensitive (about 400 nm), and its sensitivity peaks about 30 nm later; the L cone sensitivity reaches the longest wavelengths to which we are sensitive (about 700 nm), and the M cone peak sensitivity is shifted about 30 nm below that of the L cone. It is now known that these different types of cones are the product of different types of opsin proteins that produce three different photopsin combinations, and the cone types have been well-characterized experimentally, both through behavioral and biochemical means (Bowmaker & Dartnall, 1980; Schnapf, Kraft, & Baylor, 1987; for reviews: Lee, 2008; Shapley, 2019). Historically, it is worth noting that these three cone types were first postulated by Thomas Young, and later theoretically evidenced by Hermann von Helmholtz, in the 19th century, leading to what is called the "Young-Helmholtz trichromatic theory" (Young, 1802; von Helmholtz, 1867).

While each cone type is differentially sensitive to different wavelengths, this alone is not sufficient for color perception. This is because wavelength and intensity are confounded within a single cone type: a cone may produce an identical signal from a high intensity of a suboptimal wavelength or from a lower intensity of an optimal wavelength, in accordance with the "principle of univariance" (Naka & Rushton, 1966). In practice, the functional neuroanatomy of the retina produces greater complexity, such that the percept triggered from an individual cone may be influenced by its surrounding cone types (e.g., Sabesan et al., 2016, where stimulating different individual L or M cones produces color percepts of white, green, or red). In any case, taking the "color blindness" of an individual cone type into account, the presence and comparison of signals from multiple photoreceptors types can be taken as a prerequisite for color perception.

The potential advantage of the number and spectral sensitivities of the different cone types has been a topic of great interest in color perception research. In particular, theories that suggest the purpose of color perception is to distinguish different wavelengths of light suggest that the cones are optimized to this extent (e.g., Abrams, Hillis, & Brainard, 2007; Foster, 2011). However, the three types of opsins present in the human eye are derivatives of photoreceptor development over a great expanse of evolution, which were not optimized for our species. To make this point, and a salute to an interesting recent history, I will briefly address phylogenetic studies of the cone opsin types in the following.

Phylogenetic studies have used the genes coding for different opsin types, first reported only about 30 years by Nathans et al. (1986), to make inferences about evolutionary development of color perception. Accordingly, it has been found that four cone opsin genes originated early in vertebrate evolution, approximately 540 million years ago (Collin & Trezise,

2004). Human cone types trace back to Eutherian mammals, which diverged about 148 million years ago, having retained two of the original four opsin genes: the primary variety of S-cone opsin (peak sensitivity between 360 to 445 nm) and the L-cone opsin (peak sensitivity at approximately 560 nm; Solomon & Lennie, 2007; Jacobs, 2009). In early, old-world (Catarrhine) primates, approximately 40 million years ago, the L-cone is thought to have mutated into a secondary type, the M-cone (peak sensitivity slightly lower the L-cone, at approximately 530 nm): this is evidenced by their phylogeny, and further substantiated by the presence of both the L- and M-cone type opsin genes being positioned nearby on the X chromosome, and being over 96% genetically identical (in contrast, the S-cone opsin gene is located on chromosome 7, and is only about 40% identical) (Nathans, Thomas & Hogness, 1986; Yokoyama & Yokoyama, 1989; Wassle, 2004; Solomon & Lennie, 2007; Jacobs, 2009; Neitz & Neitz, 2011). Additionally, the L-cone type opsin genes are present in multiple copies, making cross-over mutations highly likely (see Neitz & Neitz, 2011 for a review); indeed, L- and M-cone types are both present in one species of new-world monkeys, who diverged from old-world monkeys approximately 35 million years ago: the howler monkey (Jacobs, 1996; Schrago & Russo, 2003).

Thus, the great variability and inconsistencies in phylogeny speak against any type of optimization in the spectral sensitivities of the cone types (Thompson, Palacios, & Varela, 1992; Thompson, 1995). In further opposition to cone optimization, there are subtle differences in peak sensitivity for the M, and especially L, pigments occurring in humans, with only slight effects on color perception (Neitz & Jacobs, 1986; review: Neitz & Neitz, 2011). Moreover, beyond the cones, color perception is known to be influenced by another class of retinal photoreceptors: the rods (peak sensitivity at approximately 500 nm; McCann & Benton 1969; Smith & Pokorny 1977; Buck, 2004). Recently, reports have been made that humans possess an

additional photosensitive cell type, intrinsically photosensitive retinal ganglion cells (ipRGCs), the influence of which on color perception is as of yet unknown (Horiguchi et al., 2012; review: Lucas, 2013). Moreover, about 8% of the human population is considered to have some form of color vision impairment (NIH), and some human females may be tetrachromats (Jordan & Mollon, 1993; Jordan et al., 2010), but the differences on such individuals' color perception appear modest (e.g., Jordan et al., 2010; Boehm, MacLeod, & Bosten, 2014), perhaps as a result of adaptation (Webster, Juricevic, & McDermott, 2010). Indeed, the number, beyond two or three, and precise spectral tuning of cone types may not be a crucial factor for color perception (for a behaviorally-driven comparison across species with 2 to 12 cone types, see Marshall & Arikawa, 2014). Instead, the potential purpose of color perception must be considered in a visual system that extends far beyond its initial stages in the cone photoreceptors, and even further up to behavior.

1.4. The bases of color vision: the post-receptoral retinocortical pathway

The nuanced color perception of humans can be better understood as a product of the signals beyond the cones, i.e., the post-receptoral processing of the inputs from different cone types. The first stages of post-receptoral processing lie in the *retinocortical pathway* for responses to color, the network of neural cells passing from the photoreceptors through the retina and out of the eye to the lateral genicular the lateral genicular nucleus (LGN) of the thalamus. This retinocortical pathway has been examined in detail (although mysteries remain), largely through the use of single-cell recordings in non-human, old-world primates (for reviews: Rodieck, 1998; Dacey, 2000; Gegenfurtner & Kiper, 2003; Solomon & Lennie, 2007; Conway, 2014; Lee, 2014; Shapley, 2019).

To briefly trace this pathway at a cellular and molecular level: the decrease in excitatory neurotransmitter from a photon-absorbing cone in the retina may inhibit (i.e., decrease the action potential firing rate of) its synapsed on-center bipolar cell, or else excite its synapsed off-center bipolar cell. In both cases, this interaction is mediated by lateral horizontal cells, contributing to the spatial field sensitivity. Subsequently, the biopolar cells synapse onto one or more cone-specific ganglion cells, with mediation from lateral amacrine cells. The resulting change in firing rate of the ganglion cells is transmitted out of the retina to the lateral genicular nucleus (LGN) of the thalamus *via* the ganglion cell axons forming the optic nerve. At the level of the ganglion and LGN cells, this capitulates in a single-opponent and subtractive comparison of the responses from the different cone types; in the LGN, this occurs distinctly at the parvocellular layers (largely L *vs.* M cone comparisons) and koniocellular areas (S contrasts).

These two contrasts (L *vs.* M and +S *vs.* -S) define the primary axes of so-called "cone-opponent" color spaces, which are supplemented by a third, brightness contrast (Derrington, Krauskopf, & Lennie, 1984; MacLeod & Boynton, 1979; **Figure 1.1C**). These cone-opponent color spaces aim to reflect the way that color signals are processed at the end of the retinocortical pathway, i.e., the way that the thalamus will relay signals to the cortex. Note that such color spaces have been used extensively in color vision research, and despite their groundings in retinocortical processing, have often been found to relate to behavioral phenomena (e.g., Gegenfurtner & Kiper, 2003). It is important to remember, however, that the responses at the LGN represent the activity of one part of an integrated visual system, and thus should not be interpreted independently from cortical processes. Additionally, these cone-opponent pathways also appear to have been highly conserved throughout evolution (Solomon & Lennie, 2007).

While individual cone types are "color blind", the comparison of their signals through the retinocortical pathway enables usage of the wavelength information, providing the bases for color perception. Indeed, the importance of human trichromacy is not only in the presence of three cone types, but especially in the comparison of the signals from these cone types, enabling a three-dimensional visual space of hue, brightness, and saturation (Young, 1802; von Helmholtz, 1867; Barlow, 1982). Historically, the finding of opponent channels (DeValois et al., 1958) resonated in color perception research, in relation to the earlier "opponent process" theory of Edwald Hering (1920; see DeValois, Abramov, & Jacobs, 1996). However, Hering's proposed primary channels of perceptually-defined red *vs.* green and blue *vs.* yellow do not quite map onto the cone-opponent channels (see Jameson & D'Andrade, 1997; Lee, 2014), which instead are typically named as red *vs.* blue-green and yellow-green *vs.* purple (e.g., see Webster et al., 2000 and Emery et al., 2017). The perceptual experience of color is indeed not fully accounted for at the retinocortical pathway stage. For a dramatic example, compare a color space created through behavioral experimentation (scaled to be perceptually uniform; **Figure 1.1D**) to the color space reflecting the retinocortical organization (**Figure 1.1C**).

1.5. The bases of color perception: cortical responses

Responses to color extend from the LGN to the primary visual cortex (V1), and a network of color-responsive visual cortical areas, including V2, V3 (including V3A), V4 (particularly the ventral area, V4v), and VO (for cortical-focused reviews: Gegenfurtner, 2003; Conway, 2014; Johnson & Mullen, 2016; **Figure 1.1A**). In this section, the visual cortical areas will be briefly addressed in turn, starting with V1.

Early studies on cortical responses to color focused on *color-selective* cells or areas, i.e., cells responding more, or exclusively, to color than non-color visual stimuli, especially in V1.

Such cells were predicted from the separate chromatic (parvo- and konio-cellular) and luminance (magnocellular) retinogeniculate pathways: a cell in the parvo- or konio-cellular pathway might be expected to respond well to color stimuli, but not to luminance stimuli. Experimentally, color-selective cells or areas were defined by sensitivity to chromatic over achromatic stimuli. In V1, color-selective cells were found: typically in small (less than 0.1 mm in diameter) cytochrome-oxidase rich "blobs" of the macaque brain (Ts'o & Gilbert, 1988).

However, color and luminance have been shown to interact in V1 (e.g., contributing to form perception: see Shapley, Hawkin, & Johnson, 2014), such that *color-responsive* cells, sensitive to both color and luminance in roughly equal extent, have become at least as much a point of interest. This widened the field conceptually, as while most color-selective cells are singe-opponent, being low-pass tuned for spatial frequency, many color-responsive cells are double-opponent, being band-pass tuned for spatial frequency and potentially also selective for orientation. It also widened the field in practice: color-selective cells constitute only about 10% of cells in macaque V1, compared to about 40% for color-responsive cells (see again Shapley, Hawkin, & Johnson, 2014). In the last few decades, neuroimaging has revealed in V1 of the human brain both color-selective (Engel & Furmanski, 2001; Wade et al., 2008; but see also Mullen, Chang, & Hess, 2015), and color-orientation integrating responses (Engel, 2005; Sumner et al., 2008). Yet, responses to V1 may not relate to color *perception,* as exemplified in cases where early visual signals and perceptual reports do not correspond, such as in blind sight (chromatic perception without V1 activation) or the presence of typical neural responses in the case of impaired color vision, i.e., dyschromatopsia (e.g., Brent, Kennard, & Ruddock, 1994; Stoerig & Cowey, 1090; Crognale et al., 2013)*.*

In visual area V2, macaques have been shown to have color-selective responses in cytochrome-oxidase rich, narrow columns, termed "thin stripes", of about 0.1-0.3 mm (Tootell et al., 1983; see also Xiao et al., 2003; Conway et al., 2007). Very recently, such stripes have been shown as color-selective in humans with high-field fMRI (Nsar, Polimeni, & Tootell, 2016). The stripes in V2 are thought to extend into color-selective columns in V3 in non-human primates (Tootell et al., 2004), again being only very recently investigated in humans (Nsar, Polimeni, & Tootell, 2016; Dumoulin et al., 2017). Yet despite the relation of color-selective responses to neuroanatomy in V2 and V3, relatively little is known about the functional properties of responses to color in these areas, despite extensive recordings therein (see Engel, Zhang & Wandell, 1997; Mullen et al., 2007; Wade et al., 2008; Brouwer & Heeger, 2009; Mullen, Chang, & Hess, 2015; Persichetti et al., 2015).

Instead, more anterior areas have been researched more extensively, perhaps due to their apparent relation to the way that color is perceived. Indeed, later visual cortical areas (V4, VO, and patches in the fusiform gyrus) have been taken as reflecting high-level differences in color perception (Zeki, 1973; Meadows, 1974; Luek, 1989; Zeki, 1990; Zeki et al., 1991; Allison et al., 1993; Martin et al., 1995; Sakai et al., 1995; Hadjihakani et al., 1998; Zeki & Bartels, 1999; Bartels & Zeki, 2000; Liu & Wandell, 2005; Bouvier & Engel, 2006; Simmons et al., 2007; Murphey, Yoshor & Beauchamp, 2008). These areas will be addressed separately, although their functional activity has not yet been well distinguished, particularly in VO and the fusiform gyrus patches.

The earliest studies on a potential "color center" with functional neuroimaging of the human brain focused on visual area V4 (Luek, 1989; Zeki et al., 1991), also known as human/ventral V4 (hV4, V4v). This research was based on previous research in non-human

primates, indicating V4 as containing color-selective columns (Zeki, 1973; although note that these relatively anterior regions are especially complicated by the lack of clear homologies across (human and non-human) primate species (e.g., Meadows, 1974; Wade et al., 2008). It was also indicated from lesions studies in humans producing achromatopsia and dyschromatopsia, i.e., the lack or impairment of color perception, respectively (Verrey, 1888; Meadows, 1974; Jaeger, Krastel & Braun, 1988; Zeki, 1990). A relatively recent meta-analysis on studies of lesions producing achromatopsia (Bouvier & Engel, 2006), however, was unable to dissociate color-impairing lesions as being in V4 or more anterior regions, as described in the following.

A color-selective area has been reported in the retinotopically-defined VO, although this area has been contentiously (Winawer & Witthoft, 2015) termed "V8" (Hadjihakani et al., 1998), or non-retinotopic "V4a" (Zeki & Bartels, 1999; Bartels & Zeki, 2000). This area has drawn interest in that it has been shown to relate to perceptual judgements of color (e.g., Liu & Wandell, 2005; Mullen et al., 2007; Brouwer & Heeger, 2009; but see also Goddard et al., 2011).

Color-selective responses have also been reported in a region of the fusiform gyrus anterior to VO in the human brain (Martin et al., 1995; Beauchamp et al., 1999; Beauchamp et al., 2000; Simmons et al., 2007; Murphey, Yoshor & Beauchamp, 2008; see Fig. 6 of Wade et al., 2008; Slotnick, 2009; Lafer-Sousa, Conway, & Kanwisher, 2016). While responses in this region have not been reported in all studies (e.g., Zeki et al., 1991; McKeefry & Zeki, 1997; Hadjikhani et al., 1998; Chao, Haxby & Martin, 1999; Wade et al., 2002), it is possible that functional neuroimaging recordings in this region are considerably limited by signal resolution issues (e.g., Winawer et al., 2010; see Lafer-Sousa, Conway, & Kanwisher, 2016), or by task-specific restrictions (see Simmons et al., 2007); note that intracerebral EEG responses have also been

recorded in this region (Murphey, Yoshor & Beauchamp, 2008). While it remains to be better

characterized, at this point in time this region has already been hypothesized to relate to

conceptual color knowledge and color-object associations (Simmons et al., 2007).

1.6. The purpose of human color perception?

To summarize up to this point, color perception derived from the development of

photoreceptors, which were likely selected to be sensitive to subsets of wavelengths of light

relevant for organisms interacting with objects in their environments. A number of cone

photoreceptor types were highly conserved throughout hundreds of millions of years of

evolution; the emergence of trichromacy in old-world primates may have occurred more-or-less

randomly from a likely genetic mutation, rather than presenting some targeted advancement to

optimal color perception, as has been theorized. In any case, the presence of multiple cone

photoreceptor types, together with their comparative post-receptoral rentiocortical pathways,

laid the basis for human color perception.

What may have been the benefit of color perception? In one of the two view previously

mentioned, the utility of color perception is thought to be for extracting objective wavelength

information form surfaces vs. illuminant (dominant in computational perspectives), or on the

optimization of color perception for imagined behavioral utility (dominant in adaptive

perspectives and information theory). However, the central theory addressed here is that color

perception may have been beneficial for organisms to categorize things in their environments

(Hardin, 1992; Hatfield, 1992; Thompson, 1995; to some extent, Johnson & Mullen, 2016).

While the conflicts between these views will be further addressed in the Discussion, it

may already be said that these views may address different levels of color processing,

specifically the color processing at the level of *sensation* or *perception.* Theories on wavelength

processing may address color *sensation,* the process of sensing, and perhaps responding

automatically to, different wavelengths of light; e.g., many species use wavelength information

to locate light environments or to facilitate hardwired, "wavelength-specific behavior" (Kelber &

Osorio, 2010). On the other hand, theories on color categorization more fully address color

perception, which relates to higher-level cognitive function. Indeed, while many organisms may

be said to have color sensation or color vision, color *perception* is distinct.

While color sensation requires only color-sensitive cells and post-receptoral pathways,

color perception requires the conjunction of developing neural systems that were able to learn

from experience (Kelber & Osorio, 2010). This definition of color perception opens color-

processing to influences outside of a color-selective system, e.g., in forming association of colors

with smells, tastes, affects, language, etc. It also necessitates an examination of color perception

in neural areas capable of such association: the cortex. (Note that this view of the role of color

perception is not in opposition to the low-level, sensory contributions of color, as for contrast,

segmentation, and form perception (reviews: Gegenfurtner & Kiper, 2003; Shapley & Hawken,

2011; Jonson & Mullen, 2016); however, it interprets such sensory contributions of color in a

secondary role to perceptual contributions.)

1.7. Color categories

If the purpose of color perception is thought to be for categorization, the notion of categories

must be examined further. Color categories may be, and have been, defined in a myriad of ways.

Here, a color category is defined merely as a perceptual grouping of visual inputs differing in

their physical properties (wavelength or complex spectral reflectance). Color categorization

appears to be fundamental to the way in which we perceive color, and likely contributes to

phenomena such as color constancy (seeing objects as the same color under different

illumination colors), color memory (associating an object or scene with specific colors), and object recognition (e.g., Thompson, 1995).

Accordingly, physically different stimuli within a category are perceived as more similar than would be predicted, and stimuli crossing category boundaries are perceived as less similar (Harnad, 1987). Additionally, color categories may be best exemplified by a prototype, also known as a focal color, providing the most pure exemplar of that category. Behavioral studies have provided evidence for these aspects of color categorization: increased sensitivity and/or decreased response time in discriminating similar colors crossing, *vs.* not crossing, a category boundary (Bornstein, 1987; Uchikawa & Shinoda, 1996; Pilling et al., 2003; Gilbert et al., 2006; Winawer et al., 2007; Roberson, Pak & Hanley, 2008). Additionally, the memory of stimulus color has been shown to shift towards the categorical prototype (Boynton et al., 1989; Uchikawa & Shinoda, 1996; Bae et al., 2015). However, behavioral measurements of categorical color perception are limited in that they may be explained either by perceptual phenomenon, or post-perceptual, decisional and/or linguistic factors in making responses (e.g., see Webster & Kay, 2012; Witzel & Gegenfurtner, 2015).

Neural studies have been employed to investigate categorical perception, with inconsistent results. With neuroimaging, a categorical color effect was claimed by Bird et al. in the middle frontal gyrus and the left cerebellum (2014), which was not replicated in a subsequent study (Persichetti et al., 2015). In the latter study, however, no categorical effect was found in any of the targeted visual areas (V1, V2/3, and V4). One study reported categorical effects with functional near-infrared spectrography in infants over the bilateral occipito-temporal cortices (Yang et al., 2016). This is generally consistent with categorical effects reported with electroencephalogram (EEG) in human adults, typically extending over the

occipito-parietal cortex (Fonteneau & Davidoff, 2007; Thierry et al., 2009; Anthanasopoulos et al., 2010; Clifford et al., 2010; Mo et al., 2011; He et al., 2014; Forder, He, & Franlkin, 2017). However, while a number of EEG studies report categorical effects, the event-related potential component affected and even the direction (increase or decrease) of its change are not consistent: for example, early effects were found in some studies (Forder, He, & Franklin, 2017, reporting a decreased across-category magnitude) and not others (only after 200 or 300 ms: Clifford et al., 2012; He et al., 2014); effects are also sometimes reported in terms of latency shifts (Fonteneau & Davidoff, 2007; see also Hanley, 2015, for a short review). Note that there is only limited evidence that color categorization may also be present in non-human species (e.g., pigeons: Wright & Cumming, 1971; chicks: Jones et al., 2001; goldfish: Poralla & Neumeyer, 2006), suggesting that this aspect of color perception is relatively high-level, beyond simple color sensation.

1.8. Transition to Experiment 1

The first of the experiments presented here will have the least emphasis on color categories *per se.* Instead, this experiment will look for more general neural correlates of a perceptual phenomenon, namely that blues appear less saturated than yellows of physically matched saturation. This study will also investigate perceptual phenomena at the individual participant level, probing whether observers of #thedress image may be identified from their EEG signals as perceiving the dress fabric as white-gold or blue-black (which is arguably a categorically binary bias for an ambiguous image). By comparing contrasts of chromatic-chromatic (e.g., blue-yellow) responses and achromatic-chromatic (e.g., gray-yellow) responses, this study is able to take the first step in examining the sensitivity of high-density EEG to probe color-specific *vs.* color-responsive signals, and the correlations of these signals with perceptual reports.

Chapter 2

Study 1: Neural correlates of perceptual color inferences as revealed by #thedress

_____

Study 1: Neural correlates of perceptual color inferences as revealed by #thedress

Talia L. Retter, O. Scott Gwinn, Sean F. O'Neil, Fang Jiang & Michael A. Webster

---

2.1. Abstract

Color constancy involves disambiguating the spectral characteristics of lights and surfaces, for example to distinguish red in white light from white in red light. Solving this problem appears especially challenging for bluish tints, which may be attributed more often to shading, and this bias may underlie the individual differences in whether people described the widely publicized image of #thedress as blue-black or white-gold. To probe these higher-level color inferences, we examined neural correlates of the blue-bias, using frequency-tagging and high-density EEG to monitor responses to 3-Hz alternations between different color versions of #thedress. Specifically, we compared relative neural responses to the original "blue" dress image alternated with the complementary "yellow" image (formed by inverting the chromatic contrast of each pixel). This image pair produced a large modulation of the EEG amplitude at the alternation frequency, consistent with a perceived contrast difference between the blue and yellow images. Further, decoding topographical differences in the blue-yellow asymmetries over occipito-parietal channels predicted blue-black and white-gold observers with over 80% accuracy. The blue-yellow asymmetry was stronger than for a "red" vs. "green" pair matched for the same component differences in LM- or S-cone contrast as the blue-yellow pair, and thus cannot be accounted for by asymmetries within either pre-cortical cardinal mechanism. Instead, the results may point to neural correlates of a higher-level perceptual representation of surface colors.

2.2. Introduction

Our perceptual experience of color arises through a complex transformation of the initial responses in three classes of retinal cone photoreceptors into extended cortical representations (e.g., for reviews: Dacey, 2000; Gegenfurtner, 2003; Lee, 2004; Solomon & Lennie, 2007; Conway et al., 2010; Shapley & Hawken, 2011; Conway, 2014; Johnson & Mullen, 2016). Within this processing stream, the representation shifts from the proximal stimulus - such as the cone contrasts at different points in the scene - to include causal inferences about the distal properties of the stimulus, such as the inferred surface reflectance. A well-studied example of these inferences is color constancy, in which the visual system forms a representation of surface color that is relatively independent of the spectrum of the incident lighting (Foster, 2011). Many different processes contribute to color constancy (Foster, 2011; D'Zmura & Lennie, 1986; Smithson, 2005; Shevell & Kingdom, 2008), from low-level sensory adjustments, e.g., adapting to the average chromaticity in the scene (Land & McCann, 1971; Brainard & Wandell, 1992; Hurlbert 1998; Smithson 2005; Foster 2011), to learned inferences about the causal structure of the world (Lotto & Purves, 2002), to potentially conceptual representations (e.g., color constancy is typically better when observers are asked to judge if two samples are the same material rather than directly judging their chromaticity; Arend & Reeves, 1986). At a neural level, differing traces of color constancy have been found throughout color-sensitive areas from the retina to the ventral occipito-temporal cortex (e.g., Gegenfurtner, 2003; Foster, 2011; Smithson, 2005; Walsh, 1999). Thus, it remains unclear at which point the representation of color more closely resembles the observer's percepts than the retina's signals (Engel, Zhang & Wandell, 1997; Wandell et al., 2000; Brouwer & Heeger, 2009).

We explored high-order color percepts and how they are manifest in neural measurements of chromatic responses with use of an ambiguous color image characterized by large individual differences in its perceptual interpretation. In 2015, this image of #thedress sparked global interest because people differed vehemently and persistently over whether the dress itself appeared "blue-black" (i.e., blue with black stripes) or "white-gold" (i.e., white with gold stripes). A common explanation for the differing percepts of the dress was that individuals differed in the inference of a distal stimulus property, i.e., whether they saw the dress to be in direct light (blue-black) or in shadow (white-gold) (e.g., Brainard & Hurlbert, 2015; Gegenfurtner, Bloj & Toscani, 2015; Lafter-Sousa, Hermann & Conway, 2015; Winkler et al., 2015; Witzel, 2015; Chetverikov & Ivanchei, 2016; Hesslinger & Carbon, 2016; Toscani, Gegenfurtner & Doerschner, 2017; Wallisch, 2017; Witzel, Racey & O'Regan, 2017). The individual differences in this inference have in turn been attributed to the special ambiguity of blue percepts (Winkler et al., 2015), in line with the gamut of chromaticities in the dress image being largely distributed along the natural "blue-yellow" daylight locus (Gegenfurtner, Bloj & Toscani, 2015; Lafter-Sousa, Hermann & Conway, 2015; Winkler et al., 2015, Witzel, Racey & O'Regan, 2017). Here, we used the dress image to investigate neural correlates of both 1) the perceptual asymmetries in the representations of blue and yellow and 2) individual differences in the perception of blue, defining white-gold and blue-black dress observers.

In the first case, perceptual blue-yellow asymmetries may again be related to the ambiguity of blue as a property of the surface or illumination. Bluish hues may pose a special challenge to color constancy because they correspond to the hue of cast shadows, and thus observers may be more likely to attribute bluish tints to the diffuse lighting (e.g. from the sky) rather than to the object. In fact, individuals tend to underestimate the blue of actual shadows

(Churma, 1994) and show better color constancy (less sensitivity to an illuminant change) for blue illuminants (Pearce et al., 2014). They are also more likely to call a bluish chromaticity "white" than the equivalent (complementary) yellow chromaticity, and thus may perceive blues as reduced in contrast (Winkler et al., 2015). Consistent with this, forming a "color negative" of the dress by inverting the chromatic contrasts from blue to yellow removed the ambiguity and thus the observer differences in the reported color (such that almost all observers now agreed that the dress stripes appeared yellow; Gegenfurtner, Bloj & Toscani, 2015; Winkler et al., 2015). This is potentially because yellow tints are inconsistent with shading, since natural blue lighting from the sky is diffuse while natural yellow lighting from the sun is directional. Moreover, these effects are specific to the blue-yellow axis: when the dress colors are rotated off this axis (e.g., along a reddish-greenish axis), the reds and greens appear more similar in saturation and there is again little disagreement in how people describe the colors (Gegenfurtner, Bloj & Toscani, 2015; Winkler et al., 2015).

Thus, we first tested for *group-level* neural responses correlated with the reduced perceived contrast of blue. To this end, we compared electroencephalogram (EEG) response asymmetries to paired blue-yellow versions of the dress, as well as paired green-red versions of the dress. The differences in chromatic contrast along the L-M and S-(L+M) cardinal chromatic axes were constructed to be identical for the blue-yellow and green-red stimulus pairs, but combined in opposite phase (see **Figure 2.1a** and Methods). Thus, differences in the responses to the blue-yellow vs. green-red pairs could not be accounted for by the separable cardinal color mechanisms representing pre-cortical color coding (Derrington, Krauskopf, and Lennie, 1984) (though asymmetries within either cardinal mechanism would be expected to produce (the same) asymmetric responses within either the blue-yellow or green-red pair). This comparison

has been applied in a number of previous studies to test for the separability of the cardinal axes

(e.g. Goddard et al., 2010; McDermott et al. 2010). To provide a reference for an extreme

contrast difference (achromatic to chromatic), we additionally measured electrophysiological

response differences to a pair of gray-yellow dress images. Overall, we predicted that group

differences in neural responses to blue-yellow would be greater than those to green-red (in line

with larger perceptual blue-yellow asymmetries: Winkler et al., 2015) but smaller than those to

gray-yellow (an extreme achromatic-chromatic contrast), even though again the blue-yellow and

green-red pairs were matched for their low-level color differences.
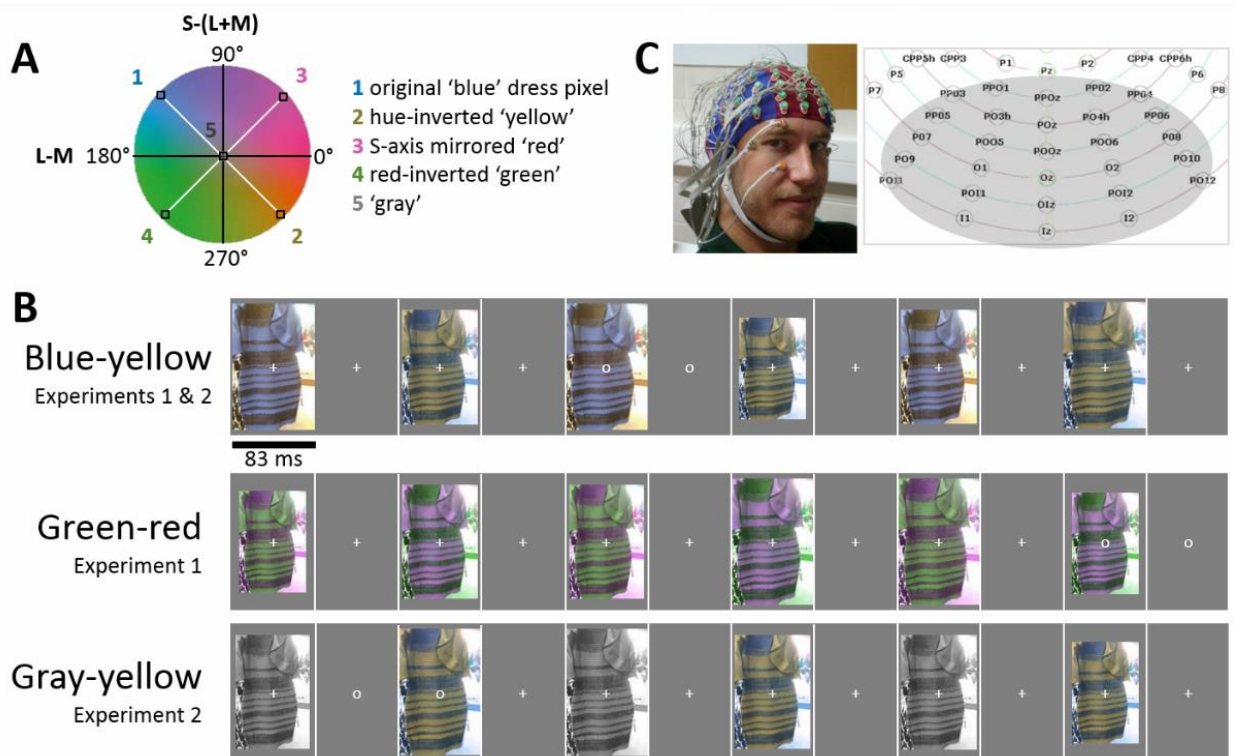
Figure 2.1. A) A scaled version of the MacLeod-Boynton chromaticity diagram showing the

construction of the stimuli. The chromatic contrast of each pixel in the original "blue" image

(e.g., point 1) was inverted to form the yellow image (e.g., point 2). In turn, the red and green

images (e.g. points 3 and 4) were formed by reflecting the blue yellow contrasts along the L-M or

equivalently S-(L+M) axes. Consequently, the blue-yellow and green-red pairs had the same

component L-M and S-(L+M) contrast, but combined in opposite phase. Additionally, another

independent transformation was applied to convert each pixel of the original dress image into

achromatic gray (point 5). **B)** *Three experimental conditions comprised of testing in order blue-*

yellow, green-red, and gray-yellow pairs of dress stimuli. **C)** *Left: A 128-channel ActiveTwo*

BioSemi EEG system was used for the recordings. Right: A section of relabeled posterior electrode

positions on a 2D scalp map. Analyses were performed on a 28-channel occipito-parietal region-

of-interest (highlighted in gray), encompassing all occipital, occipito-parietal, occipitoinferior,

and inferior channels.

In the second case, we assessed *individual* differences in the blue-yellow percepts. Here,

we reasoned that white-gold and blue-black observers would be identifiable with a system-level

measure of visual cortical responses (recorded with high-density over the occipito-parietal

cortex), again given the extensive traces of surface/illuminant resolution throughout the human

visual system (e.g., Gegenfurtner, 2003; Foster, 2011; Smithson, 2005; Walsh, 1999). Neural

correlates at this level have not been found in previous studies. Instead, one previous

neuroimaging study reported differences across observers only in frontal and parietal "higher

cognition" cortical areas when contrasting the dress to uniform color patches (Schlaffke et al.,

2015). This effect was interpreted as modulation of the percepts by top-down, post-perceptual

processes. Other studies have pointed instead at low-level visual influences, such as spectral

sensitivity differences from variations in macular pigment density (Rabin et al., 2016) or normal

variations in pupil diameter (Vemuri et al., 2016). In this vein, neural correlates of visual evoked

potential waveforms at a single medial-occipital electrode with differences in perception of the

dress were reported (Rabin et al., 2016), although these low-level findings were not reliable at the individual participant level.

We took a novel approach to explore neural correlates of individual differences in perception of the dress, hypothesizing that differences across white-gold and blue-black observers would manifest as differences in the recorded blue-yellow EEG response differences. While blue-black and white-gold observers both rely on high-level assumptions about the source of illumination in this image, the differences in these assumptions result in different perceived contrasts of the dress surface color, which in turn may predict different contrast responses to the surface color. Specifically, we predicted that observers who perceived the dress as white-gold might represent the blue hues in the image as a lower effective contrast, leading to blue-yellow amplitude differences largest over medial-occipital channels sensitive to early-stage contrast differences (Kulikowski et al., 1994; Crognale et al., 2013). Additionally, since these response asymmetries potentially reflect a lower effective stimulus contrast in the blue image, we predicted greater similarities in blue-yellow and gray-yellow asymmetries for these observers, in terms of response amplitude, topography, and phase. Conversely, observers reporting the dress as blue-black might show responses to the blue and yellow pair that are more similar to those between green and red, i.e., not differing in perceived contrast, but relying on chromatic-chromatic distinctions, possibly from later-stage visual areas projecting beyond the occipital midline of the scalp (e.g., Anllo-Vento, Luck & Hillyard, 1998). These observers in particular are expected to have larger gray-yellow than blue-yellow responses. Such differences between the two perceptual groups would lay the foundation for classification of observers as white-gold or blue-black based on their blue-yellow response asymmetries.

To monitor neural asymmetries, we used fast periodic visual stimulation and high-density electroencephalogram (FPVS-EEG; also referred to as "frequency-tagging" or "steady-state visually evoked potentials"; e.g., Regan, 1966; Rossion, 2014a; Rossion, 2014b; Norcia et al., 2015). Generally, in this approach, stimuli presented at a fixed frequency generate EEG responses locked to that frequency, which can be identified objectively in the temporal frequency domain with a high signal-to-noise ratio. Here, we applied a paradigm variant designed specifically to measure response asymmetries, or differences in the relative responses to two stimuli (e.g., Tyler & Kaitz, 1977; Ales & Norcia, 2009; Coia et al., 2014; Retter & Rossion, 2016a; Retter & Rossion, 2017; reviewed in Norcia et al., 2015). In this symmetry/asymmetry paradigm, the stimulus alternates between two images (see **Figure 2.1B**), generating responses at the presentation frequency (F = 6 Hz) and its harmonics, but potentially also at the alternation rate ($F/2$ = 3 Hz) and its unique harmonics if differences in the responses to the two images (e.g., blue and yellow dresses) are present. In other words, common (symmetrical) visual responses to both stimuli are tagged at 6 Hz, while differential (asymmetrical) responses to the two stimuli are tagged at 3 Hz. As a concrete example, suppose a grating is shown 6 times per second, but alternates between horizontal and vertical. The EEG response will modulate at 6 Hz (the stimulus presentation rate). However, if the magnitude of response to the two gratings differs (e.g., because the horizontal grating has a lower contrast and thus produces a weaker neural signal), then the EEG response will also show a modulation at the alternation rate of 3 Hz, reflecting the asymmetry in the neural responses. Here we test for response asymmetries which might arise from the perceptual color contrast differences between blue and yellow versions of the dress image.

By using FPVS to record implicit responses to briefly presented images (167 ms SOA), we limited post-perceptual attentional or decisional modulation of the response to any one image (e.g., Rossion, 2014a; Norcia et al., 2015). By using high-density EEG, we also expanded our recording beyond a traditional medial-occipital channel, which has been shown to relate dominantly to early-stage visual cortical responses (Kulikowski et al., 1994; Crognale et al., 2013; see also Anllo-Vento, Luck & Hillyard, 1998 and the Discussion). Therefore, this paradigm was optimal for investigating both group- and individual-level perceptual effects that relate to complex visual inferences about surface and lighting color, which again may emerge from throughout early- and late-stage visual areas. At a practical level, discovering sensitive and reliable neural correlates of perceptual reports of color appearance would provide important foundations for future studies, e.g., for testing the development of (blue-yellow) color perception in infants. At a theoretical level, investigating these neural correlates allowed us to explore the visual representation of higher-order aspects of color perception.

2.3 Materials and Methods

Participants

Fourteen participants, recruited from students and staff at the University of Nevada, Reno, took part in the primary experiment (Experiment 1). Their ages ranged from 20-30 years old (M = 23 years; SD = 3.2 years). Nine were male, and two were left-handed. A novel group of fourteen participants took part in a second experiment, none of whom had participated in Experiment 1. Their ages ranged between 21-41 years old (M = 26 years; SD = 5.2 years), five were male, and one was left-handed. All reported normal or corrected-to-normal visual acuity and normal color vision. They gave signed, informed consent prior to participation in the experiment, which was approved by the University of Nevada, Reno's Institutional Review

Board, and conducted in accordance with the Code of Ethics of the World Medical Association

(Declaration of Helsinki).

Stimuli

Experiment 1 used two stimulus pairs (**Figure 2.1B**). One pair included the original image

of #thedress (Roman Originals, 2018; made famous on Swiked, 2015), and an image formed by

inverting the chromaticity of each pixel across both the L-M and S-(L+M) axes to the cone-

opponent color (see **Figure 2.1A**). Note that this inversion maintained the same luminance at

each pixel and thus altered only the chromaticity. Specifically, the vector defining the

chromaticity of each pixel was effectively rotated 180 deg within a cone-opponent color space,

so that the inverted color was equal in magnitude (cone-contrast) but opposite in direction

relative to the achromatic point. The space was a modified version of the MacLeod-Boynton

chromaticity diagram centered on a nominal gray value equivalent to the chromaticity of

illuminant C (CIE 1931 x,y = 0.310, 0.316), and scaled to roughly equate threshold sensitivity

along the cardinal L-M and S-(L+M) cone-opponent axes of the space (Winkler et al., 2015). We

refer to these images as the blue-yellow (original-inverted) pair. The second pair was formed by

inverting the pixel chromaticities of the blue-yellow pair along only the L-M (or S-(L+M)) axes of

the space. This changes the hue of the original dress from blue to red, and the yellow

complement to green. We refer to these images as the green-red pair.

Importantly, the green-red pair has the same component L-M and S-(L+M) chromatic

contrast as the blue-yellow pair, but the components are combined in opposite phase.

Consequently, the two pairs are matched for their signals along the independent L-M and S-

(L+M) dimensions that are thought to be the principal or cardinal color directions along which

color is coded in the retina and geniculate (Krauskopf, Williams & Heeley, 1982). Experiment 2

used the same blue-yellow pair but compared to a third pair corresponding to the yellow image

of pair 1 and a grayscale image of the dress, wherein each pixel has the same luminance but the

chromaticity of the nominal gray. This gray-yellow pair was included to assess the EEG responses

to an actual (rather than perceived) asymmetry in the chromatic contrast of the images.

The stimuli were sized to a width of 215 pixels and height of 327 pixels, and were

presented on a gray background (with a luminance of 34.5 cd/m2, equivalent to the medium

gray level of the screen) on a 21 inch cathode ray tube (CRT) monitor (NEC AccuSync 120), with a

120 Hz screen refresh rate. The monitor was gamma-corrected based on calibrations obtained

with a PhotoResearch PR655 spectroradiometer, and was controlled by a standard PC. In

Experiment 1, at a viewing distance of 80 cm, the images subtended a height of 6.8 degrees of

visual angle. In Experiment 2, stimuli were viewed at a distance of 57 cm, changed to correspond

with other experiments in the same testing session; they consequently subtended a height of

9.5 degrees of visual angle. Though percepts of #thedress have been found to change with size

and spatial frequency (Lafter-Sousa, Hermann & Conway, 2015; Dixon & Shapiro, 2017),

informal assessments suggest that the size change between the experiments did not impact

observers' color judgments of the images (in each Experiment, 5/14 observers reported seeing

the dress as white-gold).

Fast Periodic Visual Stimulation (FPVS) Procedure

Setting up the EEG system lasted about 30-40 minutes, with two experimenters

preparing the headcap (alternating across participants which side of the cap they put the

conductive gel). Capped participants were positioned in front the CRT monitor and used a

keyboard to start testing trials and give responses. Viewing was binocular and in a room

illuminated only by the experimental and acquisition displays. A symmetry/asymmetry fast

periodic visual stimulation (FPVS) design was used (e.g., Tyler & Kaitz, 1977; Ales & Norcia, 2009; Coia et al., 2014; Retter & Rossion, 2016a; Retter & Rossion, 2017; reviewed in Norcia et al., 2015). As noted, in this paradigm, two images are presented in alternation, leading to two distinct frequency-tagged responses expected in the EEG recording. At the image presentation rate (6 Hz), responses common to the two images, i.e., symmetrical responses, are expected. At the rate at which the images repeat (6 Hz/2 = 3 Hz), aspects of the responses differing between the two images, i.e., asymmetrical responses, are expected. Note that in most previous applications of this paradigm, one of the stimuli is adapted to prior to the alternation to enhance intra-population response differences (e.g., see Figure 2 of Ales & Norcia, 2009, investigating directional motion), but adaptation is not necessary when the amplitude and phase of these differences is already substantial at the neural population level (e.g., Coia et al., 2014, investigating a chromatic illusion). Here, we aimed to investigate the inherent, unadapted neural response asymmetries to paired color images.

Images were presented with a 50% duty cycle square wave at 6 Hz, resulting in each image being displayed at full contrast for 83.3 ms, followed by 83.3 ms of the background. The processing of each image likely persists to some extent until it is interrupted, such that rapid serial visual presentation paradigms have led to behavioral and neural response signatures within less than 20 ms presentation duration (Keysers et al., 2001; Potter et al., 2014). While the display time of each image here is brief, a study by Foster, Craven and Sale (1992), showed that illuminant vs. surface color changes were detected extremely rapidly, even below 83 ms. At each image presentation, the size varied from 90-110% of the size of the original image in 10% steps to reduce pixel-based image repetition effects (see Dzhelyova & Rossion, 2014). As described in the Introduction, in Experiment 1 there were two experimental conditions, in each

of which a pair of images of the dress were presented in alternation: 1) blue-yellow, alternating the original bluish and hue-inverted yellowish images of the dress; and 2) green-red, alternating the greenish and reddish images of the dress. In Experiment 2, there were also two experimental conditions, the first of which repeated the blue-yellow condition of Experiment 1. The second, gray-yellow condition, consisted of alternating a grayscale and the color-inverted image of the original dress (**Figure 2.1B**).

Each testing sequence lasted for 50 s, immediately preceded and followed by a jittered 2-3 s presentation of a white fixation cross in the middle of the gray background, in order to establish fixation before recording and prevent abrupt movements on trial completion. Participants were instructed to fixate on this cross, which remained present throughout the testing sequence, superimposed on the presented images. To encourage fixation and sustained attention during trials, the cross would briefly change to an open circle (persisting for 200 ms) eight times throughout each sequence at random time points, and participants were instructed to press the space bar each time they detected the change.

Participants viewed four repetitions of the sequences for each of the two conditions, in an individually randomized order, leading to a total recording time of 6.7 minutes. Given the short testing time, participants also took part in additional experiments during the same session, none of which concerned color perception. Stimuli were presented with Java SE Version 8.

EEG acquisition

EEG was recorded with a 128-channel BioSemi ActiveTwo EEG system. The Ag-AgCl Active-electrodes were organized in several sizes of head caps in the default BioSemi configuration, which centers around nine standard 10/20 locations on the primary axes (BioSemi B.V., Amsterdam, Netherlands; for exact coordinates, see

http://www.biosemi.com/headcap.htm). The default labels of BioSemi (organized in four groups

(A-D) of 32) were relabeled to closely match those of a more conventional 10/5 system

(Oostenveld & Praamstra, 2001; for exact relabeling, see Rossion et al., 2015, Figure S2; for a

relevant example, see also **Figure 2.1C**). Offsets of each electrode, relative to the common mode

sense (CMS) and driven right leg (DRL) feedback loop, were held below 40 mV. In addition,

vertical and horizontal eye movements were recorded with four flat-type Active-electrodes,

placed above and below the right eye and lateral to the external canthi. Recordings were

digitized at a sampling rate of 2048 Hz and saved in BioSemi Data Formats (BDFs), and then

down-sampled offline to 512 Hz to reduce file size for processing.

EEG analysis: Preprocessing

Data were processed with Letswave 5, an open source toolbox

(http://nocions.webnode.com/letswave), running over MATLAB R2013b (MathWorks, USA).

After importation of the recorded BDFs, data were filtered with a fourth-order zero-phase

Butterworth band-pass filter, with cutoff values of high-pass 0.05 Hz and low-pass 120 Hz, as

well as a 60 Hz fast-Fourier transform (FFT) notch filter with a width of 0.5 Hz to remove 60 Hz

electrical noise and its second harmonic. To correct for noise from eye-blinks in two participants

blinking the most frequently in Experiment 1, i.e., more than two times per s (M = 0.11; SD =

0.13 blinks/s), and for three participants in Experiment 2 (M = 0.12, SD = 0.22 blinks/s),

independent-component analysis (ICA) was used to remove a single component accounting for

blink activity. Channels which had artifacts (deflections of greater than 100 μV) across two or

more testing sequences were linearly interpolated with 3-5 pooled neighboring channels (six or

fewer channels per participant; Experiment 1: M = 1.8; Experiment 2: M = 0.57). Data were then

re-referenced to the common average of the 128 EEG channels and segmented to 50 s per

testing sequence, corresponding to exactly 300 image presentation cycles at 6 Hz and 150 image repetition cycles at 3 Hz. Testing sequences were averaged in time for each participant, preserving phase-locked responses evoked by image presentation and reducing non-phase-locked noise.

EEG analysis: Frequencies-of-interest

Asymmetrical responses, i.e., responses differing between the two images presented in each sequence, are expected at 3 Hz and its unique, odd harmonic frequencies (i.e., 9 Hz, 15 Hz, etc.; see Procedure). Symmetrical responses, in common to each of the two images presented in each sequence, are expected at the image presentation rate of 6 Hz and its (even) harmonic frequencies (i.e., 12 Hz, 18 Hz, etc.). In order to determine the number of harmonics to analyze for each of these two fundamental frequencies, data from Experiment 1 was Fourier-analyzed to obtain the frequency-domain amplitude spectra (see below) based on activity pooled across all channels and grand-averaged across participants. Z-scores were computed at each frequency bin, x, with a respective baseline defined as 20 surrounding frequency bins, excluding the immediately adjacent bins ($Z = (x - \text{baseline mean}) / \text{baseline standard deviation}$) (e.g., Retter & Rossion, 2016b; Srinivasan et al., 1999). Harmonic frequencies with responses significant at $Z > 2.32$, $p < .01$ (one-tailed, testing signal>noise) were used in subsequent analyses: this included five unique harmonics of 3 Hz (i.e., 3, 9, 15, 21, and 27 Hz) and seven harmonics of 6 Hz (i.e., 6, 12, 18, 24, 30, 36, and 42 Hz) in both conditions (here, equivalent numbers of harmonics would be selected if $p < .05$ were used). Z-score values ranged from 3.15 to 15.9 at 3 Hz and its harmonics (peaking at 15 Hz), and from 2.83 to 125 at 6 Hz and its harmonics (peaking at 6 Hz). The same harmonic frequency ranges were used for analysis in Experiment 2.

EEG analysis: Region-of-interest

A single occipito-parietal region-of-interest (ROI) was defined for response amplitude quantification, encompassing all 28 occipital, occipito-parietal, occipito-inferior, and inferior channels. This expansive ROI was chosen to include potentially diffusive visual responses across occipito-parietal regions (e.g., Anllo-Vento, Luck & Hillyard, 1998; see also Forder et al., 2017; Thierry et al., 2009) and the potential neural sources considered in the Discussion. It was validated post-hoc that it included the channels producing the maximal amplitude at 3 Hz and 6 Hz and their unique harmonics, despite variance across conditions at 3 Hz and its unique harmonics (e.g., the two electrodes giving the maximal responses were Oz and OIz in the blue-yellow condition vs. POO6 and O2 in the green-red condition).

EEG Frequency-domain analysis: Amplitude

A discrete Fourier Transform (Fast Fourier Transform; FFT) was used to convert the data into an amplitude (μV) frequency spectrum, normalized by the number of samples output. This spectrum had a range of 0-256 Hz and a resolution of 0.02 Hz. Quantification of the comprehensive responses tagged at 3 and 6 Hz were computed as a sum of the significant harmonics of each respective frequency (Retter & Rossion, 2016b). First, a baseline-subtraction was performed to reduce differences in noise-level across the frequency spectrum (e.g., being generally higher at lower frequencies and increasing locally in the alpha band), as well as across participants. The baseline of each frequency bin, x, was defined with 20 surrounding frequency bins, excluding the immediately adjacent bins, as well as the local minimum and maximum (e.g., Retter & Rossion, 2016b; Rossion et al., 2012). Finally, the baseline-subtracted amplitude of each significant frequency was combined at each channel. Grand-averaged summed-harmonic responses were computed for display of group-level frequency spectra and topographies. For

further comparison of response topographies, normalization was applied using McCarthy and

Wood's (1985) method to remove overall amplitude differences across conditions.

In Experiment 1, to statistically compare the asymmetrical responses at 3 Hz and its

summed harmonics across the two conditions, a paired-sample t-test was performed over the

occipito-parietal ROI (see above), one-tailed given the specific hypothesis that larger blue-yellow

than green-red asymmetries would be observed. In Experiment 2, a one-tailed paired-sample t-

test was again performed on the occipito-parietal ROI of the summed-harmonic response to

compare the two conditions, constrained by the hypothesis that the gray-yellow condition

would produce a larger asymmetry at 3 Hz and its unique harmonics than the blue-yellow

condition. In both Experiments 1 and 2, the symmetrical responses at 6 Hz and their summed

harmonics were compared separately with two-tailed paired-sample t-tests over the same ROI,

given that there was no predicted directionality of differences between conditions. In

preparation for these paired-samples t-tests, the normalcy of the distribution of differences was

confirmed with Shapiro-Wilk's test (p > .05).

EEG Frequency-domain analysis: Phase

Additionally, the FFT cosine phase spectrum was similarly computed. Phase was

considered over the average of only a few medial-occipital channels (POOz, Oz, and OIz), since

the phase appeared variable across the scalp (data not shown). Since the reliability of phase

depends on the recorded amplitude, phase values averaged across participants at each

frequency and channel were weighted by the corresponding response amplitude for each

participant. Mean amplitude-weighted phase differences were calculated, and compared across

independent samples with the Watson-Williams test, using the CircStat MATLAB toolbox

(Berens, 2009); mean amplitude-weighted phase differences across paired samples were

compared with a circular Hotelling test (van den Brink, 2014).

Perceptual differences (Experiments 1 and 2 combined)

To compare the EEG responses with the individual differences in perceivers' reported

color perception of the dress, i.e., blue-black or white-gold, the data from the blue-yellow

condition were combined across Experiments 1 and 2. Note that despite the change in viewing

distance across the two experiments, the blue-yellow 3-Hz response did not differ across groups

in terms of amplitude (0.02 μV mean difference), peak response topography (maximal response

at the same two channels) or phase (2 deg mean difference). As one participant in the first

experiment did not report a perceptual group, this sample included 27 different participants.

There were 5 white-gold perceivers in each Experiment 1 and Experiment 2, leading to a total of

10 white-gold and 17 blue-black perceivers. Mean perceptual-group data were examined as

above for amplitude and phase differences, except with independent-samples one-tailed t-tests,

given the hypothesis that white-gold would have larger blue-yellow summed-harmonic 3 Hz

asymmetries than blue-black participants. Equal variances were confirmed with Levene's test (p

> .05).

Additionally, summed-harmonic 3 Hz response topographies were explored. First, these

topographies were normalized according to the method of McCarthy & Wood (1985), to

compensate for amplitude differences across individuals. Then, significant differences across

perceptual groups were tested with a leave-one-participant-out decoding analysis (e.g.,

Poldrack, Halchenko & Hanson, 2009; Coggan et al., 2016). In this analysis, data from each

participant is sequentially left-out and compared to the average of the remaining blue-black and

white-gold observers at each channel within the occipito-parietal ROI; each participant is

assigned the perceptual label of the group giving the higher correlation across channels, i.e., a winner-take-all approach (e.g., Jacques, Retter & Rossion, 2016). A permutation test (5,000 permutations) with Monte Carlo randomization of perceptual group was used to create a null distribution from which reference a significance score (p-value) was derived. The mean of this null distribution for the blue-black observers was 53.6% (95% CI: [53.3%, 54.0%]), and 44.9% (95% CI: [44.5%, 45.2%]) for the white-gold observers. In addition, a control decoding analysis was performed identically with the 6 Hz response topographies, which are not frequency-tagged to chromatic asymmetries but still may reflect general individual differences. In this case, the mean of the permutation distribution for the blue-black observers was 54.5% (95% CI: [54.2%, 54.9%]), and 44.1% (95% CI: [43.8%, 44.5%]) for the white-gold observers.

2.4. Results

Experiment 1: Blue-Yellow vs. Green-Red responses

To test for an overall blue-yellow asymmetry, we first compared the 3-Hz responses to the blue-yellow alternation vs. the green-red alternation. As noted, these image pairs were matched for their chromatic contrasts along the L-M and S-(L+M) axes, and thus for their effective strength in pre-cortical color mechanisms. As also noted, the difference along each axis might itself lead to an asymmetry (e.g. since both image pairs alternated between +S and –S signals, and there are known differences in the coding of S-cone increments and decrements; Tailby, Solomon & Lennie, 2008; Dacey, Crook & Packer, 2014; Wang, Richter & Eskew, 2014). However, these early-level asymmetries predict identical 3-Hz responses for both image pairs, while a stronger asymmetry for blue-yellow would instead implicate a higher-level transformation of the pre-cortical color signals.

As expected, significant asymmetric responses were found at 3 Hz and its harmonics for both the blue-yellow and green-red image pairs, but were stronger for the blue-yellow pair (**Figure 2.2A**). Pooled across all 128 channels, the response was significant at four additional unique harmonics, i.e. 9, 15, 21, and 27 Hz, in both conditions (all Z's >2.32, p's <.01). These harmonic responses were baseline-subtracted and summed to create a comprehensive response profile (Retter & Rossion, 2016b). A comparison of the amplitude of the summed-harmonic 3-Hz response, calculated over a 28-channel occipito-parietal ROI (see Methods), revealed a significantly larger response for the blue-yellow, with a medium effect size (M = 0.44 µV, SE = 0.069 µV) than green-red condition (M = 0.31 µV, SE = 0.073 µV), t_{13} = 1.86, d = 0.51, p = .043 (**Figure 2.2B**). Indeed, 10 of the 14 observers has a positive difference (blue-yellow > green-red).
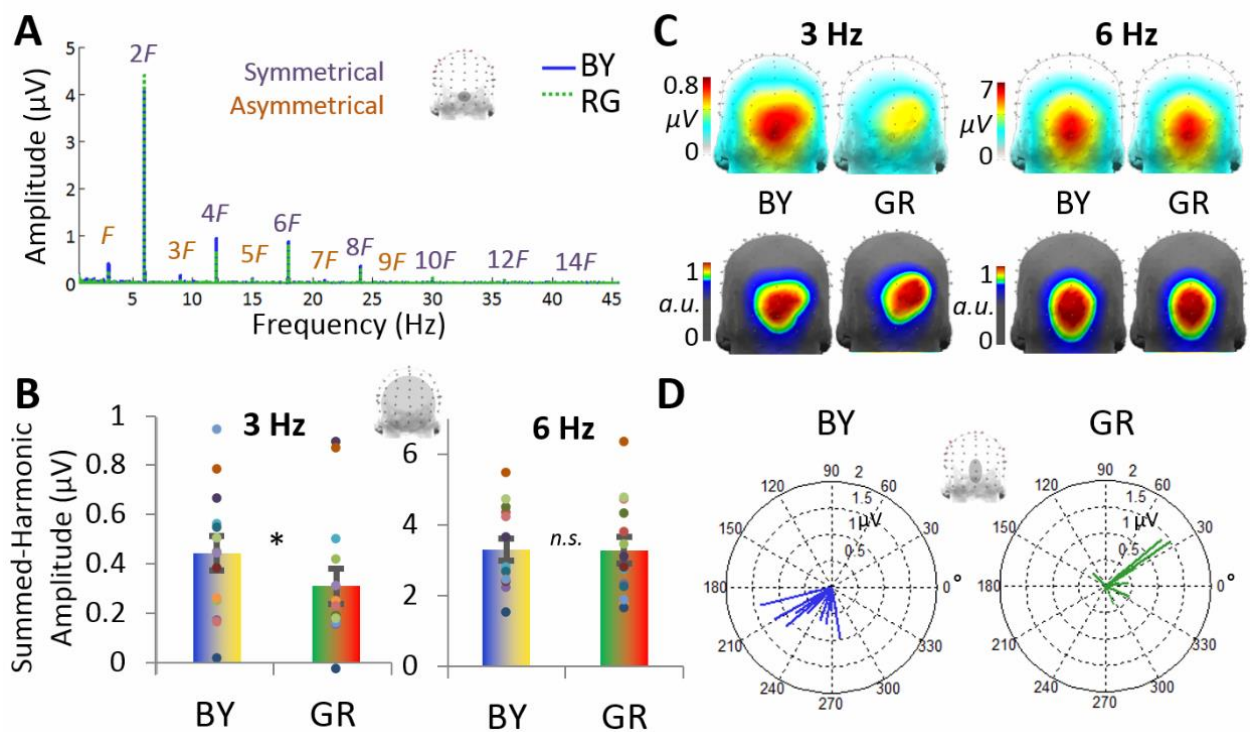
Figure 2.2. Experiment 1 EEG results for the blue-yellow (BY) and green-red (GR) image pairs (N = 14). **A)** The asymmetrical response at 3 Hz (F) and its unique harmonics is evident in the baseline-

*subtracted frequency spectrum, shown here for channel OIz. Its unique, asymmetrical harmonics are labeled up to 27 Hz (9F), the highest frequency giving a significant response at the group level across all 128 channels. Thesymmetrical response at 6 Hz (2F) and its harmonics are plotted in the same manner, up to 42 Hz (14F). **B**) The summed-harmonic baseline-subtracted amplitudes over the occipito-parietal ROI for each 3 and 6 Hz. Individual data are shown with dots, paired by color. **C**) The topographical distribution of the data partly shown in part B, at 3 and 6 Hz (top row). The corresponding normalized topographies are also plotted to emphasize the spatial differences, occurring within the occipito-parietal ROI (bottom row). **D**) The phase of the 3 Hz response over the average of channels POz, Oz, and OIz. Data are shown with separate vectors for each individual participant, with the angle of the vector representing the cosine phase and the length of the vector representing the baseline-subtracted amplitude over these channels at 3 Hz.*

Although our experimental hypothesis here targeted response amplitudes, we aimed additionally to exploit the richness of FPVS-EEG data in terms of spatial and temporal information. The phase of the 3-Hz response, showing relative latency differences, was also considered for the two conditions (**Figure 2.2D**). The mean phase of the blue-yellow response was 237 deg; SE = 7.73 deg; for the green-red response it was 29.8 deg (SE = 12.4 deg), a highly significant difference, $F_{2,12} = 17.0$, $p < .001$. The absolute difference between the phase for the two conditions across each participant was on average 202 deg (SE = 15.3 deg). This phase difference is somewhat close to that of a 180-deg phase reversal, which would indicate that differences in latency and/or amplitude within each stimulus pair were inverted across stimuli in the blue-yellow and green-red conditions (note that the blue and green images were shown first in their respective sequences). This phase inversion could reflect differences in the polarity of

the cone contrasts for the two image pairs, and thus, as described above, the latency responses

to both pairs are consistent with a common (in phase) baseline asymmetry in the response to

the S-cone (or L-M cone) contrasts in the images. (In other words, if the latencies in the

responses were measured relative to only the S-cone or only the L-M cone modulation in the

stimuli, then they would be similar for the blue-yellow and green-red pairs). By this account, the

asymmetrical responses between blue and yellow are superimposed on top of the response

differences from any cardinal axis asymmetries common to both the blue-yellow and green-red

pairs.

The summed-harmonic 3-Hz response scalp topographies were distributed across the

occipito-parietal channels in both the blue-yellow and green-red conditions (**Figure 2.2C**, top

row). While in both conditions the maximal responses encompassed the same five channels (Oz,

OIz, POO6, O2, and POOz), in the blue-yellow condition the response was maximal over channels

Oz and OIz (each 0.76 μV), and in the green-red condition the response was maximal over

channels POO6 and O2 (each about 0.53 μV). Given differences in amplitude across conditions,

the response topographies were normalized for display. The normalized topographies appeared

to show a slightly more dorsal and rightward response topography for the green-red than blue-

yellow condition (**Figure 2.2C**, bottom row).

Finally, symmetrical 6 Hz responses, reflecting visual responses common to the

presentation of both stimuli, were examined as a control, with the prediction that there would

be no differences here across conditions. The 6-Hz responses were significant up to 42 Hz in

both conditions (**Figure 2.2A**). A statistical comparison of the summed-harmonic 6-Hz response

amplitude, again calculated over the occipito-parietal ROI, indicated no differences across

conditions (blue-yellow: M = 3.32 μV, SE = 0.31 μV; green-red: M = 3.29 μV, SE = 0.37 μV), $t13$ =

1.96, d = 0.022, p = .85 (**Figure 2.2B**). The 6-Hz response topographies also appeared to be

similar across conditions, with the maximal channel along the occipital midline: first at OIz,

followed by Oz, Iz, and POOz in both conditions (**Figure 2.2C**). Additionally, the phase of the 6 Hz

responses showed no systematic differences between the pairs (blue-yellow = 169 deg; SE =

5.98 deg; green-red = 179 deg; SE = 8.58 deg), F2,14 = 1.74, p = .22.

Experiment 2: Blue-Yellow vs. Gray-Yellow responses

To further assess the basis for the blue-yellow asymmetries, we compared the

amplitude of asymmetries when the blue-yellow pair was instead compared to a gray-yellow

pair, for which the two images differed in actual (as opposed to potentially perceived) chromatic

stimulus contrast. The distribution of harmonic responses was similar to that found in the first

experiment: asymmetric responses at 3 Hz and its odd harmonics persisted up to 27 Hz in both

conditions (**Figure 2.3A**). As expected, the amplitudes of the summed-harmonic 3-Hz response

over the 28-channel occipito-parietal ROI were significantly lower for the blue-yellow (M = 0.46

μV, SE = 0.079 μV) than gray-yellow condition (M = 0.66 μV, SE = 0.068 μV), t13 = 2.77, d = 0.73,

p = .008 (**Figure 2.3B**), with a medium effect size. The stronger asymmetry for gray than blue is

not surprising given that the gray-yellow pair included an actual (physical) chromatic contrast

difference in the stimuli. However, this effect is consistent with the conjecture that the stronger

asymmetry for blue-yellow than green-red is due to differences in the effective (perceptual)

chromatic differences in the stimuli.
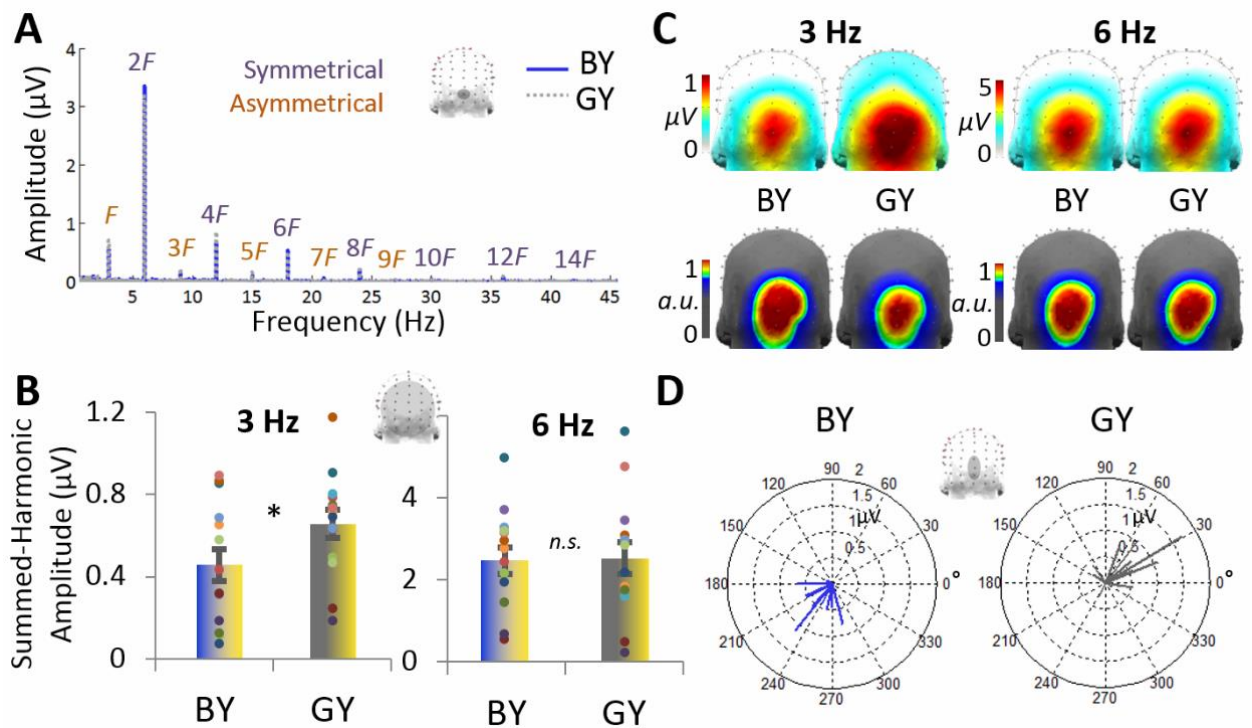
Figure 2.3. Experiment 2 EEG responses for the blue-yellow (BY) and gray-yellow (GY) pairs (N = 14). **A)** As in Figure 2.2 of Experiment 1, channel OIz is plotted in the baseline-subtracted amplitude frequency domain. **B)** Responses were quantified at the occipito-parietal ROI over the labeled harmonic frequencies for each the asymmetrical 3 Hz and symmetrical 6 Hz responses shown in Part A. Individual data are shown with dots, paired by color. **C)** The topographical distributions of the data partly shown in Part B, for 3 and 6 Hz (top row). The corresponding normalized topographies are shown below (bottom row). **D)**. The 3 Hz phase over the average of POz, Oz, and OIz. Individual participant data is plotted in separate vectors, with the angle representing the cosine phase and the length representing baseline-subtracted amplitude over these channels at 3 Hz.

In terms of temporal information, the mean phase of the 3-Hz response was 235 deg (SE = 8.46 deg) in the blue-yellow condition was different from the gray-yellow condition, 38.0 deg (SE = 10.8 deg), $F_{2,14}$ = 10.5, p = .002 (**Figure 2.3D**). The absolute difference in phase across the conditions was 185 deg (SE = 11.6 deg). Again, a speculative explanation for these phase-reversal effects is how the stimuli differed in terms of the activation they produced in S-cone and L-M cone pathways (e.g., Derrington et al., 1984, Rabin et al., 1994; see also Goddard et al., 2011). Spatially, the scalp distribution of the 3-Hz responses did not appear to differ considerably across the blue-yellow and gray-yellow conditions (**Figure 2.3C**, top row). In both conditions the two channels at which the response was maximum were Iz and OIz (about 0.90 μV in the blue-yellow vs. 1.89 μV in the gray-yellow condition). Indeed, despite a more focal gray-yellow response at the group-level, the normalized topographies also appeared similar, giving the same five maximum channels in the same order across conditions: Iz, OIz, Oz, POI2, and O2 (**Figure 2.3C**, bottom row).

Symmetrical 6-Hz responses, again reflecting the visual responses common to the presentation of both stimuli, were not predicted to differ across conditions. These 6-Hz responses were present in both conditions up to 42 Hz (**Figure 2.3A**). The summed-harmonic 6-Hz response amplitudes did not differ between the blue-yellow (M = 2.48 μV, SE = 0.068 μV) and gray-yellow (M = 2.53 μV, SE = 0.40 μV) conditions, t_{13} = 0.33, d = 0.040, p = .75 (**Figure 2.3B**). The topographies of these responses were not different across conditions, centered around the midline, with the same maximal three channels: OIz, Oz, and Iz (**Figure 2.3C**). Finally, the phase of these responses was also similar across conditions (blue-yellow: 51.5 deg (SE = 15.4 deg); gray-yellow: 121 deg (SE = 18.7 deg)), $F_{2,12}$ = 1.90, p = .19.

Individual differences in the dress percepts

The preceding results point to clear differences in blue vs. yellow responses at the group level. Again, a second aim of our study was to explore individual differences in these asymmetries. In the simplest case, we might expect observers who described the dress as white-gold to exhibit stronger blue-yellow asymmetries than blue-black observers. However, across participants in both Experiments 1 and 2, there were no significant differences in summed-harmonic 3-Hz response amplitude over the occipito-parietal ROI for blue-black (M = 0.47 µV, SE = 0.056 µV) and white-gold perceivers of the original dress (M = 0.41 µV, SE = 0.050, t_{25} = 0.56, d = 0.22, p = .29, one-tailed), seen in alternation with the hue-inverted yellowish dress, with a small effect size (**Figure 2.4A**). This null result in amplitude differences across perceptual groups may be due to several reasons, e.g., the large amount of inter-individual variability in response amplitude within both perceptual groups, or as a lack of statistical power (see the Discussion). However, this finding is also in line with behavioral evidence that the two groups show only weak overall differences in their saturation boundaries for blue and yellow (Winkler et al., 2015).
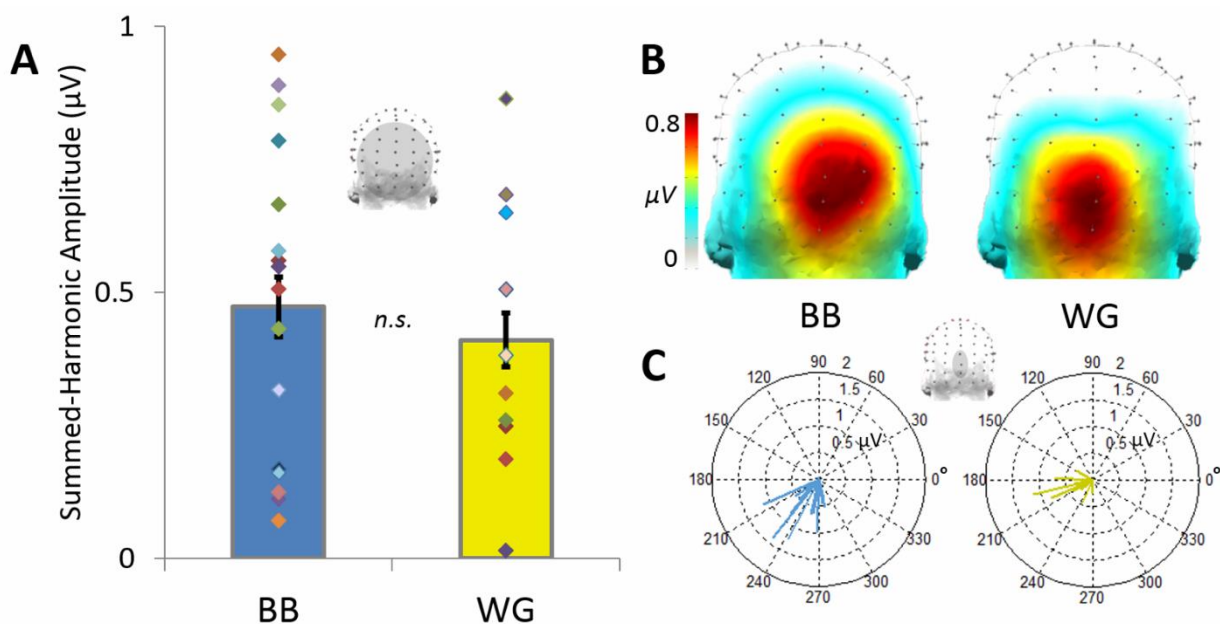
Figure 2.4. *The blue-yellow summed-harmonic 3-Hz responses across blue-black (BB) and white-gold (WG) observers.* ***A)*** *The mean response amplitude does not significantly differ across blue-black and white-gold perceivers over the occipito-parietal region-of-interest; individual participant amplitudes, indicated by randomly colored diamonds, occur over a wide range in each group of observers. Error bars indicate ± one standard error from the mean.* ***B)*** *Response amplitudes are nevertheless distributed with apparent spatial differences within the occipito-parietal ROI across the perceptual groups (see also* ***Figure 2.5***). ***C)*** *The phase of the responses across blue-black and white-gold perceivers. Individual phase values, taken from the small medial-occipital ROI indicated above, are plotted according to cosine phase angle, with the length of each vector determined by the respective amplitude.*

Interestingly, there were also notable topographical differences across the two groups in terms of the summed-harmonic 3-Hz responses, with the white-gold observers displaying more focal medial occipito-inferior responses (**Figure 2.4B**), as would be predicted from dominant input from early cortical visual areas (compare to the 6-Hz visual responses in Figures 2.2C and 2.3C; see also Kulikowski et al., 1994; Crognale et al., 2013). Normalized topographies were plotted with a color map scaled to emphasize these group differences (**Figure2. 5A**). The differences also appeared reliable across individual observers within the blue-black and white-gold groups (**Figure 2.5B**). To statistically test the reliability of the topographical differences across the perceptual groups, we applied a decoding analysis correlating 3 Hz summed-harmonic response amplitudes across electrodes in the occipito-parietal ROI. This revealed a significant correct decoding accuracy of 82.4% (14/17 observers; *p* < .001) for blue-black and 80.0% (8/10 observers; *p* = .003) for white-gold observers (**Figure 2.5C**). Despite the focused occipito-parietal responses, this effect was robust: a homologous decoding applied across all

128 channels still gave significant results across the perceptual groups (blue-black accuracy: 76.5%, p = .048; white-gold accuracy: 70%, p = .025). Finally, a control decoding of perceptual group using the response at 6 Hz, expected to capture individual variance but not reflect perceptual differences, failed to produce results above chance level: only 40.0% (4/10; p =.47) of white-gold observers were accurately classified, and 47.1% (8/17; p = 0.32) of blue-black observes.
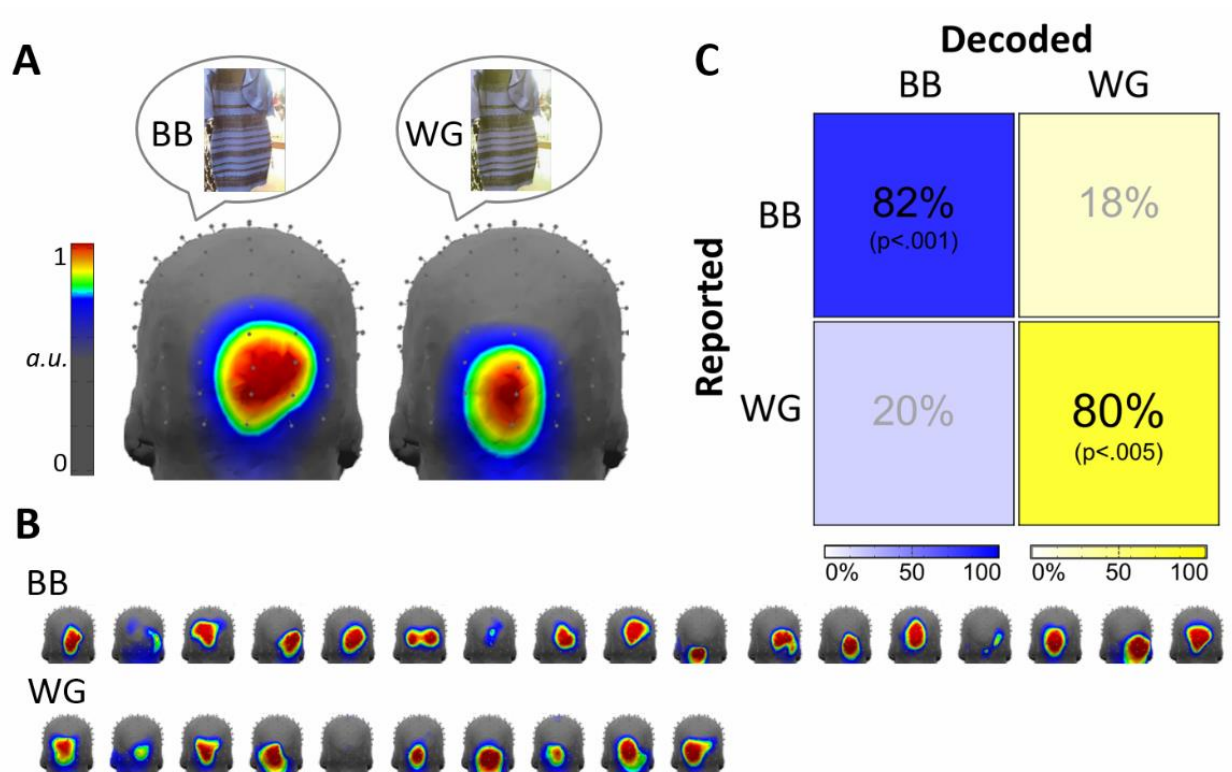
Figure 2.5. *A) Topography of summed-harmonic blue-yellow asymmetry (3 Hz) responses for blue-black (BB) and white-gold (WG) observers. Illustrative dress images are intended to represent perceptual differences; the dress stimuli presented were identical for both groups. Response topographies are normalized across all 128 channels. B) The corresponding data of each individual observer, sorted by reported perceptual group, plotted to the same scale as in section A. C) Decoding accuracy of white-gold and blue-black observers based on correlating the*

spatial distribution of responses over the occipito-parietal region-of-interest with a leave-one-

participant-out across-groups approach.

Given our hypothesis that the blue-yellow asymmetries of white-gold observers would

more closely match gray-yellow (achromatic-chromatic) asymmetries, and those of blue-black

observers would more closely match green-red (chromatic-chromatic) asymmetries, we applied

a similar topographical decoding analysis to sort the blue-yellow asymmetries across all 27

observers into gray-yellow or green-red groups. These results matched white-gold observers to

gray-yellow with 90.0% accuracy (9/10; *p* = .003) and blue-black observers to green-red with

70.6% accuracy (12/17; *p* = .042). This supports the observation that the white-gold 3-Hz

response topography is reminiscent of that of the gray-yellow topography (Figure 2.3C, for

comparison), while the blue-black topography is more similar to the green-red topography

(Figure 2.2C, for comparison).

Further, there was a slight difference in phase apparent across perceptual groups at 3

Hz (**Figure 2.4C**). The mean phase of the blue-black perceivers was 241 deg (*SE* = 5.38 deg),

while that of the white-gold perceivers was 227 deg (*SE* = 9.10 deg); this difference was not

significant, $F_{1,26}$ = 2.67, *p* = .11. The mean difference was only 13.8 deg. This difference most

likely corresponds to an 11.8 ms difference between the response latency across perceptual

groups, although the present analysis does not allow us to say whether the asymmetry response

of white-gold observers precedes that of blue-black observers or the converse.

2.5. Discussion

In this study we used high-density FPVS-EEG to examine the neural representation of ambiguous

color percepts, focusing on two aspects of color ambiguity that have been demonstrated

behaviorally. The first is the general within-observer tendency for blues to be perceived as more

achromatic than equivalent (complementary) yellows (Winkler et al., 2015). The second was the

pronounced between-observer differences in blue percepts revealed by #thedress. Both of

these effects appear specific to chromatic variations along the natural daylight locus, because

the behavioral differences largely vanish for stimuli varied along other (non-blue-yellow) axes of

color space. Moreover, the differences cannot be accounted for by variations in spectral

sensitivity, because contrast thresholds for detecting the blue and yellow stimuli are similar

(Winkler et al., 2015). Thus, the asymmetries are likely to reflect inferences or priors for natural

lighting and how these shape higher-order distal percepts of color in terms of illuminants and

surfaces, particularly in regard to blue. Our measurements thus point to neural signatures of

these higher-order color representations, at stages closer to participants' subjective experience

of color.

Electrophysiological correlates of blue-yellow asymmetries

We first explored neural correlates of perceptual blue-yellow asymmetries, in

comparison to those of equivalent chromatic-contrast along a non-daylight axis (green-red) and

to an actual physical chromatic contrast difference (gray-yellow). Consistent with percepts

observed behaviorally (Winkler et al., 2015), asymmetries in the responses to the blue-yellow

alternation were greater than to green-red, but less than to gray-yellow.

The differences in the blue-yellow variants of the dress compared to green-red were

substantial: the asymmetric (summed-harmonic 3 Hz) response amplitude for blue-yellow was

44% larger than for green-red over occipito-parietal channels, with a medium effect size. Note

again that these two dress image pairs were matched for their component contrasts along the

cardinal opponent axes, and thus the differences across conditions are unlikely to be accounted

for by the independent signals along the L-M or S-(L+M) axes. As noted, the asymmetries

common to both the blue-yellow and green-red pairs could reflect common influences of early color coding, such as the variations that both stimuli presented between S cone increments and decrements (e.g., Tailby, Solomon & Lennie, 2008; see Wool et al., 2015 for an example with local field potentials). This factor could also account for the phase relationship between the blue-yellow and green-red 3 Hz signals. However, these early factors cannot account for the larger amplitude for the blue-yellow difference.

In turn, this suggests that the representation of color, as indexed by the asymmetry responses, is not governed by the separable cardinal geniculate axes but instead involves a transformation of these axes. Such transformations have been indicated in a variety of previous studies pointing to neural representations that more closely parallel perceptual color metrics (e.g., Brouwer & Heeger, 2009) or to either weaker or stronger neural responses along the non-cardinal blue-yellow axis (e.g., Brouwer & Heeger, 2009; Conway, 2009). Neural correlates of higher-order aspects of color have also been observed in high-density EEG measurements showing that red and blue produced different responses in an attentional selection task (Anllo-Vento, Luck & Hillyard, 1998). Our results suggest that this transformation is evident *within* the blue-yellow axis, again presumably as a weakened or differentially attributed response to blue.

The blue-yellow asymmetry was also significantly weaker, with a medium effect size, than the gray-yellow modulation, which again was 44% larger. This difference is not surprising, given the extensive reports of reliable differences when comparing color vs. grayscale stimuli (e.g., Goddard et al., 2011; Goffaux et al., 2005; Zhu, Drewes & Gegenfurtner, 2013; Lafer-Sousa, Conway & Kanwisher, 2016). However, this control contrast further supports the possibility that the perceptual differences driving the blue-yellow asymmetries were consistent with the "effective" (perceived) contrast of the patterns. Finally, the fact that all three stimulus pairs

produced different levels of asymmetry provides support that it was in fact the chromatic

differences in the stimuli driving these response differences.

Perceptual differences: white-gold vs. blue-black observers

In our sample of 27 participants across the two experiments, 17 participants described

the dress as blue-black and 10 as white-gold, in line with an approximate 2:1 ratio of blue-black

to white-gold observers (with a large sample size: Lafter-Sousa, Hermann & Conway, 2015).

Analyses of the individual differences in the summed-harmonic 3-Hz blue-yellow response

topographies turned out to provide a highly reliable classifier of the individuals' percepts. These

decoding analyses separated blue-black from white-gold observers with over 80% accuracy,

significantly above chance ($p <. 005$ for both groups). This outcome is in spite of the fact that

significant asymmetries in blue-yellow responses were not found in five of the participants, and

that amplitude differences between the groups were not manifest in the averaged asymmetrical

signals averaged across the occipito-parietal ROI (Figure 2.4A). A control decoding of observers'

symmetrical (summed-harmonic 6-Hz) responses was not successful (neither group was

classified with accuracy above chance-level). Thus the decoding effectively discriminated the

observers only for the tagged asymmetry frequency where they would be expected to differ.

The amplitude of the asymmetry response was not diagnostic of white-gold or blue-

black perception, perhaps as the result of great inter-individual differences in response

amplitude on the scalp, which may be due to physiological factors unrelated to the processes of

interest, e.g., cortical folding orienting dipole sources, and skull thickness (Luck, 2005). However,

this null result may be influenced by many factors, including a lack of statistical power. Note that

at the traditional chromatic visual evoked potential (VEP) recording site, medial-occipital

electrode Oz, amplitude differences were also not found across groups: 0.85 µV (*SD* = 0.51 µV)

blue-black vs. 0.78 μV (*SD* = 0.51 μV) white-gold. Phase differences were also not significant at

the group level, and were not reliable for categorizing individual participants (note the

overlapping ranges in Figure 2.4C). The success of our decoding was thus possible only because

we used high-density EEG.

Note that the performance of this decoding was determined using a binary split of

individuals into either white-gold or blue-black based on their descriptions of the dress, and was

thus based on how observers labeled the dress colors and not necessarily how they perceived

them. It has been shown that across observers there may be a continuum of saturation percepts

of the dress's color (Gegenfurtner et al., 2015; Witzel et al., 2017). Indeed, individual differences

in perceived saturation may have contributed to the wide variety of blue-yellow asymmetry

amplitudes in both perceptual groups (see Figure 2.5A). Such differences may be influenced by

the extent to which individuals interpret the lighting of the dress as direct or indirect, and thus

the extent to which they attribute the bluish tint to the surface or illuminant. As such the

differences across individuals may reflect relatively high-level visual inferences regarding

illumination, it has also been suggested that these differences may reflect differences in the

pattern of lighting observers are exposed to: early-rising "larks" vs. late-rising "owls" may have

different learned illumination priors. By this account late-risers are likely exposed to more

artificial, yellower light, and thus may tend to more frequently report perceiving the dress

(rather than the lighting) as blue (Wallisch, 2017; Lafer-Sousa & Conway, 2017).

Yet, despite the possible graded variation in the dress percepts, the fact that the

classifier could discriminate the two groups indicates that the neural signals carried sufficient

information about these categorical differences, or that there was at least a strong relation

between the percepts and the labels (e.g., so that those who described it as blue by and large

saw it as more blue). Categorical effects in perception of the dress have also been reported: approximately 9/10 individuals are satisfied by using the terms white-gold or blue-black to describe its colors (Lafter-Sousa, Hermann & Conway, 2015). Here, we hypothesize that a categorical interpretation of the dress as chromatic (blue) or achromatic (white), may lead to the blue-yellow alternation as either a chromatic-chromatic (perceived blue-yellow) or achromatic-chromatic (perceived white-yellow) asymmetry, which may differentially activate different sets of neural sources (as will be discussed in the follow section), leading to the reliable topographical differences across perceptual groups.

One test of this hypothesis was performed through our comparison of white-gold and blue-black observers' blue-yellow dress asymmetries to the green-red and gray-yellow dress asymmetries. We hypothesized that the topographies of blue-black observers' blue-yellow asymmetries would resemble those of green-red asymmetries, while the topographies of white-gold observers' blue-yellow asymmetries would resemble those of gray-yellow asymmetries. A topographical decoding analysis was applied across experiments, which was able to classify 90% of white-gold observers' blue-yellow asymmetries as more similar to gray-yellow than green-red, and 71% of blue-black observers as more similar to green-red than gray-yellow (both p's < .05; see Results).

To further test this hypothesis, we would predict that blue-black, but not white-gold observers, have larger blue-yellow asymmetry amplitudes than blue-black observers *relative* to their gray-yellow asymmetry amplitudes in Experiment 2. To follow up on this here, we performed an extra comparison of white-gold observers' responses, which revealed no significant differences with a small effect size between blue-yellow (M = 0.54 μV, SE = 0.126 μV) and gray-yellow asymmetries (M = 0.67 μV, SE = 0.158 μV), t_4 = 1.63, d = 0.40, p = .18 (two-

tailed, paired-sample). Conversely, the blue-black observers had a medium effect-size, significantly lower blue-yellow (M = 0.41 μV, SE = 0.103 μV) than gray-yellow asymmetries (M = 0.65 μV, SE = 0.208 μV), t_8 = 2.30, d = 0.92, p = .025 (one-tailed, paired-sample), again consistent with a higher effective blue contrast in the blue-black observers. Note however that an interaction between perceptual group (blue-black and white-gold) and condition (blue-yellow and gray-yellow) could not be tested appropriately, due to the small number of participants per perceptual group in the second experiment (9 blue-black and 5 white-gold observers).

The lower accuracy for identifying blue-black observers as closer to green-red responses may be due to differences in the responses to each of these pairs of colors (akin to differences in blue and red EEG responses reported by Anllo-Vento, Luck & Hillyard, 1998). Differences in population-level responses to different colors may also be predicted by intracranial EEG and imaging studies (e.g., Brouwer & Heeger, 2009; Murphey, Yoshor & Beauchamp, 2008; Kuriki et al., 2011). Potential sources of these differences are discussed in the following section. Note that since roughly equal proportions of white-gold and blue-black observers were present in the green-red and gray-yellow groups (5/13 vs. 5/14, respectively, green-red and gray-yellow topographical differences were likely not driven by differences across white-gold or blue-black individuals.

Some differences in ocular anatomy and physiology have been reported across blue-black and white-gold observers of the dress (Rabin et al., 2016; Vemuri et al., 2016), and genetic factors have been estimated to account for about a third of the variation in the percept (Mahroo et al., 2017). Additionally, in our data, variability in the asymmetric modulations to green-red stimuli also occurs across observers, but is unlikely to be correlated with the (negligible) differences in the relative perceptual salience of the red and green hues. As noted, one previous

study investigating neural markers of perception of the dress found small group-level

differences in early-stage cortical processing (Rabin et al., 2016). Here, stimulus sets were

balanced for pre-cortical color signals, such that while other early-level processes might

contribute to the percepts, they are unlikely to be the primary factor. In contrast, another study

reported correlates of perception of the dress with late-stage frontal and parietal "higher

cognition" areas, such as those involved in attention or decision making (Schlaffke et al., 2015).

While it is possible that these "post-perceptual" factors play a role, our results point to neural

traces at stages that are likely both perceptual and high-level.

We attribute our asymmetry responses to perceptual rather than "higher cognition"

processing, because they are predominant over inferior occipito-parietal cortical areas

associated with visual responses. Moreover, these responses are elicited from participants naïve

to the experimental design and without a stimulus-related task, such that here is no incentive

for selective modulation of attention to either stimulus or for post-perceptual decision or task-

related processes. Finally, we attribute them to high-level perception because the pattern of

responses corresponds more closely to the observers' percepts than to the spectral sensitivities

of early color coding.

Potential sources of the EEG response asymmetries to color

Although we cannot target the specific sources of the neural asymmetries reported

here, we can hypothesize as to their origins (neural sources may be better identified in future

studies with the aid of spatially precise neuroimaging). Cortical responses to color extend from

early occipital visual areas along much of the ventral visiocortical stream. However, in terms of

perceptual correlates at a population-level, several studies have pointed to the importance of

more anterior, ventral occipito-temporal cortical (VOTC) regions. These areas were originally

implicated by studies of patients with damage to these areas presenting with achromatopsia or dyschromatopsia, i.e., complete or partial loss of color perception (e.g., Verrey, 1888; Meadows, 1974; Jaeger, Krastel & Braun, 1988; Zeki, 1990; Bouvier & Engel, 2006). The importance of VOTC regions in color coding, particularly the fusiform and lingual gyri, has been further supported by neuroimaging (e.g., Brouwer & Heeger, 2009; Goddard et al., 2011; Lueck et al., 1989; Zeki et al., 1991; Liu & Wandell, 2005; Mullen et al., 2007) and intracerebral EEG studies (Murphey, Yoshor & Beauchamp, 2008; Allison et al., 1993; see Conway & Tsao, 2009 for single-cell correspondence in macaques).

Asymmetries between color and grayscale images

Given the wealth of previous neuroimaging studies, we expected that achromatic vs. chromatic (gray-yellow, and white-gold observers' blue-yellow) response asymmetries would arise from a network of implicated color-sensitive visual regions, including the occipital lobe, dorsolateral occipital cortex, and areas of the ventral posterior fusiform and lingual gyri (e.g., Goddard et al., 2011; Lueck et al., 1989; Mullen et al., 2007; Sakai et al., 1995; Hadjikhani et al., 1998; Beauchamp et al., 1999). Such areas have also been associated with attention to color with neuroimaging (Corbetta et al., 1990; Corbetta et al., 1991), and of particular relevance here, EEG source localization (Anllo-Vento, Luck & Hillyard, 1998).

Here, these asymmetries presented maximally over medial ventral occipital channels (OIz, Iz, then Oz), and were similar to the response to stimulus presentation in general at 6 Hz and its harmonics (occurring maximally at OIz, Oz, then Iz) (see Figures 2.3C and 2.4B). Despite a slightly ventral shift in the response, this correspondence suggests a lack of specialized processing for these summed-harmonic 3-Hz asymmetries. Further, in a previous study of cerebral dyschromatopsia (in this case, lesions primarily to an extensive region of the bilateral

ventral occipito-temporal cortex), chromatic VEPs were unaffected at the single recording site

Oz (Crognale et al., 2013). This was taken as evidence that, at least at early response

components over this channel, the chromatic VEP was characterized by responses from early

visual areas. Similarly, macaques with lesions of a higher-level visual region (V4) also showed

preserved occipital chromatic VEPs, attributed to responses from early areas (V1 and V2)

(although these animals also showed preserved wavelength discrimination abilities; Kulikowski

et al., 1994). Taken together, we propose that the achromatic-chromatic asymmetries reported

here, maximal over ventral medial occipital channels, are driven by early visual processes.

Blue-yellow vs. green-red asymmetries

In contrast, the topography of the green-red asymmetries (and blue-black observers'

blue-yellow asymmetries, to a lesser extent) is maximal over a relatively more dorsal and

laterally translated (i.e., rightward) region of the scalp (see Figures 2.2C and 2.4B). In the green-

red contrast, the response was maximal over channels POO6, O2, then Oz, while in the blue-

yellow contrast for blue-black perceivers it was maximal at OIz, Oz, then O2. Both these

summed-harmonic 3-Hz responses, sensitive to the chromatic differences between paired

images, are spread more laterally across the occipito-parietal cortex than the summed-harmonic

6-Hz responses to stimulus presentation. Population-level differences in the responses to

numerous different colors have been reported with voxel-pattern classification throughout the

occipital lobe and ventral visual areas (e.g., Brouwer & Heeger, 2009; Kuriki et al., 2011; Parkes

et al., 2009). Supporting the perceptual relevance of such activation, responses in the fusiform

gyrus following fMRI-adaptation have been shown to correlate with perceptual color after-

images (Sakai et al., 1995; Hadjikhani et al., 1998). Moreover, electrical stimulation in human

participants in the posterior fusiform and lateral lingual gyri and dorsolateral occipital cortex

evoked color percepts (Allison et al., 1993; Schalk et al., 2017); further, in the fusiform gyrus, the

evoked percept matched the color preference of the stimulation site (Murphey, Yoshor &

Beauchamp, 2008). Thus, EEG asymmetries to different color pairs may have their primary

sources in the posterior fusiform gyrus (where EEG sources were modeled by Anllo-Vento, Luck

& Hillyard, 1998), with additional inputs from the lateral lingual gyrus, dorsolateral occipital

cortex, and more general (early) visual areas.

The shift in the maximal response towards the occipito-parietal cortex is in line with an

increased contribution of more specialized visual areas. For example, differences in responses to

the "unique hues" were reported by (Forder et al., 2017) in a late EEG response component

including more dorsal channels (P1, Pz, and P2), and an effect of language categories on

discriminating light vs. dark blue in Greek speakers was reported over occipito-parietal channels

(Thierry et al., 2009). In our case, the differences in responses between blue-black and white-

gold observers cannot be driven by stimulus attributes, lending support to chromatic VEPs being

capable of reflecting perceptual aspects of color vision, particularly over regions of the ocipito-

parietal cortex extending beyond the posterior midline and traditional Oz recording site.

Applying the FPVS approach to high-order color perception: strengths and limitations

The present results provide another illustration of the power and sensitivity of the FPVS

method for characterizing visual processes (Norcia et al., 2015). First, the blue-yellow

comparison replicated extremely well across entirely different groups of 14 participants. In both

experiments, its amplitude was close to 0.45 µV (0.44 µV in Experiment 1 and 0.46 µV in

Experiment 2). The response was maximal at the same two channels, Oz and OIz across

experiments, and had a similar phase of about 236 deg (237 deg in Experiment 1 and 235 deg in

Experiment 2). Furthermore, by using high-density EEG and inspection of amplitude, phase, and

topography response attributes, the approach was highly sensitive to differences in the neural responses to our paired images. This demonstrates the use of FPVS-EEG for providing high-order color-selective neural responses. Another advantage of this paradigm is that we were able to obtain these results with short SOAs (167 ms between images; a 333-ms repetition rate for each image) and without a stimulus-related task.

With our paradigm, a limitation was imposed by the presentation of stimuli in alternation at 6 Hz: we were not able to dissociate clearly the responses to each image within a testing sequence. Thus, we cannot say with certainty which way the response amplitude or latencies differed between blue and yellow, or the direction of this difference across blue-black or white-gold observers. Additionally, we chose not to use a current-source density (CSD) transform of our data in investigating the topographic responses. While CSD is reference-free and accounts for volume conductance contributions, it is less sensitive to electrophysiological sources deeper in the brain, and less reliable for electrodes at the border of the montage (Luck, 2005); however, the results of CSD-transformation on the topographies of the blue-black and white-gold participants was checked, and did not appreciably change the results (data not shown). Finally, a potential confound of our paradigm is that most observers are now highly familiar with the original image of the dress, so that the blue-yellow pairing modulated familiarity while both versions of the green-red pair were novel. However, the finding that the 3 Hz responses were strongest for the gray-yellow pair (again both novel), argues against this account.

A robust neural correlate for blue-yellow differences both within and across observers opens opportunities for exploring how these perceptual asymmetries emerge. As we have noted, the special ambiguity of blues may reflect experience with light and shading in the

natural environment. Developmental studies suggest that infants can begin to disambiguate

shadows by the age of about seven months (e.g., Granrud, Yonas & Opland, 1985; Sato,

Kanazawa & Yamaguchi, 2016). However, little is known about how or how long it takes children

to learn about the correlations between color and shading, and how this might influence their

color percepts. The paradigms we devised could be readily extended to track this development

and potentially reveal how infants might experience the colors in #thedress. More generally, our

results suggest that EEG responses to color, particularly those situated away from the occipital

midline, are reflective of perceptual experiences of color, and thus not attributable to early-

stage chromatic processing. Therefore, they underline the possibility of exploring perceptually

relevant system-level responses to color in the human brain.

2.6. Transition to Study 2

The study on the dress demonstrated neural correlates of perceptual phenomena, as measured

with high-density EEG and frequency-tagging. This study built on previously reported perceptual

phenomena from the Visual Perception Lab in particular (Winkler et al., 2015). Ultimately, we

aim to look forward to other perceptual phenomena. In Study 2, we will begin by taking a

foundational step, looking more precisely into the relationship between cone-opponent and

perceptual influences on these EEG responses. There were two specific hopes for Study 2: first,

that it might provide reference data, generalizable across participants, with which to predict

which color an observer is perceiving; and second, that it might demonstrate similar neural

responses to perceptually grouped color categories, overpowering retinally-driven inputs.

    In doing so, we will attempt to map differential response to different colors,

parametrically sampled in twelve steps around a cone-opponent color space, again applying

high-density EEG and frequency-tagging. As in Study 1, we will use a stimulus presentation rate

of 6 Hz, i.e., a stimulus-onset-asynchrony (SOA) of 167 ms. However, unlike in in Study 1, instead

of using a symmetry/asymmetry paradigm, we will present a target stimulus (e.g., blue) at a

lower proportion, 1 out of 6, of base stimuli (of other colors). Accordingly, target stimuli will be

tagged at: 6 Hz/6 = 1 Hz. This presentation paradigm allows for tracking target-selective

responses in the time-domain, similar to event-related potentials, after selectively filtering out

responses synchronized to the stimulus presentation rate and its harmonics (e.g., Retter &

Rossion, 2016). In exchange, it limits the interpretability of target stimulus phase: given the

complexity of the response over the large time window allotted (1 s SOA between target

stimuli), the response amplitude is not dominated by the first harmonic, but is distributed across

many harmonic frequencies. The temporal analysis here will thus focus on time-domain

responses, and in particular, their nuanced spatio-temporal dynamics.

Chapter 3

Study 2: Differential cortical responses to color depart from cone-opponent mechanisms

_____

Study 2: Differential cortical responses to color depart from cone-opponent mechanisms

Talia L. Retter, Fang Jiang, Bruno Rossion & Michael A. Webster

_____

3.1. Abstract

Dissociable electroencephalogram (EEG) responses to different colors have been reported, but a comprehensive mapping of these responses has not yet been produced. Such mapping would have theoretical contributions, illuminating whether variations in cortical responses to different colors are better explained through cone-opponent mechanisms or by higher-level perceptual influences. Such mapping would also have practical contributions, enabling a reference for whether a response is specific to an associated color, and potentially enabling the decoding of which color an observer is looking at. Here, we measured color-specific responses to 12 different hue angles, parametrically sampled at 30° steps around a cone-opponent color space. Stimuli were presented at 6 Hz; within each sequence, 1 of the 12 target colors appeared periodically at 1 Hz within testing sequences containing five other non-periodically appearing colors. Color-specific responses to the target hue were recorded at 1 Hz and its unique harmonics with high-density EEG over occipito-parietal channels. These responses had similar amplitudes and scalp topographies. However, these color-specific responses appeared to differ in their spatiotemporal dynamics. Interestingly, the differences across different colors seemed to reflect perceptual color categories more than cone-opponent metrics. These results suggest that cortical responses to color are organized to be reflective of color perception, more than retinocortical inputs. Practically, they provide further evidence that the EEG responses to

different colors might be decoded across observers, particularly in the case of few and perceptually salient colors.

3.2. Introduction

A mapping of neural responses to different colors from the human brain has not yet been produced. However, there are many reasons to think that this would be possible, in light of what is known about the neurophysiological structure of responses to color throughout the human visual system (for reviews: Dacey, 2000; Gegenfurtner & Kiper, 2003; Solomon & Lennie, 2007; Conway, 2014; Lee, 2014; Johnson & Mullen, 2016; Shapley, 2019). If produced, such a mapping might lead to theoretical contributions, e.g., in illuminating the pathway through which color signals from retinal cone-opponent mechanisms are transformed into cortical activity relating more directly to our perceptual experience. Additionally, such a mapping would enable the decoding of the color at which an observer is looking, which has applications for brain-computer and brain-machine interfaces (e.g., Yang & Leung, 2013; Rasheed & Marini, 2015).

Neural responses to color have been measured in the human brain with neuroimaging, implicating the involvement of a network of occipital and ventral occipito-temporal visual areas (V1, V2, V3, V4v, VO, and more anterior regions of the fusiform gyrus; e.g., Lueck et al., 1989; Corbetta et al., 1990; 1991; Zeki et al., 1991; Martin et al., 1995; Engel, Zang, & Wandell, 1997; Hadjikhani et al., 1998; Beauchamp et al., 1999; Liu & Wandell, 2005; Mullen et al., 2007; Simmons et al., 2007; Wade et al., 2008; Brouwer & Heeger, 2009; Kurikie et al., 2015; Lafer-Sousa, Conway, & Kanwisher, 2016; Nsar, Polimeni, & Tootell, 2016). While neuroimaging has been used to decode responses to different colors, this typically relies on pattern classification analyses across voxels that requires training and testing within the same participant (Parkes et al., 2009; Brouwer & Heeger, 2009; Goddard et al., 2010; see also Kuriki et al., 2011, using an

adaptation paradigm). That is, there is not pattern of activity across voxels that is indicative of a response to a specific color that generalizes across individuals, preventing a useful cartographic description.

Neural responses to color have also been measured in humans with electrophysiological recordings, typically in the form of non-invasive electroencephalogram (EEG). Discriminable responses to different colors of light were reported in the earliest chromatic event-related potential (ERP) and frequency-tagging studies (Regan, 1966; Riggs & Sternheim, 1968). Such differences are readily interpretable in light of the difference in latency across retinal cone-opponent pathways (L *vs.* M and S *vs.* L/M), with S-cone stimulation lagging about 12 ms behind L and M cone stimulation (Lee et al., 2009). Indeed, S-cone isolating stimuli have been shown to produce ERPs with a lower amplitude and longer latency than L and M-cone isolating stimuli (Robson & Kulikowski, 1998; Rabbin et al., 1994; see also Kulikowski, Robson, & McKeefry, 1995). Furthermore, electrophysiological responses may be expected to be influenced from cortical areas in which the responses to color relate more to observers' perception than to cone-opponent mechanisms (e.g., Komatsu et al., 1992; Hadjikhani et al., 1998; Liu & Wandell, 2005; Murphey et al., 2008; Brouwer & Heeger, 2009; Conway & Tsao, 2009), predicting additional, non-linear differences in EEG responses.

One major limitation of previous EEG studies is that a single recording electrode in the mid-occipital cortex (Oz) has typically been used (e.g., Robson & Kulikowski, 1998; Rabbin et al., 1994; Kulikowski, Robson, & McKeefry, 1995; Gerth et al., 2003). A number of recent studies applying high-density EEG have shown responses to color that extend across the parietal and inferior-occipital cortices, likely carrying information from additional cortical sources (e.g., Anllo-Vento, Luck & Hillyard, 1998; Thierry et al., 2009; Forder et al., 2017). Here, we exploited the

spatio-temporal resolution of high-density EEG in an attempt to provide a cartography of human neural responses to color.

Specifically, we combined high-density EEG with a frequency-tagging paradigm, preserving temporal information (Rossion et al., 2015; Jacques, Retter, & Rossion, 2016; Retter & Rossion, 2016). We investigated twelve different colors, distributed evenly around a cone-opponent color space, for which the responses must be generalized across large changes in luminance and saturation, as well as discriminable from those to the other colors in the stimulation sequence.

3.3. Materials and Methods

Participants

Sixteen participants (18 – 32 years old; M = 24.2 years; SD = 4.15 years) were recruited from the University of Nevada, Reno, campus to participate in this experiment. Eleven identified as female, and five as male; 15 reported being right-handed, and one as left-handed. All participants reported normal color vision and normal or corrected-to-normal visual acuity. The participants gave signed, informed consent prior to experiment, which was approved by the University of Nevada, Reno's Institutional Review Board and conducted in accordance with the Code of Ethics of the World Medical Association (Declaration of Helsinki).

Stimuli

Twelve colors were chosen as stimuli for the experiment, selected from even sampling around a cone-opponent color space (**Figure 3.1A**). Each stimulus was composed of one color, in the form of circles with Guassian tapered edges. The color space used was a modified version of the MacLeod-Boynton chromaticity diagram, defined by a horizontal L-M axis and vertical S-L+M axis, and centered on a nominal gray value equivalent to the chromaticity of illuminant C (CIE

1931 x,y = 0.310, 0.316), and scaled to roughly equate suprathreshold sensitivity along the cardinal axes.

The colors were sampled starting from 0 degrees in consistent 30 degree steps. Note that about half of these hue angles corresponded to colors typically described with basic color terms. Although there are great inter-individual differences, English-speaking observers generally employ basic color terms at the following hue angles of this color space (Webster et al., 2000; Emery et al., 2017): red: 0 degrees; purple: 60 and 90 degrees; blue: 150 degrees; green: 210 and 240 degrees; yellow: 300 degrees; and orange: 330 degrees. The other hue angles are typically described with combinations of these terms, e.g., blue-green: 180 degrees; yellow-green: 270 degrees.

This experiment aimed to isolate the chromatic dimension, apart from the influences of luminance and saturation. To this end, we introduced a wide range of variance in the stimuli (Thorpe et al., 1996; Rossion et al., 2015). Ultimately, each hue angle was represented with 18 stimuli, varying in three luminance levels, three saturation levels, and two spatial frequency levels of local luminance noise (**Figure 3.1B**). The mean luminance was varied in three steps between 28 and 50% of the monitor maximum; the mean saturation was likewise varied in three steps between 56 and 100% of the monitor maximum. Additionally, to control for inconsistencies across individuals and the visual field, such as caused by retinal inhomogeneities, luminance variation was added within each image in the form of blurred luminance checks (see Barbu, Harlow, & Plant, 1994; Regan, Reffin, & Mollon, 1994). These checks were sized at one of two spatial frequencies.
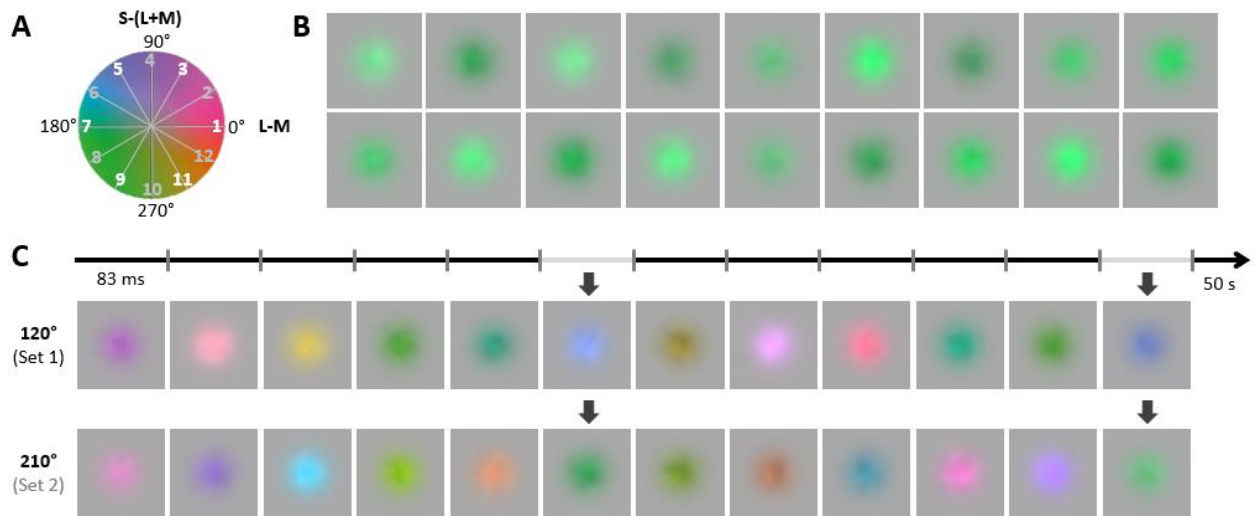
Figure 3.1. A) *The twelve hue angles used in the experiment were evenly sampled in 30 degree*

steps, starting from 0 degrees. ***B)*** *The range of variation in luminance, saturation, and local*

luminance noise, exemplified at one hue angle (210 degrees). ***C)*** *The experimental design,*

illustrated with two example hue angle conditions.

Experimental Design

Each color defined an experimental condition, such that there were 12 conditions in

total. To record specific responses to each color, we employed a categorization paradigm with

EEG and frequency-tagging (Rossion et al., 2015; Jacques, Retter, & Rossion, 2016). In this

design, stimuli are presented at a constant rate (here, 6 Hz), with a potential category of stimuli

presented as a fixed rate within this image stream (here, 1 Hz). Thus, the potential category-

selective response is expected at 1 Hz and its specific harmonics, while a general response to

image presentation is expected at 6 Hz and is specific harmonics. This category-selective

response relies on both the discrimination of this category from the other stimuli, as well as the

generalization across different exemplars defining the category. In the case where a category-

selective response is not produced, no significant response occurs at this frequency; in contrast,

as long as the participant is perceiving the visual stimuli, a significant does occur at the stimulus-presentation frequency (Rossion et al., 2015).

In this design, each of the 12 colors was presented as the potential category-selective stimulus in different 50-s testing sequences (**Figure 3.1C**). This stimulus appeared consistently at the 1 Hz rate, while the non-target stimuli appeared in a random order. So that the targeted color appeared the same number of times as the other colors throughout each testing sequence, the stimuli were broken into two sets of six, with the first set comprising 60 degree steps starting from 0 degrees, and the second set comprising 60 degree steps starting from 30 degrees. Thus, in each sequence, the target appeared as every one out of six stimuli, with all stimuli presented with equal frequency across the sequence. Participants were presented with four sequence repetitions for each condition, leading to a total of 3.3 minutes of recording per condition, and a total of about 40 minutes. The order of condition sequences was fully randomized for each participant.

Each trial began with 1 – 2 s of a centrally presented, gray fixation cross (with a luminance 80% of that of the background, to ensure continuous visibility), serving to orient attention, followed by 1 s of a gradual increase in stimulus contrast (fade-in), to avoid startle and abrupt eye movements. The 50-s testing sequence (the only part retained for subsequent analysis) was then following by 1 s of fade-out and another 1 – 2 s of the fixation cross. Throughout the trial, including during the fade-in and fade-out periods, stimuli were presented at 6 Hz, with a 50% squarewave duty cycle, such that upon each presentation cycle, stimuli appeared at full contrast for 83 ms, followed by the background screen alone for 83 ms. To reduce pixel-influenced responses (Dzhelyova & Rossion, 2014), as well as to increase variation in the spatial frequency of the local luminance noise, the size of each stimulus presentation

varied in five steps from 92 – 108%. The fixation cross remained superimposed on the colored

stimuli constantly throughout the trial.

Participants viewed the stimuli on a Display++ LCD with a 120 Hz screen refresh rate,

which was gamma-corrected based on calibrations obtained with a PhotoResearch PR655

spectroradiometer, and controlled by the stimulation computer running Windows. Participants

viewed the monitor from a distance of 80 cm, in a testing room illuminated only by the

stimulation and acquisition computer monitors. The mean luminance of the stimuli was

matched by the luminance of the gray background. Stimulus presentation was performed with

Java SE.

Task

Participants were instructed to attend to the colors during the sequences, while fixating

on the fixation cross. Their task was to press on a key (the space bar), each time it briefly (250

ms) changed shape into an open circle. This task was used to both reduce eye movements and

encourage sustained attention, while keeping participants naïve to the experimental

manipulation (e.g., as in previous studies with this paradigm: Rossion et al., 2015; Retter &

Rossion, 2016; Or, Retter, & Rossion, in press). Fixation cross shape changes occurred 8 times

per sequence, at random intervals constrained by a 500 ms minimum.

EEG acquisition

EEG data was recorded with a 128-channel BioSemi ActiveTwo EEG system, using Ag-

AgCl Active-electrodes (BioSemi B.V., Amsterdam, Netherlands). This system has default

electrode locations that are centered around nine standard 10/20 locations on the primary axes,

and for a reference uses a feedback loop of two additional channels positioned within the

headcap array (a common mode sense and driven right leg; for exact coordinates, see

http://www.biosemi.com/headcap.htm). The BioSemi labels were relabled to closely match those of a more conventional 10/5 system (Oostenveld & Praamstra, 2001; for exact relabeling, see Rossion et al., 2015, Figure S2). In addition, electrooculogram (EOG) signals were recorded with four flat-type Active-electrodes, located above and below the right eye and lateral to the external canthi. The offset of each electrode was help below 40 mV following setup with conductive gel, and the unfiltered recordings were registered at a sampling rate of 512 Hz.

EEG analysis: Preprocessing

Letswave 6, an open source toolbox (http://nocions.webnode.com/letswave), running over MATLAB R2018b (MathWorks, USA), was used to (pre)process the data. Filtering was performed through the application of a fourth-order, zero-phase Butterworth band-pass filter, cutting off frequencies below 0.1 Hz and above 100 Hz. Additionally, to extract contamination from electrical noise at 60 Hz, a fast-Fourier transform notch filter was applied at 60 and 120 Hz, with a width and slope of 0.2 Hz.

Correction for muscular artifacts related to eye blinks was performed through an independent-component analysis, removing a single component accounting for this activity, for participants who blinked more than 0.1 times/s. Correction for artifact-contaminated channels (those containing deflections beyond ±100 µV in two or more testing sequences) was performed through linear interpolation with 3-5 symmetrically-surrounding and directly neighboring channels. A maximum of six channels was interpolated this way per participant).

To complete preprocessing, data were re-referenced to the common average of the 128 EEG channels.

EEG analysis: Frequency-domain transform

The preprocessed, individual testing sequences were cropped in separate 50-s epochs. The testing sequences were then averaged in time by condition, to relatively emphasize activity phase-locked to the stimulus presentation. A discrete, fast Fourier transform (FFT) was then used to transform the amplitude of the data from the temporal frequency into the frequency domain, with a normalization for the number of samples output. The resulting spectrum had a range of 0-256 Hz, and a frequency resolution of 0.02 Hz.

EEG analysis: Harmonic frequencies-of-interest and region-of-interest (ROI)

Frequency-tagged responses are predicted at the stimulation frequency of each the color-specific (1 Hz) and the stimulus-presentation (6 Hz) responses. Further, responses are expected at the harmonic frequencies of these fundamental ($2f$, $3f$, etc.). The range of harmonic frequencies to consider depends on the temporal dynamics of the specific response (e.g., Retter & Rossion, 2016; Jacques, Retter, & Rossion, 2016). We used an *a-priori* range of harmonic frequencies from an earlier study on cortical color-specific responses with frequency tagging, from 1-30 Hz, excluding stimulus-presentation responses; for stimulus-presentation responses, we also used the previously defined range up to 42 Hz (Retter et al., 2017).

An occipito-parietal ROI was determined from the maximal color-specific channels across all conditions, quantified across harmonics from 1-30 Hz (see below): this consisted of 21 contiguous channels centered over the medial inferior-occipital cortex (see **Figure 3.3**). This ROI encapsulated all of the top 10 channels in every condition, and on average 87% (SD = 3.6%) of the maximal 21 channels across conditions. Note that this ROI was also used to verify the significance of the color-specific harmonic frequencies-of-interest: after the data were grand-averaged across all participants, at least two harmonics were consecutively significant only up to

30 Hz in two conditions (Z>2.32; p<.01; see, e.g., Retter & Rossion, 2016, for more details on this analysis).

EEG analysis: Quantification and statistics

To summarize the results of each condition for quantification and subsequent statistics, the harmonics-of-interest and ROI channels were collapsed. To this end, a sliding baseline-subtraction was applied across the frequency spectrum, with the baseline defined by the 20 surrounding frequency bins, once excluding the local minimum and maximum; the harmonics of interest were then summed (Retter & Rossion, 2016) and pooled across the channels of the ROI.

Statistical analyses were performed on the response amplitudes using a one-way repeated-measures analysis of variance (ANOVA), with the single factor of *condition* (with 12 levels).

3.4 Results

Frequency-domain analysis

Color-specific responses, frequency-tagged at 1 Hz and its unique harmonics, were present in all twelve color conditions (**Figure 3.2**). Again, these responses reflect discriminatory responses of the

periodically occurring color, in contrast to the responses to the other colors in the testing sequences, and generalized across large variations in saturation, luminance, and luminance contrast.
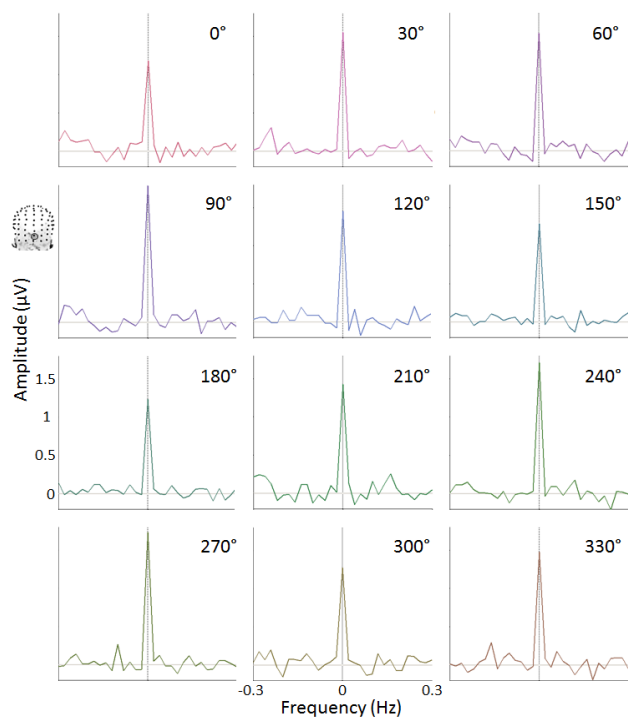
Figure 3.2. Frequency-domain spectra. Baseline-subtracted data at the color-selective response frequency summed across its unique harmonics (1 to 30 Hz), at electrode OIz. These frequencies-of-interest are centered at 0 Hz on the display, with the surrounding frequency bins shown for comparison; baseline noise level is 0 μV.
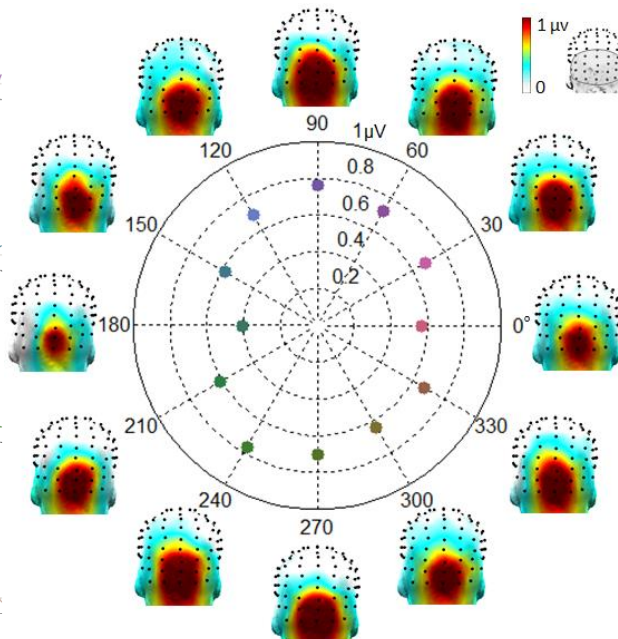
Figure 3.3. Amplitude and topography of summed-harmonic responses. Degrees on the polar plot represent hue angle, while the distance from the origin of each marker plot represents the amplitude for that hue condition at the occipito-parietal ROI as shown at the top right.

In all conditions, the color-specific responses were maximal over the medial-occipital cortex, peaking at channels OIz and Iz, but the responses diverged subtlety across conditions in their amplitude and spread within the occipito-pareital ROI (**Figure 3.3**; **Table 3.1A**). Quantified across this ROI, the response amplitude varied slightly across conditions, with the amplitude at 180° appearing the lowest, and the amplitude at 90° and 240° appearing the highest. A repeated-measured ANOVA with 12 levels of *condition* revealed a medium main effect, $F_{11} = 2.42$, $p = .008$, $\eta_p^2 = 0.14$. Removing the 180° condition was sufficient to abolish this effect: $F_{10} = 1.05$, $p = .40$, $\eta_p^2 = 0.07$. Overall, although color-specific responses could be recorded in the

frequency-domain EEG signal, these responses were not discriminable from one another in terms of amplitude.

Amplitude (SE)	0°	30°	60°	90°	120°	150°	180°	210°	240°	270°	300°
A) Color-specific	0.57 (0.10)	0.68 (0.11)	0.71 (0.09)	0.76 (0.11)	0.69 (0.11)	0.58 (0.12)	0.40 (0.10)	0.61 (0.11)	0.77 (0.11)	0.70 (0.14)	0.64 (0.12)
B) Stimulus-presentation	1.23 (0.20)	1.23 (0.22)	1.26 (0.26)	1.29 (0.23)	1.28 (0.24)	1.26 (0.23)	1.27 (0.25)	1.24 (0.24)	1.27 (0.25)	1.20 (0.23)	1.29 (0.24)

*Table 3.1. Amplitude (µV) of the color-specific (**A**) and stimulus-presentation (**B**) responses, baseline-corrected and summed across harmonics (1-30 Hz, and 6-42 Hz, respectively).*

In comparison, the stimulus-presentation responses did not differ in amplitude or topography across conditions (**Figure 3.4**; **Table 3.1B**). The 12 levels of *condition* did not generate an appreciable main effect of amplitude across the same occipito-parietal ROI, F_{11} = 0.47, p = .92, η_p^2 = 0.03.
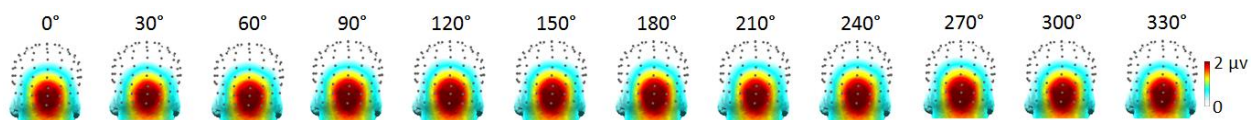
Figure 3.4. Stimulus-presentation summed-harmonic response topographies.

Time-domain analysis

Variations in the timecourse of the color-specific responses were evident over the occipito-parietal ROI. These responses were maximal over the medial occipital channels, where the timecourse of the responses varied across color conditions (**Figure 3. 5**). Interestingly, while

some conditions showed pronounced differences, others appeared highly similar. For example, conditions 240° and 270° were almost identical in timecourse, with a small positive peak at about 66 ms, a negative peak at 105 ms, a positive peak at about 193 ms, a negative peak at about 231 ms, and a small positive peak at about 265 ms (differences in peak latency across conditions ranging from 0 to 8 ms). In contrast, relative to these the condition at 150° was highly opposing in timecourse: there was a delayed onset with a positive peak first at 134 ms, a *negative* peak at 185 ms, a *positive* peak at 232 ms, and a *negative* peak at 269 ms.
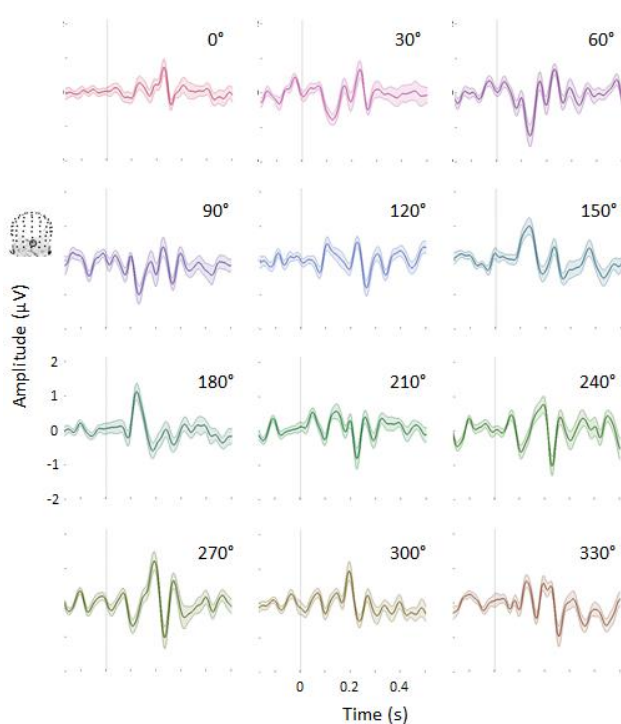
Figure 3.5. Time-domain response waveforms at electrode OIz.

The similarities and differences across conditions were more pronounced when investigated across the entire scalp, particularly the occipito-parietal channels (**Figure 3.6**). The responses spread across the occipito-parietal channels, sometimes with components peaking over the lateral parietal channels, e.g., at 175 ms in conditions of 90° (a negative response lateralized over the right parietal channels), and 330° (a positive response lateralized over both the right and left parietal channels).

In particular, some conditions showed highly similar response patterns: 30°, 60°, and 90°; 120° and 150°; and 210°, 240°, and 270°.
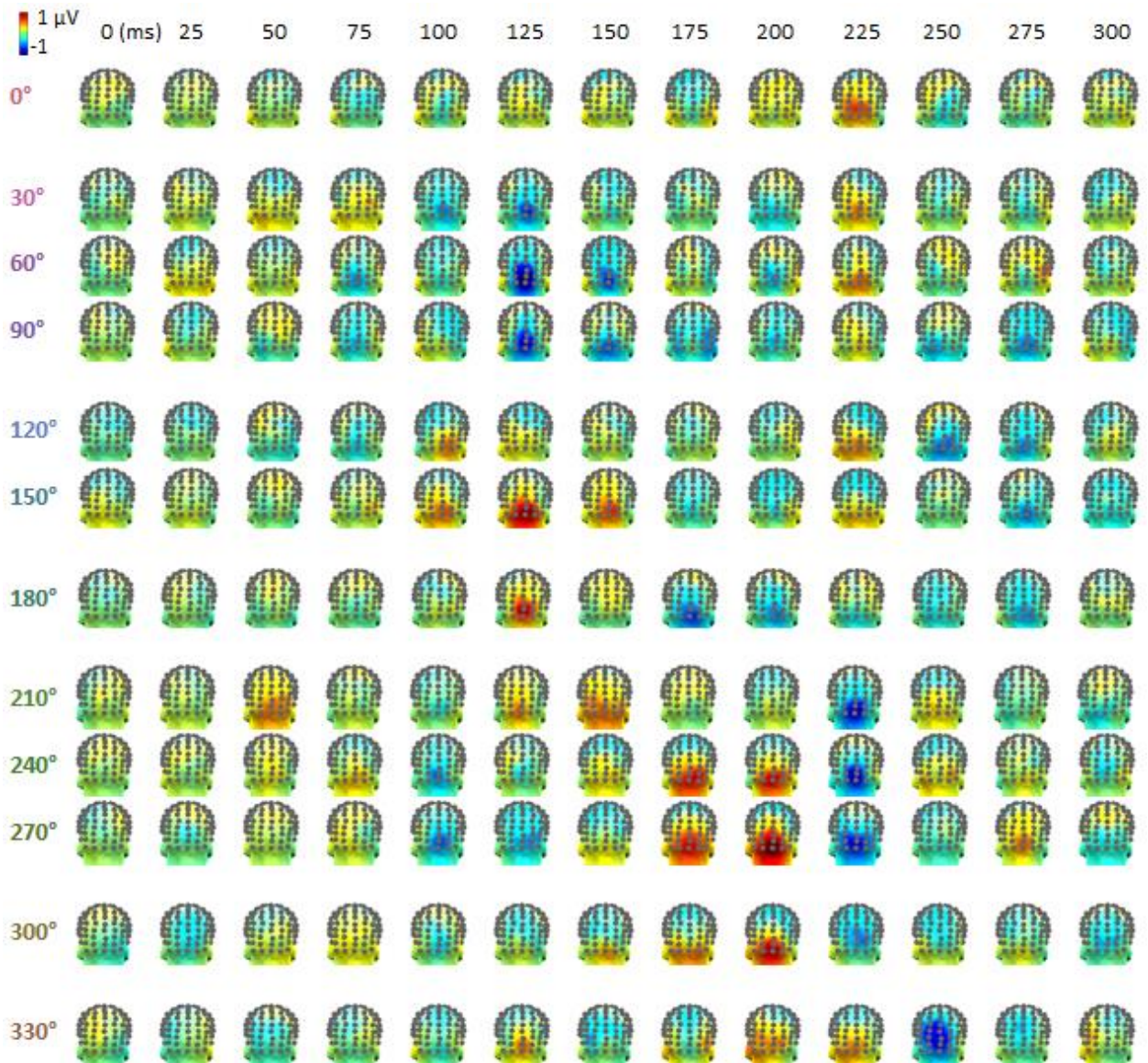
Figure 3.6. *Time-domain response topographies. Spacing between rows indicate a possible grouping of some conditions with similar response profiles, potentially corresponding to perceptual categories.*

3.5. Discussion

Specific response to different hue angles in the frequency-domain

We recorded color-specific response to every hue angle, indexed by the responses at 1 Hz and its unique harmonics. The color-specific responses were typically of similar amplitude and similar scalp topographies across hue angles.

The presence of color-specific EEG responses is in line with early EEG studies showing differentiable responses to different wavelengths of light (Regan, 1966; Riggs & Sternheim, 1968). In the study by Regan (1966), the different frequency-tuning of frequency-tagged responses to red, yellow, and blue light were characterized: differences were present in a frequency range from about 10-20 Hz; consistent with the present study, differences in amplitude across colors were not present below about 10 Hz. In the study by Riggs & Sternheim (1968), simultaneous electroretinogram and EEG were recorded, and cortical responses were shown to sometimes be more sensitive than retinal responses to some small changes in wavelength, suggesting a transformation of retinal signals by the time of cortical processing. Note that these studies used on a few recording electrodes, and did not investigate the spatial attributes of the responses.

In terms of scalp topographies, to our knowledge this is the first study to extensively characterize the spatial attributes of responses on the scalp with high-density EEG. However, previous studies have descriptively reported asymmetries in the topography of responses to paired colors: red and blue: Anllo-Vento, Luck & Hillyard, 1998; red and green: Retter et al., 2017; blue and yellow: Retter et al., 2017). One reason the response topographies may not have been highly distinctive here is that each target hue angle was compared to five other hue angles in each testing sequence, such that the differential response produced was in broad competition. Another possibility is that the responses recorded here to different hue angles are

produced by a common set of neural sources, or at least, from neural populations that are not spatially dissociable on the scalp.

Thus, although these responses indicated distinct responses to different colors, they were not readily dissociable from each other. The one exception was at 180°, wherein the amplitude of the response was weaker than for the other conditions. One possible explanation of this effect is that this color is ambiguous in that it contains equal amounts of blue and green (Webster et al., 2000; Emery et al., 2017a). Perhaps in the experimental conditions used here, in which the order of the non-periodic colors was fully randomized in each sequence, the 180° hue was sometimes perceived as green, and sometimes perceived as blue, based on the preceding (and/or following) color. For example, when following 120°, the 180° hue might appear green, and when following 240°, the 180° hue might appear blue. Given the opposing responses produced when a color is perceived as blue or green (i.e., the responses at 150° and 210°), this could account for a competition across different categorical perceptions, which could reduce the neural response amplitudes (e.g., Keysers & Perret, 2002; Retter & Rossion, 2016). Alternatively, this hue could be consistently perceived as blue-green, and produce a lower neural amplitude for another, unknown reason.

Again, the responses recorded here likely isolate differences in hue, rather than differences in luminance and saturation, given that there were large variations in these latter parameters at every stimulus presentation. Additionally, stimuli were presented with local luminance noise at variable spatial frequencies at each stimulus presentation, to further control for variations in luminance perception across the visual field (e.g., Barbur, Harlow, & Plant, 1994; Regan, Reffin, & Mollon, 1994). More generally, it may be noted that this frequency-tagging EEG paradigm has been validated to produce selective responses though a number of

previous studies, which have shown that the generated responses are, e.g., category-specific, unexplained by low-level image properties (at least with the image sets tested), and immune to temporal predictability (Rossion et al., 2015; Jacques, Retter, & Rossion, 2016; Quek & Rossion, 2017).

Spatiotemporal EEG responses cluster by perceptual color category rather than by cone-opponent mechanisms

The responses that appeared similar to spatiotemporal dynamics were colors that are typically given the same color terms across observers (Webster et al., 2000; Emery et al., 2017a; Emery et al., 2017b). Although there is not perfect agreement in the color spaces used, this previous data may provide some insights into the way that these colors are categorized perceptually. Starting at the 0° position and moving counterclockwise: at 0°, individual observers are in nearly full agreement that this color is termed red. Purple is typically used from 30° to 120°: individual observers are in strong agreement at 60° and 90°, and less so at 30° and 120°, sometimes calling these last hues red and blue, respectively. Blue is used in between 120° and 150°, more consistently closer to 150°. Blue-green is the description given at 180°, with high agreement across observers. Green usually spans from 210° to 270°, with the former sometimes being called blue-green, and the latter sometimes called yellow-green. Yellow is used at 300°; and orange at 330°. Note that these color terms are given with time in between stimulus presentations and unlimited time for hue scaling; here, the relative order of stimuli presented in rapid sequences likely also has a considerable influence on the perception of the color category perceived.

These color names correspond well with the apparent grouping of spatiotemporal EEG responses across colors. Some responses seemed markedly different at similar hue angle steps

with different color names: e.g., positive medial-occipital responses at 150° (typically called

blue) and negative responses at 90° (typically called purple), at 125 ms, In comparison, an

equidistant color from 90° also called purple, at 30°, also showed a negative response at 125 ms.

More generally, colors appeared to be grouped across adjacent hue angles in ways that are

credible with perceptual groupings: distinct spatiotemporal responses separated 0° and 30°, but

similar responses occurred from 30° to 90°, in a range which hues may be perceived as purple.

Similar responses were also seen at 120°-150°, which may be perceived as blue; and similar

responses occurred from 210°-270°, which may be perceived as green. While these findings

require more investigation, if reliable they would provide evidence for neural correlates of

categorical perception of colors.

It may have been that the differences in the spatiotemporal responses were driven by

the parametric differences in hue angle, defined according to cone-opponent mechanisms: this

does not appear to be the case. Responses at the opposite ends of the cardinal cone-opponent

pathways are not more different than responses at other intermediate hue angle contrasts. For

example, responses at orthogonal cone-opponent axes are also not particularly pronounced:

responses at 0° and 270° are not more different than those at 150° and 240°. This is surprising,

given that previous studies have reliably reported lower amplitude and longer latency for S-cone

than L and M-cone isolating stimuli (Rabbin et al., 1994; Kulikowski, Robson, & McKeefry, 1996;

Robson & Kulikowski, 1998). However, one possible explanation for this difference is that

previous studies have relied on grating stimuli, in which both ends of the opponent axis are

represented in alternate stripes. Accordingly, it may be that stimuli along the LM-axis may be

more similar and at earlier time points (both producing a medial-occipital negativity around 75

ms; see Figure 3.6) than along the S-axis (a medial-occipital negativity around 75 ms for 90°, but

a positivity at this time for 270°). Thus, it may be that grating stimuli presenting two colors at once are not optimal for targeting color-specific response.

Overall, these responses thus appear to reflect higher-level perceptual responses than early-level, retino-cortical inputs. This is in line with previous studies reporting perceptually-defined responses to colors, typically in higher-level visual areas (e.g., Komatsu et al., 1992; Hadjikhani et al., 1998; Liu & Wandell, 2005; Murphey et al., 2008; Brouwer & Heeger, 2009; Conway & Tsao, 2009). It is possible that a concert of neural areas collectively contribute to the neural responses recorded here, first at a global network level, such that from the onset responses are perceptual and category-selective.

Implications for decoding color-specific responses across observers

Again, early EEG studies on color reported differences in neural responses as a function of wavelength (Regan, 1966; Riggs & Sternheim, 1968). However, these responses were not generalized across individuals, and in later studies the interest appeared to be placed more in discriminating responses within individual participants, and typically by means of functional neuroimaging (e.g., Parkes et al., 2009; Brouwer & Heeger, 2009; Goddard et al., 2010; Kuriki et al., 2011).

Here, we hypothesized that selective responses to different colors would be predicted from the neurophysiological structures of early, retinal and lateral geniculate nucleus, responses to color, such as the delay of the S *vs.* L-M pathway, and delay of the +S *vs.* −S signals (e.g., Dacey, 2000; Gegenfurtner & Kiper, 2003; Solomon & Lennie, 2007; Conway, 2014; Lee, 2014; Johnson & Mullen, 2016; Shapley, 2019). However, the responses we recorded did not seem to reflect the characteristics of these early color-responsive mechanisms. There were no pronounced differences in the latency of color-specific responses along these pathways: the −S

responses at 270° did not appear to be of longer latency than the +S responses at 90°; and the S-axis generally did not appear to be delayed relative to the LM axis (see again Figures 3.5 and 3.6). Instead, as discussed above, the distinctness of the color-specific responses appeared to be a function of the perceptual categorization of the differing hues (Figure 6). While an influence of the latter aspect was predicted, its dominance on the EEG signal is nevertheless surprising.

Whether these responses can be used to reliably decode to the color at which an observer is looking remains an open question, which could be investigated here with additional analyses. However, our data provide promising evidence to suggest that it should be possible, even across observers. This would pave the way for future studies on color perception, and also applications for brain-machine interfaces, using the perceived color as a decodable input signal (e.g., fixating on a green arrow to proceed to the next screen). Such a decoding may be strengthened by the use of high-density EEG recordings, at least providing some parietal in addition to occipital coverage (e.g., see also Anllo-Vento, Luck & Hillyard, 1998; Retter et al., 2017). Moreover, our data suggest that decoding specific colors may only be possible if the colors are perceptually distinctive, and even better, categorically distinctive.

3.6. Transition to Study 3

Here, we showed differentiable responses to different colors, which is not a novel finding, but one that lacked exploration since its earliest reports (Regan, 1966; Riggs & Sternheim, 1968). We were able to use high-density EEG and more sophisticated analyses to explore the spatiotemporal dynamics of these responses within a frequency-tagging paradigm. This provided a closer look into the ways in which these EEG responses depart from cone-opponent mechanisms, sometimes producing extremely little influence when two or more colors fell within the same perceptual color category.

In Study 3, we will push the testing of the perceptual nature of these EEG responses even further: we will examine whether neural correlates to a certain color can be produced, even in the absence of a color stimulus. To this extent, we will again make use of "memory color", i.e., color associations with familiar objects, such as yellow with bananas, again with high-density EEG and frequency-tagging. We predicted that we would be able to frequency-tag the responses to periodically appearing grayscale objects with the same color association (*vs.* grayscale objects of non-periodic color associations). In this event, we would be able to further explore the spatiotemporal dynamics of responses to implied *vs.* actual color, and again further probe the influences of perceptual interpretation *vs.* physical stimulus properties.

Compared to the design of the previous experiments, we will use a slower stimulation frequency, 4 Hz, to ensure time for recognizing and developing responses to each object (250 ms SOA). Despite this, we will continue to present a target image at 1 Hz, here requiring a 1/4 target *vs.* base stimulus proportion, with three different colors of base stimuli so that each color appears equally as often throughout the each testing sequence. Again, this design will enable investigating responses in the time domain, although potentially with more interference from the general visual stimulation response, given the increased overlap of target and base stimulus harmonic frequency responses. Importantly, such a potential distortion would be equal in both grayscale and color conditions, so that the validity of this comparison will be maintained in investigating the spatiotemporal dynamics of implied and actual color responses.

It may be noted that across these three studies, the spatial frequency content of the images will have varied enormously: from a natural, rectangular image of the dress in Study 1, to circular color patches in Study 2 (with some blurred luminance checks proving a small amount of local contrast), and finally to segmented images or drawings of objects in Study 3. The retino-

cortical cone-opponent pathways have differing spatial frequency tuning, affecting their EEG

amplitudes and latencies: while both pathways generate EEG amplitudes peaking at about 1-2

cycles per degree of visual angle, the L *vs.* M pathway remains more sensitive to higher spatial

frequencies than the +S *vs.* -S pathway (e.g., Rabin et al., 1994). It is thus possible that spatial

frequency content affects the EEG responses, although cone-opponent processes did not appear

to dominate the chromatic EEG signals recorded in Study 2. In future studies, the spatial

frequency content could be more precisely manipulated, such that its impact – or lack of impact

– on high-level color perception might be investigated. One consistent aspect of spatial

processing on color perception across these studies, however, is eccentricity: all images were

presented centrally around fixation, given that color perception is optimal in the foveal region

due to its having the highest density and most regulated packing structure of cones (e.g.,

Brainard, 2015), and EEG responses to foveal chromatic stimuli produce the largest amplitudes

and signal-to-noise ratios (Gerth et al., 2003).

Chapter 4

Study 3: Early and automatic activation of color memory in visual object recognition

_____

Study 3: Early and automatic activation of color memory in visual object recognition

Talia L. Retter, Yi Gao, Bruno Rossion, Fang Jiang & Michael A. Webster

---

4.1. Abstract

Natural or man-made objects of the visual environment can be associated with specific colors, e.g., red strawberries or yellow rubber ducks, but how color and shape are related in the visual representation of objects remains uncertain. We tested 16 observers with a frequency-tagging paradigm capturing color-specific responses with high-density electroencephalogram (EEG). Different object images were presented in 50-s sequences at a rate of 4 Hz, with a characteristically yellow object appearing as every fourth stimulus, i.e., at a rate of 1 Hz. The object stimuli consisted of twenty-four images distributed across four color categories (yellow, red, green, and blue) and matched across hues for the type of object (e.g., fruits/vegetables and cartoon characters). In addition to a generic visual response to the objects at the stimulus-presentation rate of 4 Hz and harmonics, large color-selective neural responses at 1 Hz and harmonics were also observed over the parieto-occipital cortex. Critically, grayscale versions of the objects, equated for size, luminance, and luminance contrast with the colorized objects, also elicited a 1 Hz response, suggesting an automatic activation of color-selective neural activity. This yellow-selective response to the grayscale images averaged 63% of the response to actual colored objects, was reliable at the individual participant level, and had a similar but more lateralized occipito-parietal scalp topography. Color-selective responses emerged at the same post-yellow stimulus onset latency in both conditions, with the colored stimuli eliciting a larger response at a later time (approximately 140-230 ms). These observations suggest that the

neural responses to visual objects with characteristic color attributes automatically elicit the

associated color responses, suggesting a strong coupling of color and shape information in the

neural representations of prototypically colored objects. These results are in line with a

framework in which the visual world is initially perceived through associative recognition, with

additional physical details being incorporated later in time. objects in the visual cortex.

4.2. Introduction

Color and shape are fundamental attributes of any visual stimulus, but how these attributes are

related within the visual system remains poorly understood. In this study we examined how

color and shape cues are bound in object recognition. Shape alone is frequently object-specific,

and in this case can be sufficient for visual object recognition (Grossberg and Mingolla, 1985;

Biedermann 1987; Biederman & Ju, 1988). While surface attributes, such as texture and color,

are often not object-specific, they nevertheless contribute substantially to this critical brain

function (Marr & Nishihara, 1978; Tanaka, Weiskopf, & Williams, 2001). In part, color may assist

recognition by providing cues to image segmentation and thus shape, as noted above. However,

color can also play a role by defining not only where the object is but also what it is. Thus,

objects shown in color are typically recognized faster and more accurately than when shown in

grayscale (Price & Humphreys, 1987; Markoff, 1972; Wurm et al., 1993; Humphrey et al., 1994;

Tanaka & Presnell, 1999; Nagai & Yokosawa, 2003; Therriault, Yaxley, & Zwaan, 2009; Rossion &

Pourtois, 2004; Bramao et al., 2011; Hagen et al., 2014; etc).

While color may contribute more to the recognition of structurally similar objects (e.g.,

objects with non-specific shapes, such as some citrus fruit) or when an object exemplar has an

atypical or degraded shape (Price & Humphreys, 1989; Wurm et al., 1993; Tanaka & Presnell,

1999), the object class benefiting the most from the presence of color is that for which objects

have a learned association with a specific color, so-called "color-diagnostic" objects (e.g., von

Helmholtz, 1867; Tanaka & Presnell, 1999; Naor-Raz, Tarr, & Kerseten, 2003; Rossion & Pourtois,

2004; for a meta-analysis: Bramao et al., 2011; etc). Such color-specific objects are present

across a variety of object types, including natural, artificial, living, non-living, and animated: e.g.,

blueberries (blue), lobsters (red), American dollar bills (green), and Pikachus (yellow; for further

examples of color-diagnostic objects, see Table 1 of Tanaka & Presnell, 1999; Appendix 1 of

Naor-Raz, Tarr, & Kersten, 2003; Appendix A of Nagai & Yokosawa, 2003; Appendix 5 of Rossion

& Pourtois, 2004; Fig. 3 of Witzel et al., 2011).

For these objects, the specific color/object association allows color to provide a

diagnostic cue for object recognition: when color-diagnostic objects are presented in

incongruent colors, i.e., any color other than their prototypical color, object recognition

performance is lower in terms of accuracy and/or response time relative to objects presented in

congruent color and, to a lesser extent, in grayscale (Price & Humphreys, 1987; Tanaka &

Presnell, 1999; Therriault, Yaxley, & Zwaan, 2009; Hagen et al., 2014; etc). Moreover, it may be

said that this association allows objects to provide a diagnostic cue for color perception: color

naming is less accurate and/or delayed for incongruent relative to congruent color-diagnostic

objects (Bruner & Postman, 1949; Ratner & McCarthy, 1990; Naor-Raz, Tarr, & Kerseten, 2003).

For these object s, color appears to be a defining property.

This suggests that the recognition of color-specific objects by shape alone would

automatically evoke their color associations. Indeed, the perception of color-specific objects

may be drawn towards the associated color of the object, i.e., the "memory color", particularly

when the presented color is categorically ambiguous, e.g., yellow-orange, or presented under

challenging viewing conditions (e.g., Duncker, 1939; Bruner & Postman, 1949; Mitterer & de

Ruiter, 2008; Vandenbroucke et al., 2016). Memory color effects have been further

demonstrated in work suggesting that grayscale object images can appear subtly tinged with

their characteristic hue (Hansen et al., 2006; Olkkonen, Hansen, & Gegenfurtner, 2008; Witzel et

al., 2011), and that chromatic afterimages of objects appear more vivid when corresponding to

their memory colors (Lupyan, 2015). Functional neuroimaging studies have reported that color-

associated grayscale objects activate discrete visual regions of the human brain relating to color

perception, including the fusiform gyrus (Martin et al., 1995; Simmons et al., 2007; Slotnik,

2009).   More recently, these findings have inspired the successful decoding of the implied color

of grayscale color-specific images with functional neuroimaging in visual regions or whole-brain

analyses, even when subjects are performing orthogonal, i.e., non-color-related, tasks (Bannert

& Bartels, 2013; Vandenbroucke et al., 2016; Teichmann et al., 2018; 2019). However, these

studies have used only a few objects per color category (two: Bannert & Bartels, 2013; four:

Vandenbroucke et al., 2016), and have reported divergent results in terms of the cortical areas

responding to memory color (V1: Bannert & Bartels, 2013; V3, V4, VOI, LOC, and frontal areas:

Vandenbroucke et al., 2016). Yet, in light of these findings, it appears possible that color is

automatically incorporated into the visual representations of color-diagnostic objects .

However, how color and shape components of object representation are related, and in

what ways shape information might elicit an implied color response – as well as how that

response differs from the response to an actual color stimulus – remains unknown. In particular,

it is unclear at what stages of processing a specific implied color response might be elicited from

grayscale objects. Evidence has pointed to both a role for implied color in early (e.g., Price &

Humphreys, 1989; Naor-Raz, Tarr, & Kersten, 2003; Rossion & Pourtois, 2004; Lu et al., 2010;

Hagen et al., 2014; Teichmann et al., 2018) and later (e.g., Marr & Nishihara, 1978; Proverbio et

al., 2004; Therriault, Yaxley, & Zwaan, 2009; Proberbio et al., 2004; Teichmann et al., 2019) stages of object processing. However, evidence for these ideas has primarily been from behavioral studies, for which increased response times to grayscale or incongruent colors might be decisional rather than perceptual.

The few electro/magnetoencephalography (EEG and MEG, respectively) studies on this topic have produced inconsistent results. Teichmann et al. reported earlier color-specific responses to color than grayscale objects, based on the success of a multivariate pattern-analysis classifier trained on colored objects with full-brain MEG (2018), but failed to replicate this finding one year later (2019). Other studies have not reported any latency differences between event-related potentials (ERPs) evoked by color, grayscale, or incongruent color objects (Proverbio et al., 2004; Lu et al., 2010; Bramao et al., 2012b; Lloyd-Jones et al., 2012). In these studies, the latency of color memory effects has been inferred from the onset of amplitude differences across color vs. grayscale or congruent vs. incongruent color objects, but at the earliest components in some studies (Lu et al., 2010: N1 and later components decreased congruent color vs. grayscale/incongruent color; Bramao et al., 2012b: P1 and N1 increased color vs. grayscale), and only at later components in other studies (Provebio et al., 2004: N2 increased when attending to color for congruent vs. incongruent shapes; Lloyd-Jones et al., 2012: P2 and P3 decreased for congruent vs. incongruent color; Bramao et al., 2012b: N400 increased for diagnostic vs. non-diagnostic color). Additionally, these studies averaged across different color categories (e.g., averaging yellow, green, red, etc. object responses), despite evidence that the spatiotemporal dynamics of EEG responses to different colors can differ substantially (e.g., Regan, 1966; Riggs & Sternheim, 1968; Allison et al., 1993; Anllo-Vento, Luck & Hillyard, 1998).

In the present study, we quantify the magnitude and temporal dynamics of automatically evoked object-diagnostic color responses with a frequency-tagging EEG approach designed to isolate color-specific neural responses. First, we quantify the color-specific neural responses to prototypically colored objects, using frequency-tagging to isolate these responses from the generic responses to visual stimulation and from the effect of color on these generic responses. Second, using grayscale versions of these objects, we quantify the contribution of any implied color signal to this neural response . Finally, we compare the temporal dynamics in the neural responses to physical vs. implied color-specific responses. Our findings indicate that while the raw effect of color alone on visual object stimulation responses is relatively modest , color-diagnostic object shape alone can evoke substantial color-specific neural responses. Moreover, the implied color response emerges as early in time as the corresponding responses for actual colored objects, with the neural responses for the two types of stimuli diverging only later in time. These results are in line with a framework in which the visual world is initially perceived through associative recognition, with additional details being incorporated later in time.

4.3. Materials and Methods

Participants

Sixteen participants (18 - 35 years old; M = 24.5 years; SD = 5.27 years) took part in the experiment. Eleven identified as female, and five as male ; twelve as right-, and three as left-handed. All reported normal or corrected-to-normal visual acuity, as well as normal color vision . All participants gave signed, informed consent prior to participation. The study was conducted in accordance with the Code of Ethics of the World Medical Association (Declaration of Helsinki), and approved by the University of Nevada, Reno's Institutional Review Board.

Stimuli

Objects with a diagnostic color were chosen with considerations for color category and object type. Ultimately, 24 object images were selected, balanced for color category (red, green, blue, and yellow) and object type (fruit/vegetable, cartoon character, manmade, and animal), and controlled for low-level attributes (**Figure 4.1**).

In regards to color diagnosticity, we first selected images of 40 candidate objects, with reference to previous studies (Tanaka & Presnell, 1999; Naor-Raz, Tarr, & Kersten, 2003; Witzel et al., 2011). In an informal survey, we presented these images in grayscale to a room of 110 undergraduate students; participants were asked "what color do you think the item is?", and instructed to fill in a response sheet by circling the color that was mostly likely from the following list: red, orange, yellow, green, blue, purple, gray, and don't know. Diagnosticity of the color was assessed by the percent agreement across participants for the most frequent color selected. Objects with the highest color diagnosticity were selected while maintaining balance in color category and object type, resulting in a minimum of 93% color naming agreement on average within each color category (range: 93 to 96%).

The resulting stimuli of each color category consisted of two fruits/vegetables, two cartoon characters, one manmade object, and one animal. These include for red: strawberry, cherries, Elmo, Devil, fire extinguisher, and lobster; yellow: corn, banana, Pikachu, SpongeBob, star sticker, and rubber duck; green: broccoli, celery, Grinch, Shrek, dollar bill, and frog; blue: blueberries, eggplant, Cookie Monster, Smurf, mailbox, and whale. Note that the eggplant was actually named as purple, but was included in the blue set to match for object type. The object images were coarsely selected for similarity in visual appearance: for example, the cartoon

characters were restricted to two-dimensional renderings with similar postures, and the animals were all toy versions.

To control for low-level attributes, these objects were first isolated from their background, cropped to their external edges, and resized to a common rectangular area. A grayscale set of these images was created , and both the colored and grayscale set were equalized in terms of mean luminance and root mean-squared luminance contrast. The control for regularity in the colored images was tempered with consideration for preserving the natural object color characteristics, which may relate to typicality (e.g., that the yellow of Pickachu contains more orange than that of SpongeBob) and to preserve slight accent colors (e.g., the orange beak on the rubber duck, or the tan cookie of the Cookie Monster). To this extent, the mean hue angle of the images in a cone-opponent space was adjusted as follows: stimuli within each color category were ranked by hue angle, and this order was kept while restricting images to a 10 degree range of hue angle, with 2 degree spacing across images. For the different color categories, the mean hue angle was set to: 355 (red), 315 (yellow), 205 (green), and 135 (blue). The cone-opponent color space used was a modified version of the MacLeod-Boynton chromaticity diagram (defined by a horizontal L-M axis and vertical S-L+M axis), centered on a nominal gray value equivalent to the chromaticity of illuminant C (CIE 1931 x,y = 0.310, 0.316), and scaled to roughly equate threshold sensitivity along the cardinal axes (Winkler et al., 2015).
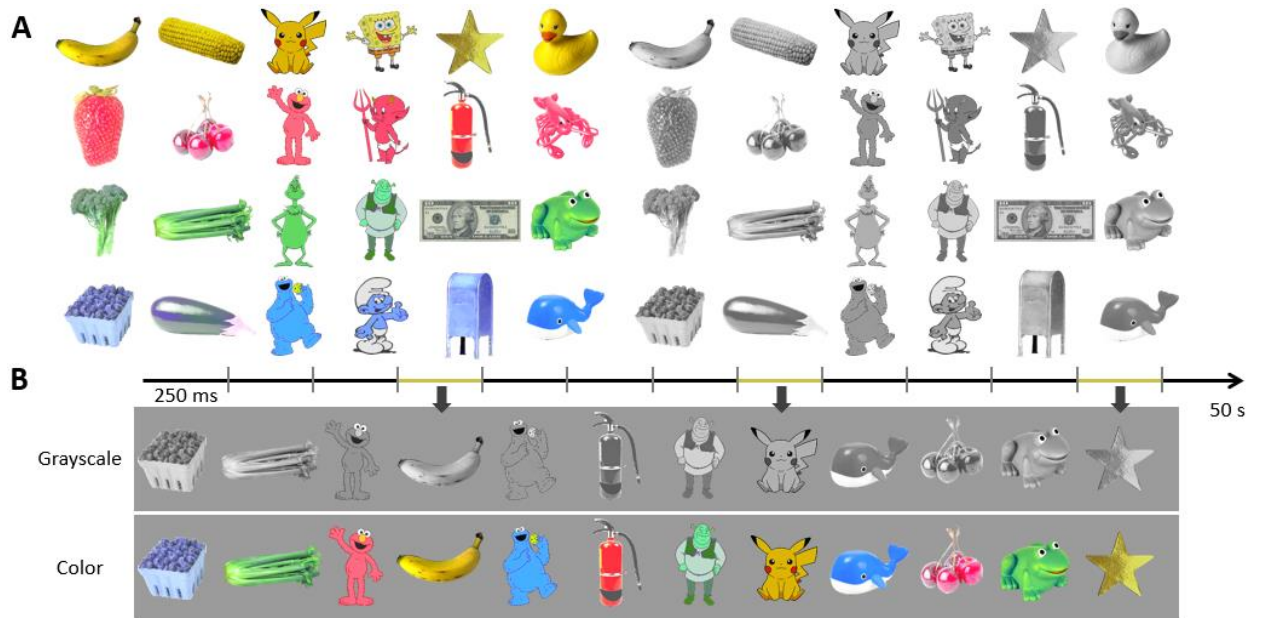
Figure 4.1. *Stimuli and experimental design.* **A)** *The 24 color-diagnostic stimuli use in the experiment, shown in color (left) and grayscale (right).* **B)** *The trial design is depicted for each the grayscale and color conditions. Stimuli were presented every 250 ms (at 4 Hz) in 50 s sequences, throughout which a diagnostically-yellow object appeared every 1 s, i.e., as every one out of four images. The order of the diagnostically-green, -red, and –blue images was fully randomized within every sequence for every participant.*

The grayscale images were also checked for higher-order image statistics, namely in terms of global contrast factor (Matkovic et al., 2005) and gist (spatial envelope; Oliva & Torralba, 2001). Global contrast factor reflects a contrast measure across a number of resolution levels that is thought to relate to perceptual contrast: this factor did not vary across images (GCF range: 13.83-14.73), $\chi^2 3 = 4.86$, $p = .18$ (Kruskal-Wallis H test, given the small number of images per category). Gist relates to visual spatial forms that can quickly and automatically be extracted from an image, and may be measured with spatial envelopes: differences in gist did not differ

across image categories (D range: 0.94-1.06), $F_{3,68} = 1.98$, $p = .13$, $\eta p2 = 0.08$ (one-way ANOVA including all paired cross-category differences for each image).

Experimental Design

There were two conditions in the experiment: color and grayscale. In the former, all images were presented in color, and in the latter, the same images were presented in grayscale. Participants were presented with four 50-s sequence repetitions for each condition, leading to a total of 3.3 minutes of recording per condition, and 6.7 minutes of recording overall. The conditions were presented in blocked order, counter-balanced across participants.

Throughout each sequence, stimuli were presented at a rate of 4 Hz, i.e., every 250 ms. With a 50% squarewave duty cycle, each image was displayed at full contrast for 125 ms, allowing for 125 ms of the gray background between successive images. Crucially, diagnostically-yellow images appeared every 1 s, at a rate of 1 Hz, within the sequence. The order of presentation of the other diagnostic colors was fully randomized within every sequence for every participant (**Figure 4.1B**). Thus, responses to diagnostically-yellow objects (i.e., color-specific responses) were expected at 1 Hz and its specific harmonics (2, 3, 5 Hz, etc.), while responses to object presentation in general were expected at 4 Hz and its harmonics. Yellow was chosen arbitrarily in the sense that any color might have been selected as the target; however, yellow has been shown to produce relatively large color-memory effects in previous studies (e.g., Hansen et al., 2006; Lee & Mather, 2019).

Participants progressed through trials at their own pace, in between which they had time to rest (close their eyes, make small movements, etc.). Upon commencement of each trial, the testing sequence was preceded by 1 – 2 s of a fixation cross, in order to orient attention and decrease exact expectation of image onset, followed by 1 s of gradual stimulus contrast increase

(fade-in), to avoid abrupt eye movements. Each sequence was followed by 1 s of fade-out and 1 – 2 s of the fixation cross, with similar logic and to delay movements upon trial completion. Only the 50-s testing sequence was retained for analysis.

The stimuli were presented on a gray background with a mean luminance of 213 cd/m2, equal to the mean luminance of the test images. The monitor was a Display++ LCD with a 120 Hz screen refresh rate, gamma-corrected based on calibrations obtained with a PhotoResearch PR655 spectroradiometer, and controlled by a standard PC. The monitor was viewed at a distance of 80 cm, such that the images subtended a mean width/length of 5.26 degrees of visual angle. To reduce size-specific responses, the size varied from 92-108% of the size of the original image in 4% steps at each image presentation (Dzhelyova & Rossion, 2014). Stimuli were presented with Java SE Version 8. Viewing was binocular and in a room illuminated only by the experimental and acquisition computer displays.

Task

Participants were instructed to attend to the images presented while fixating on a centrally presented fixation cross, which was present throughout the entire testing sequence, superimposed on the images. To encourage fixation and sustained attention, the participants' task was to press on a key (the space bar) each time they detected a brief shape change (250 ms) of the cross to an open circle. This occurred 8 times in each trial, at random intervals above a minimum of 500 ms. Participants were naïve to the experimental manipulation.

EEG acquisition

EEG was acquired with a 128-channel BioSemi ActiveTwo EEG system. This systems uses Ag-AgCl Active-electrodes, with default electrode locations centered around nine standard 10/20 locations on the primary axes, including a reference feedback loop constituted of two

additional channels (a common mode sense and driven right leg; BioSemi B.V., Amsterdam,

Netherlands; for exact coordinates, see http://www.biosemi.com/headcap.htm). The BioSemi

electrodes were relabeled to closely match those of the more conventional 10/5 system

(Oostenveld & Praamstra, 2001; for exact relabeling, see Rossion et al., 2015, Figure S2).

Additional electrooculogram (EOG) signals were recorded from four flat-type Active-electrodes,

positioned above and below the right eye and lateral to the external canthi. Following setup of

the EEG system (including insertion of a conductive gel), the offset of each electrode was held

below 40 mV. The unfiltered recordings were saved at a sampling rate of 512 Hz.

EEG analysis: Preprocessing

Data were (pre)processed with Letswave 6, an open source toolbox

(http://nocions.webnode.com/letswave), running over MATLAB R2013b (MathWorks, USA).

Data were filtered with a fourth-order, zero-phase Butterworth band-pass filter, with cutoff

values below 0.1 Hz and above 100 Hz; to remove contamination from electrical noise, a fast-

Fourier transform notch filter was also applied at 60 and 120 Hz, with a width and slope of 0.5

Hz. To correct for muscular artifacts related to eye-blinks, independent-component analysis was

applied to remove a single component accounting for blink activity in 6 participants, blinking

more than 0.2 times/s (across all participants: M = 0.16 blinks/s; SD = 0.15 blinks/s). To correct

for artifact-contaminated channels (containing deflections beyond ±100 μV in two or more

testing sequences), these channels were linearly interpolated with 3-5 symmetrically-

surrounding neighboring channels (six or fewer channels per participant; M = 3.4 channels).

After filtering and artifact correction, data were re-referenced to the common average of the

128 EEG channels.

EEG analysis: Frequency-domain transform

Preprocessed, individual sequences were isolated in separate 50-s epochs, and averaged

in time by condition, to selectively reduce activity not phase-locked to stimulus presentation.

These data were transformed into the frequency domain by means of a discrete Fast Fourier

Transform (FFT) for amplitude. This spectrum was normalized by the number of samples output;

it had a range of 0-256 Hz and a resolution of 0.02 Hz.

EEG analysis: Harmonic frequencies-of-interest

As mentioned previously, responses to diagnostically-yellow objects (i.e., yellow-

selective responses) are predicted at 1 Hz and its specific harmonics, while general responses to

visual object presentation are predicted at 4 Hz and its harmonics. While responses should occur

at harmonics beyond the fundamental frequency, they are expected within a limited range,

specific to the type of response occurring (e.g., Retter & Rossion, 2016; Jacques, Retter, &

Rossion, 2016).

In order to determine the frequency ranges of interest here, the signals were pooled

across all EEG channels and grand-averaged across participants. These data were then assessed

for significance at all harmonics of the fundamental yellow-selective and stimulus-presentation

responses for each condition, by means of Z-scores. Z-scores were calculated at each frequency

bin, x, with a local baseline defined by the 20 surrounding frequency bins (Z = (x - baseline

mean) / baseline standard deviation; e.g., Srinivasan et al., 1999; Retter & Rossion, 2016). The

maximal harmonic frequency range with contiguous significance (Z > 1.64; p<.05), exempting

one harmonic, in either condition was identified and used in subsequent analyses. For yellow-

selective responses, this range spanned 1 – 25 Hz. Note that harmonics coinciding with the

stimulus-presentation responses within this range were excluded. For the stimulus-presentation

responses, this range spanned 4 – 56 Hz. These criteria were relatively insensitive to threshold:

only one fewer yellow-selective harmonic would have been selected had a threshold of p<.01

been used.

EEG analysis: Region-of-interest (ROI) and subregions

A parieto-occipital ROI was defined post-hoc from the maximal activation across both

conditions. This ROI consisted of 24 channels, centered medially and extending symmetrically

across the left and right cortices. For the yellow-selective responses, averaged across

participants it encompassed 21 of the maximal 24 channels for both the grayscale and color

conditions; for the stimulus-presentation responses, it again encompassed 21 of the maximal 24

channels for the grayscale condition, and 22 for the color condition. For more specific response

localization, this ROI was further broken into three subregions (see Figure 4.2): the left (10

channels), middle (4 channels), and right (10 channels).

EEG analysis: Quantification and statistics

Responses were examined across all the EEG channels and harmonic frequencies of

interest; however, to summarize the results in quantification and statistical analyses, the

primary analyses focused on data collapsed across the ROI and subregions, and the relevant

frequencies-of-interest. Note that before harmonic responses were collapsed, a local baseline-

correction was applied (given the variable noise level across the frequency spectrum), in the

form of a baseline-subtraction. The baseline of each frequency bin, x, was defined by the 20

surrounding frequency bins, after excluding the local minimum and maximum (e.g., Rossion et

al., 2012; Retter & Rossion, 2016). Data were grand-average across participants for description

and display.

To statistically compare the responses across conditions at the occipito-parietal ROI,

one-tailed, paired-sample t-tests were performed across individual participants, with the

prediction that larger amplitude responses would be produced in the color than grayscale condition. To compare responses across conditions across the ROI subregions, a two-way repeated-measures analysis of variance (ANOVA) was performed, with factors of Condition (two levels: grayscale and color) and Subregion (three levels: left, medial, and right). In the case that Mauchly's test of sphericity was violated, a Greenhouse-Geisser correction was applied.

EEG analysis: Time domain

Data were analyzed in parallel in the time domain, following preprocessing (e.g., as in Rossion et al., 2012; Retter & Rossion, 2016; Jacques, Retter, & Rossion, 2016). To this extent, the data were first low-pass filtered with a fourth-order Butterworth filter at 30 Hz. In one case, to isolate the yellow-diagnostic object responses, the stimulus-presentation responses were selectively removed through a frequency-domain notch filter, applied at all the harmonics of 4 Hz below 30 Hz, with a width and slope of 0.02 Hz. The data were cropped in separate segments for each yellow-diagnostic object presentation, from 250 ms prior- and 750 ms post-stimulus onset. The cropped data segments were baseline-corrected by subtracting the average amplitude in the 250 ms preceding stimulus onset, a time window corresponding to one stimulus-presentation cycle. To avoid contamination from eye movements, data segments containing deflections of ± 125 μV in any EOG channel were rejected. Data segments were then averaged by condition. To determine when yellow-diagnostic response deflections significantly differed from baseline (0 μV), independent t-tests against zero were performed at every time bin from stimulus onset to 750 ms post-stimulus onset; to reduce the chance of false-positive due to the high number of comparisons, a conservative threshold of p<.01 was selected, and consecutively criteria of 15 ms (9 consecutive sampling bins) was applied. Similarly, paired-

sampled t-tests were applied to determine when the responses from the two conditions differed from each other. For description and display, data were grand-averaged across participants.

4.4. Results

Responses to visual stimulus presentation, frequency-tagged at 4 Hz and its harmonics, were of high amplitude and were significant up to 56 Hz. Most importantly, responses to yellow-diagnostic objects, frequency-tagged at 1 Hz and its specific harmonics, were apparent in the frequency-domain amplitude spectrum over the occipito-parietal ROI at the group level (i.e., pooled across individual participants) for both color and grayscale conditions (**Figure 4.2A**). These responses were significantly greater than noise at harmonic frequencies up to 25 Hz (see Methods). To describe the complete responses, these multi-harmonic responses were baseline-subtracted and summed (Retter & Rossion, 2016).

The responses to stimulus presentation were 4.35 µV (SE = 0.481 µV) for color stimuli and 3.81 µV (SE = 0.360 µV) for grayscale stimuli over the occipito-pareital ROI. This relatively small increase, of less than 15%, was nevertheless statistically significant, $t15 = 1.75$, $d = 1=0.32$, $r = 0.16$, $p = .012$. Over the same ROI, the amplitude of the response specific to yellow-diagnostic objects (**Figure 4.2B**) in the color condition was of 1.13 µV (SE = 0.098 µV). Strikingly, a response specific to yellow-diagnostic objects of 0.71 µV (SE = 0.059 µV) was elicited in the grayscale condition, about 63% of the response to colorized objects. The amplitude difference between the responses in the color and grayscale conditions was statistically significant, $t15 = 4.22$, $d = 1.29$, $r = 0.54$, $p = .0004$.

While half the participants saw the grayscale sequences first, and the other half of partiipcants saw the actual color sequences first, there was no significant order effect on the stimulus presentation responses over the occipito-parietal ROI (color *vs.* grayscale difference for

grayscale first: 0.61 µV (SE = 0.23 µV); color first: 0.48 µV (SE = 0.39 µV), t_7 = 0.22, p = .84, two-tailed). Moreover, there was also no order effect on the yellow-specific response amplitudes over the occipito-parietal ROI (color *vs.* grayscale difference for grayscale first: 0.28 µV (SE = 0.11 µV); color first: 0.56 µV (SE = 0.15 µV), t_7 = -1.29, p = .24, two-tailed). The trend was for observers of grayscale sequences first to have a smaller difference between grayscale and color responses, opposite to the potential expectation that recent exposure to these objects strengthens their color associations.
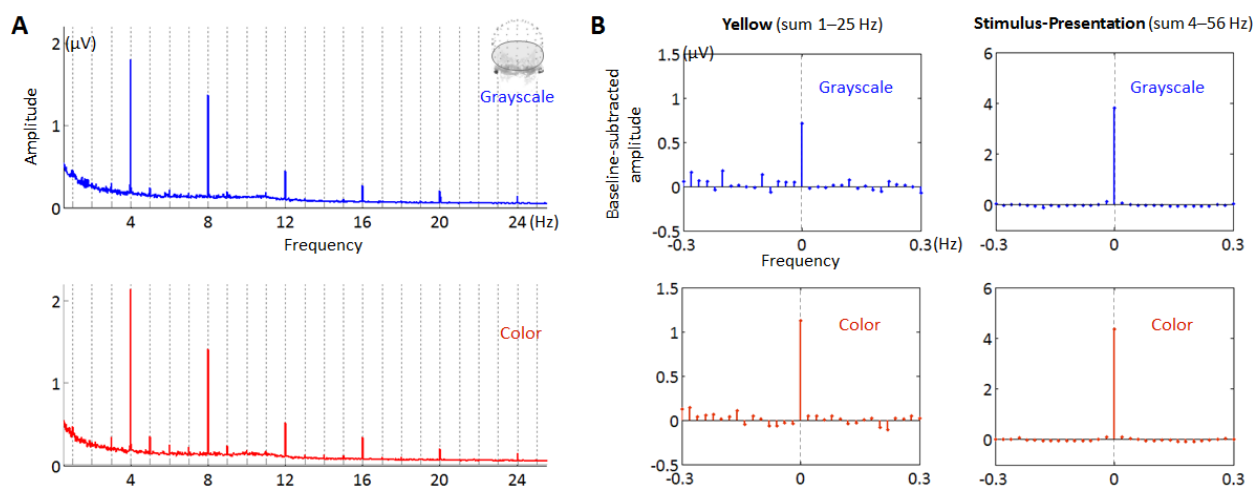
Figure 4.2. EEG responses in the frequency-domain. *A) The frequency-domain amplitude spectra for the grayscale and color conditions, plotted over the occipito-parietal ROI. Dotted vertical lines indicate the position of 1 Hz and its harmonics. B) Summed baseline-subtracted harmonic responses: the frequency-of-interest and its harmonics are combined and plotted at the 0 Hz position, with the surrounding frequency bins included in the display for comparison; noise level is at 0 µV.*

For a more detailed spatial investigation of these responses, the scalp topographies were plotted (**Figure 4.3A**) and the single occipito-parietal ROI was decomposed into its left, right, and medial subregions (**Figure 4.3B**). Visualization and analyses of these subregions

revealed that the yellow-diagnostic object amplitude difference was most pronounced over the middle occipital channels. The increase for this response in the color relative the grayscale condition was 88% over the middle subregion, compared to 52-54% over the left and right subregions. These differences held up in a repeated-measures ANOVA, with factors of condition and subregion, which yielded a moderate interaction between these factors, $F_{2,30} = 4.03$, $p = .042$, $\eta p2 = 0.37$. Note that the main effect of this ANOVA replicated the large difference of condition, $F_{1,15} = 18.7$, $p = .001$, $\eta p2 = 0.56$; the main effect of subregion was not robust, $F_{2,30} = 2.96$, $p = .084$, $\eta p2 = 0.30$, although the right subregion was consistently of moderately higher amplitude than the left at the group level. At the individual participant level, response topographies varied across participants within the occipito-parietal ROI, but were generally consistent within participants across conditions (**Figure 4.3C**). Significant responses at the occipito-parietal ROI were found in all but one participant in both conditions, underlying the reliability of the main finding that both grayscale and color images are sufficient to elicit selective responses to yellow-diagnostic objects.
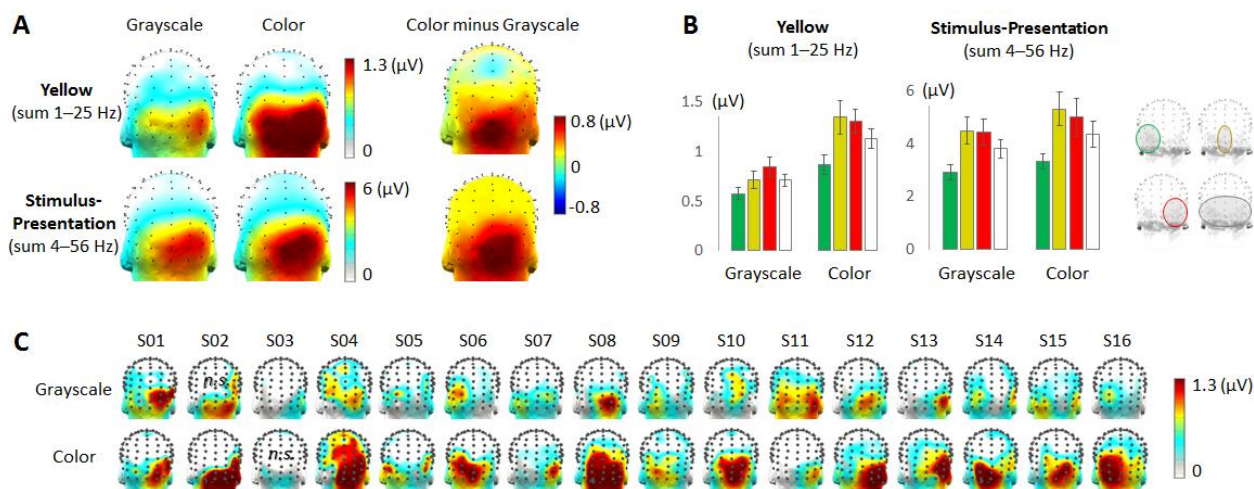
Figure 4.3. *Frequency-domain response scalp topographies at the group and individual levels.* **A)** *Summed-harmonic response scalp topographies in the grayscale and color conditions, as well as*

*their differences. **B)** Quantification of the summed-harmonic responses at the occipito-parietal ROI and its three subregions: left, medial, and right. **C)** Individual participant, yellow-diagnostic summed-harmonic response scalp topographies.*

For comparison, an investigation of the spatial attributes of the stimulus-presentation responses produced no appreciable differences across conditions. Across subregions, the response for color was increased 13-14% for right and left subregions, and 18% for the medial subregion. A repeated-measures ANOVA, with factors of Condition and Subregion, did not report an interaction between these factors, $F_{1.34,20.1} = 2.11$, $p = .158$, $\eta p2 = 0.12$. The ANOVA did support the main effect of Condition, $F_{1,15} = 7.35$, $p = .016$, $\eta p2 = 0.33$, as reported previously. Here, a main effect of Subregion was also found, $F_{2,30} = 10.7$, $p = .0003$, $\eta p2 = 0.42$, with the left subregion falling below the amplitudes of the middle and right subregions. Post-hoc t-tests confirmed this difference (all t's > 2.87, d's > 0.77, r's > 0.36, p's <.012) when including the left subregion (otherwise t's < 0.65, d's < 0.11, r's < 0.06, p's > .53).

To investigate the temporal dynamics of the yellow-diagnostic responses, the data were analyzed in the time domain, both in terms of 1) overall responses and 2) responses specific to yellow-diagnostic objects. In the second case, a notch filter was applied to selectively remove the stimulus-presentation responses at 4 Hz and its harmonics, in order to isolate the responses to yellow-diagnostic objects at 1 Hz and its specific harmonics (see Methods). The data were then cropped into epochs locked by the onset time of yellow-diagnostic stimulus presentation (labeled 0 ms), and these epochs were averaged, as in traditional ERP analyses. Given the different spatial foci of responses on the scalp across time, the responses were investigated separately over the occipito-parietal subregions.

The overall responses appeared similar in the grayscale and color conditions, although the occipito-parietal subregions displayed different timecourses (**Figure 4.4A**). Slightly larger responses to the color condition were hinted at over the middle region, but the responses to yellow-diagnostic objects were obscured by the responses to other objects (appearing every 250 ms, i.e., at – 250 ms, 250 ms, and 500 ms in this figure). To isolate yellow-diagnostic object responses, we examined the waveforms notch-filtered at 4 Hz and its harmonics (**Figure 4.4B**). Note that since the response aspects common to the stimulus presentation are removed by the notch filter, if no differential response to yellow stimuli is recorded, no substantial deflections from the baseline will be present. However, this revealed a first negative deflection at the middle subregion, occuring at about the same time in the two conditions: it first reached significance at 61 ms in the grayscale, and 65 ms, in the color condition . A negative component was also seen later over the left and right subregions, first reaching significance at 119 and 125 ms over the right subregion in the grayscale and color conditions, respectively, and at 123 and 127 ms over the left subregion. In total, there were no differences in the onset latency of the yellow-diagnostic response across the grayscale and color conditions.
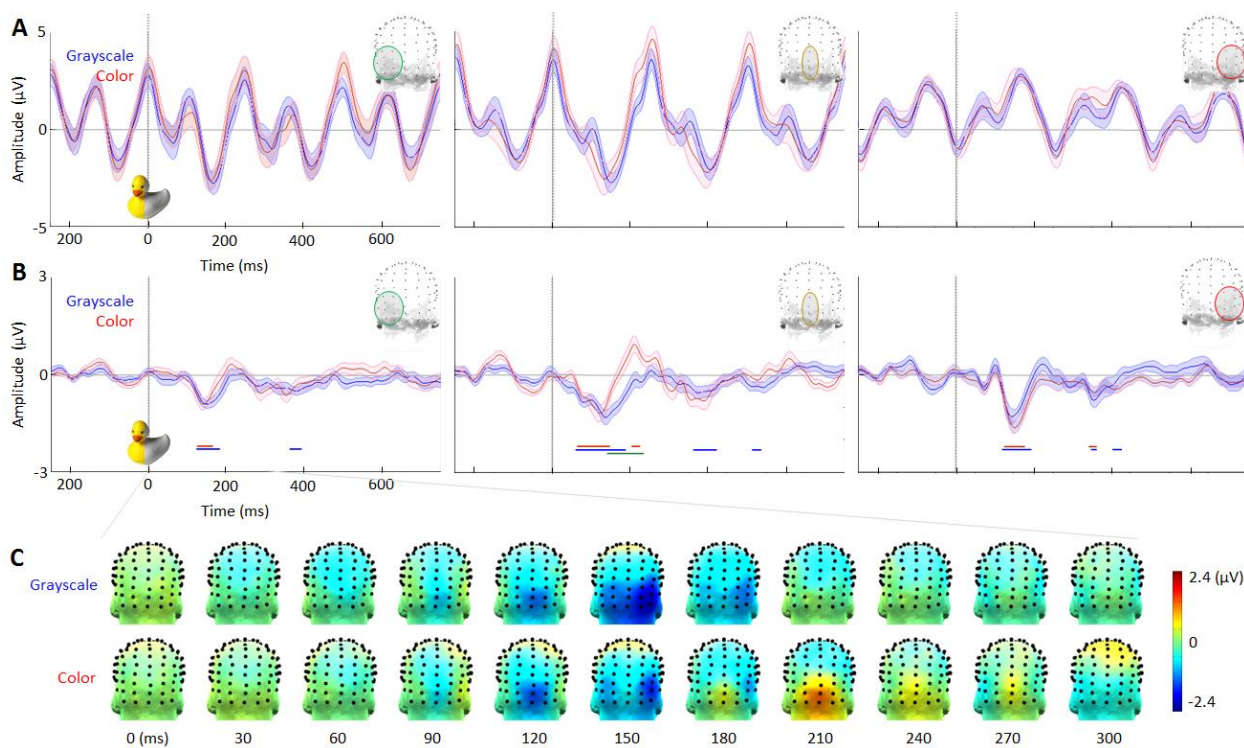
Figure 4.4. *Time-domain responses to yellow-diagnostic objects.* **A)** *Time-domain responses in the grayscale (blue waveform) and color (red waveform) conditions, related to yellow-diagnostic object stimulus onset (0 ms; exemplified with a yellow/gray rubber duck), at the three scalp subregions (left, middle, and right panels, respectively). These responses reflect the responses to all objects (presented at 4 Hz, i.e., every 250 ms) as well as the responses specific to yellow-diagnostic objects. The dark waveforms are the average across subjects, with the shaded areas indicating ± 1 SE.* **B)** *After filtering out the general visual EEG responses at 4 Hz and its harmonics, the time-course of the yellow-diagnostic object responses may be isolated. This panel is plotted as in (A), except with a different amplitude scale. Additionally, the time windows of significant deflections for each condition are indicated by solid lines below the waveforms in the corresponding color by condition; significant differences across conditions, occurring only at the middle subregion, are indicated in green.* **C)** *Response scalp topographies across time: sampled every 30 ms from stimulus onset.*

The striking difference across conditions in the time domain was at a positive

component, peaking at 211 ms, which was only present in the color condition. Paired sample t-

tests showed that this component was significantly different across conditions between 141-234

ms post-stimulus onset (p<.01; see Figure 4.4B). The scalp topography of this component was

well-centered over the middle occipital channels (**Figure 4.4C**), consistent with this subregion

producing the only color advantage in terms of amplitude across conditions in the frequency-

domain analysis (compare Figure 4.4C with Figure 4.3A). There were no other appreciable

differences across conditions in either the subregion waveforms, or the scalp topographies.

4.5. Discussion

To summarize, we designed an experiment to isolate selective responses to objects of one color

category (yellow), occurring as every one out of four stimuli presented at 4 Hz, otherwise

containing non-periodic presentations of green, red, and blue color-diagnostic objects. We

found color-specific responses reflecting the differing spatiotemporal dynamics of EEG

responses to different colors (e.g., Regan, 1966; Riggs & Sternheim, 1968; Allison et al., 1993;

Anllo-Vento, Luck & Hillyard, 1998), for stimuli with characteristic colors shown either with

actual color or in grayscale. This allowed us to compare the strength and the temporal dynamics

for these color-specific responses. Our results suggest that a robust color-selective response can

be elicited by the corresponding spatial information for a color-diagnostic object, and allowed us

to assess the spatiotemporal dynamics of these responses.

Yellow elicits selective EEG responses *vs.* blue, green, and red

Selective neural responses were recorded at 1 Hz and its harmonics to yellow objects

shown in their diagnostic physical color, differential from the responses to non-periodic

presentations of blue, red, and green objects, also shown in their diagnostic physical color (color

condition; Figure 4.2). Different   responses to different colors have been reported on the scalp

in a number of previous studies with EEG (e.g., Regan, 1966; Riggs & Sternheim, 1968; Anllo-

Vento, Luck & Hillyard, 1998; Retter et al., 2017). This is unsurprising given differences in

amplitude and latency as a function of cone-opponent cortical inputs (e.g., Robson & Kulikowski,

1998; Rabbin et al., 1994; Lee et al., 2009). However, these results have been previously

reported only at the group level, typically with a small number of electrodes, and are largely

descriptive: here, we objectively quantify color-selective responses in the frequency domain,

these responses being significant at the individual participant level (in 15/16 participants; Figure

4.3C). Our results are likely supported by the extensive spatial coverage of high-density EEG,

given the variability in the response scalp topography across individual participants, as well as

the high signal-to-noise ratio afforded by frequency tagging (Regan, 1966; Norcia et al., 2015).

There are several reasons to conclude that this response does reflect a selective

response to yellow, and does not emerge as an artifact of our paradigm. Firstly, the yellow-

selective response cannot be explained by the periodic temporal frequency of the yellow

images. The response to frequency-tagged target stimuli appearing as a proportion of images in

this type of paradigm have been shown to be immune to the temporal predictability of the

image presentation; specifically, faces appearing periodically among objects produced

equivalent responses to faces presented non-periodically among objects (Quek & Rossion,

2017). Additionally, differentiable neural responses to different image types (faces, body parts,

and houses) appearing periodically as a proportion of cross-category objects have been shown

(Jacques, Retter, & Rossion, 2016).   Secondly, the yellow-selective responses were not driven by

yellow objects occurring more of less often than objects of other colors, since each of the object

colors appeared the same number of times as the other colors on average in each testing

sequence (each color appearing on average every one out of four stimuli). While all object colors

thus on average were occurring at a rate of 1 Hz, we empirically demonstrated that no response

would occur at 1 Hz and its harmonics without a specific periodically-presented color: in a

control condition added with the last five participants, we presented all the colored objects non-

periodically, and show that no 1-Hz response is recorded in that case (**Figure 4.5**). Thirdly, the

yellow-selective response we record in this paradigm is similar in terms of scalp topography to a

yellow/gray asymmetry response reported in a previous study (Retter et al., 2017). Thus, the

response to periodic yellow objects at 1 Hz and its harmonics does appear to capture selective

responses to yellow.
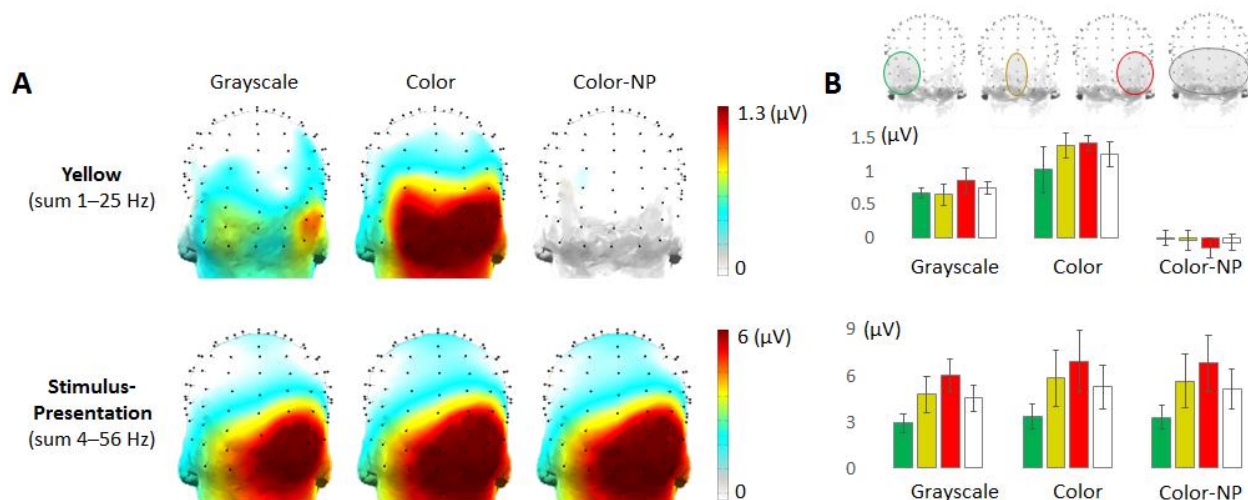
Figure 4.5. Responses to a color non-periodic (NP) control condition, in which yellow-diagnostic objects repeated non-periodically throughout the stimulation sequences (N = 5). A) No response is present at 1 Hz and its harmonics when no color is presented periodically ("frequency-tagged") at this rate. B) When quantified at the occipito-parietal ROI and its subregions, there is again no response for the non-periodic control condition at 1 Hz, however, note that the stimulus-presentation response in this condition is equivalent to that of the standard periodic color condition.

Yellow-diagnostic objects elicit selective EEG responses to grayscale images

More interestingly, we recorded selective responses to yellow-diagnostic objects at 1 Hz and its harmonics, even when all the objects were shown in grayscale (grayscale condition; Figure 4.2). As addressed in the introduction, previous studies have shown that color memory influences object perception, through a convergence of various experimental approaches. Our finding of a color-selective response to grayscale yellow-diagnostic objects suggests that the color information routinely associated with prototypically colored objects is automatically activated from the spatial cues to the object, suggesting that the neural representation of the object jointly codes the spatial and color information. Further, it suggests that these color associations are color-specific, such that the responses to implied yellow may be differentiated from the responses to other implied colors.

Previous EEG studies have instead measured effects of color memory that are non-selective to color category, i.e., contrasts of color vs. grayscale or color vs. incongruent color objects, averaging across color categories (8 different color categories: Proverbio et al., 2004; color category uncontrolled among 96 objects: Lu et al., 2010; color category uncontrolled among 54 high color-diagnostic objects: Bramao et al., 2012b; color category uncontrolled among 150 objects: Lloyd-Jones et al., 2012). Not only did these previous EEG studies report inconsistent differences in the amplitude of color vs. grayscale objects responses, but these effects cannot be taken as reflecting color-specific responses associated with diagnostic objects. In fact, when only color vs. grayscale object responses are compared, the response differences could be more related to a general effect of color, as we also observe on the 4 Hz base rate stimulation rate in our study (i.e., 15% increase). Additionally, no previous EEG study quantified the difference in response amplitude between implied vs. physical color .

Here, with our frequency-domain analysis, we quantify for the first time the relative

amplitude difference in neural responses to implicit vs. actual color objects. We show that the

amplitude of the implicit color yellow-selective responses was 63% of that of actual color over

the occipito-parietal ROI (Figure 4.3B).   Again, this amplitude difference captures the difference

in differential responses to yellow-diagnostic objects vs. objects of different diagnostic colors for

each the color and grayscale conditions. The responses in this case are reduced more than

would be expected from a general effect of color, as indexed by the responses at the stimulus-

presentation rate (where the implicit color yellow-selective responses were 88% of the

amplitude of actual color responses). This suggests that implied color elicits weaker color-

specific responses than actual color. However, this could be for a number of reasons: for

example, it is possible that the neural representations of object color are fully elicited from

implied color objects, but that the response is decreased due to variance in the amount that

color is associated with these objects for each observer.

A relatively large response to specific implied color does not relate to the perceptual

experience of color when looking at grayscale objects: color-diagnostic grayscale objects shown

in grayscale do not appear to look 63% colored but, under most conditions, actually do appear

gray (note very small effects of memory color, produced in an unnatural context: e.g., Hansen et

al., 2006, reporting 4-13% relative scaling; Lee & Mather, 2019, reporting weak chromatic

adaptation effects to achromatic implied color stimuli). However, the yellow-selective response

amplitude to implied object color in this case does not merely reflect the responses to the

perceived visual stimuli per se; rather, it reflects responses to the perceived objects recognized

from the visual stimuli. That is, in addition to the low-level (physical) visual features of the object

images, the processes of matching these features to an object (i.e., object recognition) activates

neural representations of that object that may be more extensive and high-level (abstract) than the visual features themselves. For example, consider the case in which the presentation of part of a face (e.g., the eyes) may elicit the neural response of a full face representation (e.g., Bentin et al., 1996). Or, for another example, consider "mirror neurons," which suggest that the representation of a body motion in (pre)motor brain areas may be evoked from only the visual perception of this motion; note that the pattern and rate of such neurons may not differ in response to motion or perception of motion (e.g., Kilmer & Lemon, 2013). Again, we think that the yellow-selective responses to grayscale objects with prototypical colors here reflect high-level, automatic object knowledge.

Memory color responses are not delayed relative to physical color responses

In our time-domain analysis, we show that selective yellow memory color responses to color-diagnostic grayscale objects are not delayed relative to selective yellow physical color responses to the same objects presented in color (Figure 4.4). Specifically, we showed that over the medial subregion, responses onset at 61 ms for grayscale and 64 ms for color; over the lateral occipito-temporal subregions, responses onset at 121 ms for grayscale and 126 ms for color. This suggests that neural responses to objects are influenced by their remembered color associations: objects are categorized by color with no delay between grayscale and colored images.

Here, by isolating yellow-selective responses and not averaging across multiple color categories, we have validly measured color-selective responses, again given that different colors have different temporal dynamics with EEG (e.g., Regan, 1966; Riggs & Sternheim, 1968; Allison et al., 1993; Anllo-Vento, Luck & Hillyard, 1998; Retter et al., 2017). In comparison, previous EEG studies that averaged across different color categories may have distorted color-selective

measures. Perhaps for this reason, previous EEG color memory studies have produced

incongruent results, reporting divergent differences in the amplitude of inconsistent ERP

components (e.g., at the P1 and N1 components: Lu et al., 2010; Bramao et al., 2012b; or in later

components, such as the N2, P2, P3, and N400: Provebio et al., 2004; Lloyd-Jones et al., 2012;

Bramao et al., 2012b). Note that the finding of the same neural onset latency for color and

physical memory responses is in line with one previous MEG study by Teichmann et al. (2019)

employing a multivariate pattern-analysis decoding of the color category of congruent vs.

grayscale objects, although this is in contradiction to a study one year earlier from Teichmann et

al. (2018) that reported earlier decoding of responses to physical than memory color with the

same approach. Our findings are thus important for clarifying the issue of whether or not color-

selective physical and memory color responses differ in onset latency.

These finding relates to the debate as to whether color has a secondary effect than

shape in object recognition, as addressed in the Introduction. Here, we provide direct evidence

that color is integrated into objects' representations, at the earliest stages of object processing.

This finding is in line with previous studies using very short image presentation times, which

provided indirect evidence that color has an early impact on object processing. Indeed, previous

behavioral studies have shown a color advantage in recognizing objects or scenes with

diagnostic colors, even at the shortest image presentation times (from 10 to 1000 ms per item:

Bruner & Postman, 1949; from 16-64 ms per image: Gegenfurtner & Rieger, 2000; from 13 to 80

ms per image: Hagmann & Potter, 2016). Additionally, further indirect evidence has been

provided by behavioral studies that show a consistent color advantage in accuracy of object

recognition across trials with relatively early or late response times (Rossion & Pourtois, 2004;

Hagen et al., 2014). However, it is against hierarchical views of color first being processing

selectively in early visual areas, and only later being influenced by "top-down" feedback from color memory expectations at later stages (e.g., Tanaka, Weiskopf, & Williams, 2001; Hansen et al., 2006; Bramao et al., 2012)

Note that we have addressed selective yellow-diagnostic responses that reflect differential responses, contrasting yellow responses to green, red, and blue. Thus, it is possible that the non-differential responses to physically yellow objects were faster than those to memory yellow objects. In support of this, the responses to the data unfiltered for the 4-Hz responses did appear to be onset earlier in the color condition, at least over the medial subregion (data not shown). This finding would be in line with color aiding in early sensory processing, such as image segmentation through contour enhancement (Allen, 1879; Walls, 1942, p. 463; Elsner, 1978; Frome, Buck, & Boynton, 1979; De Valois & Switkes, 1983; Gegenfurtner & Rieger, 2000; Bramao et al., 2012). However, in our design, this may have a relatively weak effect, since we used simple object images, cropped without their natural backgrounds, and without many luminance boundaries from shadows and occlusion (especially in the case of the cartoon characters). Additionally, we presented stimuli without immediate masking (at a 50% squarewave duty cycle), separated by reasonably long stimulus-onset asynchronies of 250 ms, and centrally and at a large size. Thus, it was predicted that physical color would have a role in accelerating early sensory responses to objects, but our paradigm was not particularly sensitive to this effect.

Equal onset-latencies for implied and actual yellow-selective responses are followed by a late (~140-235 ms) actual color advantage

In our time-domain analysis, we show that yellow-selective implied color responses to color-diagnostic grayscale objects emerge at the same time as yellow-selective actual color

responses to the same objects (Figure 4.4). Specifically, we showed that over the middle

occipital subregion, responses onset at 61 ms for grayscale and 64 ms for color; over the lateral

occipito-temporal subregions, responses onset at 121 ms for grayscale and 126 ms for color.

This suggests that neural responses to objects are influenced by their remembered color

associations from their onset: objects are categorized by color with no delay between grayscale

and colored images.   Our findings are thus important for clarifying the issue of whether or not

color-selective implied and actual color responses differ in onset latency.

Note that we have addressed selective yellow-diagnostic responses that reflect

differential responses, contrasting yellow responses to green, red, and blue. Thus, it is possible

that the non-differential responses to physically yellow objects were faster than those to

memory yellow objects. In support of this, the responses to the data unfiltered for the 4-Hz

responses did appear to be onset earlier in the color condition, at least over the middle

subregion (Figure 4.4A). This finding would be in line with color aiding in early sensory

processing, such as image segmentation through contour enhancement (Allen, 1879; Walls,

1942, p. 463; Elsner, 1978; Frome, Buck, & Boynton, 1979; De Valois & Switkes, 1983;

Gegenfurtner & Rieger, 2000; Bramao et al., 2012). However, in our design, this may have a

relatively weak effect, since we used simple object images, cropped without their natural

backgrounds, and without many luminance boundaries from shadows and occlusion (especially

in the case of the cartoon characters). Additionally, we presented stimuli without immediate

masking (at a 50% squarewave duty cycle), separated by reasonably long stimulus-onset

asynchronies of 250 ms, and centrally and at a large size. Thus, it was predicted that physical

color would have a role in accelerating early sensory responses to objects, but our paradigm was

not particularly sensitive to this effect.

The only appreciable difference across conditions in the time-domain analysis was at a positive component that was present only in the actual color condition (Figure 4.4). This component was significantly different from the grayscale condition between about 140-235 ms post-stimulus onset; its peak was at about 210 ms. In spatial terms, this component was centered over the middle occipital channels, in agreement with the middle subregion producing the only amplitude advantage for the color condition in the frequency-domain analysis (compare the scalp topography of the differences across conditions in Figure 4.3A with that of this time-domain component in Figure 4.4C).

This positive component is in line with a typical chromatic ERP, the CIII component (e.g., see Gerth et al., 2003). Thus, it is possible that this component is related to typical chromatic processing, rather than being related to color-shape integration in object processing. Indeed, this component may be evoked not from yellow-selective responses integrated with shape information, but from the response to physically present yellow that is not automatically evoked from the association with object shape. Alternatively, another possibility is that this component reflects an enhancement of the response to diagnostic-yellow objects from the congruent presence of the physical yellow color. Such issues could be addressed further by comparing the timecourse of the neural responses to congruent and incongruent colored color-diagnostic objects.

Together, these findings relate to the debate as to whether color has a secondary effect than shape in object recognition, as addressed in the Introduction. Here, we provide direct evidence that color memory is integrated into objects' representations early on. This finding is in line with previous studies using very short image presentation times, which provided indirect evidence that color has an early impact on object processing. Indeed, previous behavioral

studies have shown a color advantage in recognizing objects or scenes with diagnostic colors, even at the shortest image presentation times (from 10 to 1000 ms per item: Bruner & Postman, 1949; from 16-64 ms per image: Gegenfurtner & Rieger, 2000; from 13 to 80 ms per image: Hagmann & Potter, 2016). Additionally, further indirect evidence has been provided by behavioral studies that show a consistent color advantage in accuracy of object recognition across trials with relatively early or late response times (Rossion & Pourtois, 2004; Hagen et al., 2014). A relatively late effect of actual color on image processing is also in line with previous studies, e.g., in color having a late effect on enhancing image representation in memory (Gegenfurtner & Rieger, 2000).

However, our findings are not compatible with a hierarchical views of color first being processing selectively in early visual areas, and only later being influenced by "top-down" feedback from color memory expectations at later stages (e.g., Tanaka, Weiskopf, & Williams, 2001; Hansen et al., 2006; Bramao et al., 2012). Instead, our findings may be interpreted in a framework in which the visual world is perceived initially through associated recognition: i.e., the physical details of the visual world (captured through sensory processing) are not actually perceived before stimuli are recognized (refs). Instead, perceptual awareness may precede the processing of visual details, which may have relatively later effects on visual processing.

Limitations and future directions

This study used a limited number of object stimuli (6 per color category), so that a limitation was in the amount of physical difference within and across color categories. While luminance and luminance contrast were controlled in the stimulus generation, and differences in global contrast factor (Matkovic et al., 2005) and gist (Oliva & Torralba, 2001) were not significant across color categories, it remains a possibility that the stimuli have some mean

differences by color category (e.g., in curvature, local contrast across an image, etc.). A future study could use familiarity or training to test different subjects, or the same subjects across time, having different color-shape associations. For example, subjects could be trained to associate certain novel shapes with certain colors, and would be predicted to have color-memory effects in this paradigm only after this training.

Another limitation here is that in the color condition, images contain natural color information, with variation in hue and saturation within each image, and a slight variance in mean hue across images. Consequently, grayscale images are more uniform. Moreover, there may be more uniformity in the colors associated with grayscale objects: color memories have been shown to be biased by color category membership (for objects: Van Gulick & Tarr, 2010; for color patches: Boynton et al., 1989; Uchikawa & Shinoda, 1996; Bae et al., 2015; see also Bartleson, 1960). Thus, it is possible that the evoked neural responses are more consistent to the different grayscale objects within each category. Again, a training of novel shape-color associations could be used, with dissociable elements of color homogeneity and/or training time, to further explore the intricacies of these effects.

This study was limited by recording neural responses on scalp: thus, it remains unknown whether these color memory responses originate from color-selective cortical regions, or whether they are object-selective responses that have been selectively shaped by learned color associations. Indeed, it has been suggested that color memory responses originate from regions close to but external from color-selective regions, which may have been influenced by color associations (e.g., Martin et al., 1995). However, it has also been suggested that color memory responses originate from color-selective regions evoked from object shape associations (e.g., Slotnick, 2009, with a different interpretation of similar neural data as recorded by Marin et al.,

1995; see also Simmons et al., 2007). Future neuroimaging or intracerebral EEG studies with

frequency-tagging may better address this outstanding issue.

Chapter 5

Discussion

_____

_____

5.1. Summary: the retina and retino-cortical pathway cannot explain color perception

Three different cone types in the typical human retina absorb different wavelengths of light with differing probabilities, as a function of each cone type's spectral sensitivity (**Figure 1.1B**). Even at this earliest stage, it is possible that the spectral sensitivities of the cones evolved in relation to the emission spectra of functionally relevant objects in the environment (e.g., Gouras & Zrenner, 1981). Nevertheless, the specific spectral sensitivities in the human retina were likely limited in terms of their optimization, as they consist of two opsin pigments that have been conserved throughout hundreds of millions of years, with only a probable novel mutation in one of these opsins leading to trichromacy about 40 million years ago (Nathans, Thomas & Hogness, 1986; Yokoyama & Yokoyama, 1989; Wassle, 2004; Solomon & Lennie, 2007; Jacobs, 2009; Neitz & Neitz, 2011). In any case, the signals from the cones are not highly determinant in perception, as perception is often unexplained by the cone spectral sensitivities (Neitz & Jacobs, 1986; Neitz & Neitz, 2011; Jordan et al., 2010; Webster, Juricevic, & McDermott, 2010; Boehm, MacLeod, & Bosten, 2014) or the ratio of different cone types in an observer's eye (particularly the L _vs._ M cone ratio, which is highly variable across individuals; e.g., Neitz, Neitz & Jacobs, 1993; Roorda & Williams, 1999; Kremers et al., 2000; Brainard, 2015).

At the next stage of visual processing, the retino-cortical pathway takes the signals from the cones into the retinal ganglion and lateral geniculate nucleus (LGN) cells, which will eventually reach the cortex. At this stage, the signals from the cones have been integrated into two dominant comparative pathways that are single-opponent and subtractive (the L _vs._ M

pathway and the S pathway, which integrate with a brightness dimension, L+M; Young, 1802; von Helmholtz, 1867; DeValois et al., 1958; Derrington, Krauskopf, & Lennie, 1984; MacLeod & Boynton, 1979; Jameson & D'Andrade, 1997). Signals from these comparative pathways account for a number of perceptual phenomena, which has been taken as evidence of feed-forward visual processing with a high impact from the early stages (see Gegenfurtner & Kiper, 2003). However, the differences between cone-opponent (**Figure 1.1C**) and perceptual (**Figure 1.1D**) representations of color are readily apparent in the color spaces they define. The transformation of visual chromatic signals between the retinocortical pathway color space and the perceptual color space is computable, and accordingly has had a profound impact on the way in which responses to color have been understood. However, the way in which the brain performs this transformation, and the cases in which it may not be linearly predicted, remain mysteries, the understanding of which is thought to lie hidden in cortical color processing.

5.2. Color-processing in the visual cortex: hierarchical models

Dominant throughout cortical color research studies is the model that color information progresses along a visual hierarchy, progressively from area V1, to V2/V3, to V4, to LO, and potentially beyond to more anterior regions in the fusiform and lingual gyri. There is at present some acknowledgement that such a feed-forward pathway for color processing may be influenced by interactions with luminance and shape, and ultimately be complemented by feed-back in the opposite direction (e.g., Gegenfurtner, 2003; Johnson & Mullen, 2016).

Up to this point, although I have addressed color-selective responses in this order, for simplicity and ease of organization, I have not meant to imply that the feed-forward retino-cortical pathway may be extended into a largely feed-forward intra-cortical pathway. Indeed, at present, there is little conclusive functional evidence to support hierarchical processing of visual

information across early visual areas (V1, V2, and V3). At the level of single-cell recordings, despite pronounced differences in spatio-functional organization ("blobs" in V2 and the thin stripes of V2 and V3), cells with highly variable properties have been found throughout visual areas. Even in V1, multiple color-responsive cell types have been reported with variable chromatic, spatial, and chromatic-spatial tuning properties (Ts'o & Gilbert, 1988; Komatsu et al., 1992; Shapley & Hawkin, 2011); and the cells types in V2 are highly similar (Kiper et al., 1997; Moutoussis & Zeki, 2002; but see also Hubel & Livingstone, 1985). While less is known about responses to color in V3 (but see Tootell et al., 2004), the organization appears similar to that of V2 in the human brain (Nasr, Polimeni, & Tootell, 2016; Dumoulin et al., 2017). Moreover, fMRI studies on these areas in humans often fail to show appreciable differences between areas V1, V2, and V3 (and sometimes V4) in their chromatic tuning (e.g., Engel, Zhang & Wandell, 1997; Mullen et al., 2007; Brouwer & Heeger, 2009; Mullen, Chang, & Hess, 2015). Some studies report little activation in V3 (e.g., Wade et al., 2002; Conway, 2009), while others even group V2 and V3 into a single functional area (e.g., Persichetti et al., 2015). When specific functional responses within these regions are not known, it would be extremely difficult to conceive of a specific hierarchical model of functioning from V1 to V2 and V3 for color processing.

Another simplified extension of a hierarchical model of visual processing is grouping together the "early visual areas" of V1-V3, and sometimes including V4, and remarking that responses in these areas reflect low-level differences in color discriminations (similar to color *sensations*), while "late" visual cortical areas (sometimes V4, VO, and anterior regions in the lingual and fusiform gyri) reflect high-level differences in color *perception*. This construct potentially has its origins in single-cell recordings in non-human primates, contrasting the properties of cells found in V1 and V4 (although, again, note that there is some controversy in

the homology of the latter area across species): cells in V4 were reported to possess more

specific, perceptual color-tuning, while cells in V1 were reported to be more sensitive to metric-

based wavelength discriminations (Zeki, 1973; Zeki, 1983; see also Dean, 1976). Later studies

have reported similar, or even more perceptually-biased, single-cell responses in more anterior

inferior temporal cortex in non-human primates (Komatsu et al., 1992; Zeki & Marini, 1998;

Koida & Komatsu, 2007).

Human lesion studies on achromatopsia and dyschromatopsia were also taken as

support of this early/late distinction: lesions to area V4 and more anteriorly in the ventral

occipito-temporal cortex (VOTC) produced behavioral deficits in color perception (Verrey, 1888;

Meadows, 1974; Jaeger, Krastel & Braun, 1988; Zeki, 1990; Bouvier & Engel, 2006; see also

Wade et al., 2002). In contrast, lesions to human V1 did not abolish color-related behavior,

although they abolished perceptual awareness (Brent, Kennard, & Ruddock, 1994; Stoerig &

Cowey, 1090). Distinctions have also been made with fMRI in humans at area V4 or VO and

more anteriorly, in that the color-tuning of response in these areas departs from that of V1-V3

(VO: Mullen et al., 2007; V4: Brouwer & Heeger, 2009; V4: Mullen, Chang, & Hess, 2015; see also

Conway, 2009). Additionally, electrical stimulation of an intracerebral EEG contact in the medial

fusiform gyrus, thought to be consistent with VO, produced specific color percepts in a single

human patient (Murphey, Yoshor & Beauchamp, 2008). Thus, these later visual areas are

interpreted as more color-selective, reflecting more perceptually-valid representations of color

(e.g., Simmons et al., 2007; Brouwer & Heeger, 2009).

However, some perceptual color phenomenon, such as color categorization and object

color memory, have remained elusive, even in these later visual areas. For example, fMRI

studies have failed to report categorical color effects anywhere in the visual cortex, including V4

(Bird et al., 2014; Persichetti et al., 2015), although this may reflect a limitation of recording

resolution or appropriate experimental paradigms. Additionally, object color memory effects

(e.g., associating a grayscale image of a banana with yellow) have been reported in V1 (Bannert

& Bartels, 2013), rather than in late areas (but for different results, including effects in V3, V4,

and VO, see Vandenbroucke et al., 2016). Thus, while it appears possible that there is a

dissociation between more posterior (pre-V4) and more anterior (post-V4) color-responsive

regions, many questions remain as to what extent, and under what circumstances, this may be

the case (for continued retinotopic organization throughout these functional areas, with

ongoing foveal biases through VO, see Wade et al., 2002).

5.3. (Early) cortical EEG responses to color reflect high-level color perception: an

alternative system-level model

The responses to color recorded with EEG have been thought to reflect activity from early

cortical areas, instead of relating to higher-level color perception. For example, in one case, a

patient with extensive ventral occipito-temporal lesions presented with a typical chromatic

visual evoked potential at one medial occipital electrode, suggesting that color-selective

responses were driven by early visual areas alone (Crognale et al., 2013; see also Kulikowski et

al., 1994). This view has changed somewhat within the last couple decades in particular, as

higher-level categorical and hue-specific responses to color have also been reported with EEG,

particularly over a wider occipito-parietal region (e.g., Anllo-Vento et al., 1998; Fonteneau &

Davidoff, 2007; Thierry et al., 2009; Anthanasopoulos et al., 2010; Clifford et al., 2010; Mo et al.,

2011; He et al., 2014; Forder, He, & Franlkin, 2017). These studies have sometimes been

contradictory, however, in regards to the specific ERP components affected or the presence or

absence of latency shifts (e.g., for early categorical effects: Forder, He, & Franklin, 2017; for late categorical effects, later than 200 ms: Clifford et al., 2012; He et al., 2014).

Contrary to the idea that EEG responses reflect only early-stage, sensory processing of color, and contrary to a hierarchical visual model of the responses to color, the data presented here suggest that the cortical responses to color recorded with EEG reflect the activity of a high-level color-responsive network that responds without a dominant "feed-forward" progression across cortical areas. That is, in all three studies, our data provide evidence that the cortical responses to color recorded with EEG are strongly correlated with human color perception, reflecting a transformation of the organization of retino-cortical pathway color signals (see also Riggs & Sternheim, 1968, for simultaneous electroretinogram and EEG responses). Moreover, the earliest responses recorded in these studies do not appear to reflect the activation in early, sensory visual areas, but appear to be reflective of high-level color perception from early on.

In Study 3, in particular, we recorded EEG responses specific to diagnostically-yellow objects, even when all object images were presented in grayscale, suggesting that color associations play an automatic role in object recognition. Note that neuroimaging studies have concluded that memory color reflects activation from V4 or VO, which may or may not feed back into V1 (Bannert & Bartels, 2013; Simmons et al., 2007). The very presence of responses to implicit color indicates that a hierarchical progression of color-processing in early visual areas is not necessary for color perception, i.e., that responses do not need to originate in V1 (V2, and V3) in order to activate higher-level color areas (e.g., VO). Importantly, here, the responses evoked from color-diagnostic yellow objects onset as early in the grayscale as the color condition, suggesting that these EEG responses reflect the knowledge of yellow even before the physical color is fully processed. Showing that the response is not delayed for implied color *vs.*

actual color speaks strongly against the temporal progression of "early-to-late" visual areas in typical color perception.

In Study 1, we showed that gray-yellow and blue-yellow conditions produced similar EEG response asymmetries for white-gold observers of the dress (when the dress may have been perceived as white, i.e., achromatic), in spite of large physical differences in the chromaticity of the gray and the yellow dress images. Additionally, we recorded EEG responses that are reflective of perceptual blue-yellow asymmetries, being stronger than green-red asymmetries, even though the stimuli in both of these contrasts were matched for cone-opponent signals. Finally, we were also able to use individuals' EEG responses to classify them as to whether they saw "the dress" image as blue-black or white-gold. In Study 2, we recorded EEG responses that are more related in perceptual than cone-opponent terms, sometimes presenting with nearly identical spatiotemporal dynamics when classified within the same perceptual category (e.g., purple responses at 60° and 90°). Additionally, the color-specific responses recorded in Study 2 diverge in from their earliest deflections in time, rather than appearing as late-stage modifications of physically-driven inputs.

We interpret the responses recorded here to reflect high-level color perception, as they relate to perceptual experiences of color more than physical stimulus attributes. However, it may be observed that the topographies we record are typically centered over the middle occipital cortex in all three studies, although there are some more lateralized deviations extending over the parietal cortex (e.g., in the chromatic-chromatic asymmetries in Study 1, and the responses to implicit color in Study 3). One possibility is that the responses we record reflect a distribution of activation throughout the visual cortex, such that responses in relatively anterior brain areas, such as the fusiform gyrus, are activated in concert with early visual areas

that drive the EEG response amplitude, given the likelihood for such early visual areas to possess electrical dipole sources close to, and potentially projecting orthogonally to, the scalp surface where the sensors are positioned (e.g., Luck, 2005).

Another possibility is that we do record lateralized responses in each subject reflecting activity from more anterior visual areas, but that when averaging across participants, the strongest amplitudes appear to be medial as an effect of higher reliability in this area across participants (e.g., compare the topographies of individual subjects in **Figure 4.3C** to the grand-averaged topographies in **Figure 4.3A**). Overall, while our EEG data cannot speak to specific neural sources, the presence of perceptual correlates from the earliest selective neural response onsets speaks against a hierarchically evolving neural response, where early visual areas themselves drive the earliest neural responses.

Such outstanding questions could be further explored in future studies, using direct intracranial EEG or indirect functional neuroimaging approaches. For example, the relative onsets of the neural activation selective to color could be tracked more thoroughly throughout the visual cortex with intracerebral EEG. Additionally, the neural sources contributing to high-level perceptual effects, such as color-specific responses to implied color as studied in Study 3 or perception of the dress stimulus in Study 1, could be probed with fMRI, to assist in resolving ongoing controversies in these areas of research. Additionally, neural traces of high-level perceptual effects, such as color categorization, could be more fully explored at the individual level with a combination of behavioral and cortical-level recording techniques.

5.4. A return to theories on the purpose of human color perception

The central theory addressed here on the purpose of color perception is that color perception is beneficial for categorization things in the environment (Hardin, 1992; Hatfield, 1992; Thompson,

1995; see also Johnson & Mullen, 2016). While it has been stated that this theory is not incompatible with the contributions of color to early-stage, sensory visual processing, such as image segmentation and form identification (e.g., Gegenfurtner & Kiper, 2003; Shapley & Hawken, 2011; Jonson & Mullen, 2016), it emphasizes the importance of perceptual object categorization, even from earliest stages of cortical visual processing. The present results, showing EEG correlates of perceptual effects, suggest that the human cortex is an integrated processing unit, wherein structurally-distinct modules, while likely having some internal specializations, are activated in concert to produce human perception. Empirically, these results do not make any advances in addressing the purpose of color perception throughout evolution, and they could be interpreted through a number of different theories. However, this theoretical question merits some speculative consideration.

It was mentioned in the Introduction that this theory is in contrast to those that focus on the utility of color for extracting objective wavelength information from surfaces vs. illuminants in the environment. Such theories assume that the wavelength of surfaces presents *information* about distal properties in the physical world (e.g., Land, 1977; Marr, 1982; Brainard & Maloney, 2011). These theories such for support from evidence that the human visual system is *optimized* for extracting surface wavelength unambiguously under naturally occurring illuminations (e.g., Abrams, Hillis, & Brainard, 2007; Foster, 2011). These theories, however, are crippled by the necessity of defining physical properties with subjective, functionally-defined attributes. That is, they must define the amount of "information" present in the world as the range of wavelengths to which the human eye is sensitive (a problem made even more complicated by the use of digital images, with sampling metameric for human vision to the external world, but certainly not capturing the true extent of its dynamic range). Such theories

then claim that human vision is optimized to process information within that range: a rather

trivial claim, given that two photoreceptor with spectral sensitivities defining each end of an

observers' visible chromatic spectrum are present by definition. In any case, studies on

comparative color vision have provided evidence that it is highly improbable that human color

perception is optimized in this sense, given that there has been great conservation of

photosensitive pigments across species evolving in vastly different environments, with vastly

different behaviors, as well as the variability of the number and type (up to at least 12; Marshall

& Arikawa, 2014) of photosensitive pigments of species in similar environments (Thompson,

1995).

This theory of color perception also differs in some specifics from those that have

attempted to focus on the benefits of color perception, specifically primate trichromacy, for

adaptive utility in detecting objects (or the state of objects) from their backgrounds. In

particular, it has been posited that primate trichromacy may have been advantageous because it

allowed for increased ability to forage for food or to detect the health/emotional states of

conspecifics (Mollon, 1989; Dominy & Lucas, 2001; Gegenfurtner, 2003; Changizi, Zhang &

Shimojo, 2006; see also Jacobs, 2013; Carvalho et al., 2017; Wu et al., 2017). As described in the

Introduction, primate trichromacy did not evolve through an unlikely mutation; however, it may

have been conserved for its benefit to behavioral performance (e.g., Sumner & Mollon, 2000;

but see also variable differences in foraging behavior between dichromats and trichromats of

the same primate species: Caine, Osorio & Mundy, 2010 and Hiramatsu et al., 2008). It seems at

least as likely, however, that fruits or edible leaves themselves have changed their coloration to

become more attractive to animals (see Polyak, 1957; Jacobs, 2013).

As an aside, it is problematic to use modern fruits and vegetables as examples of the fruits (and the diets) of early primates at the time of the appearance of trichromacy: the old-world (Catarrhine) primates of approximately 40 million years ago likely consisted of a limited range of fruits (and leaves and nuts), not including oranges or yellow bananas, and potentially not even including bright red berries (note that plants have been extensively manipulated through agricultural breeding, in part for their color appearance, over approximately the last 10,000 years). In the case of skin color, it is also difficult to extrapolate findings of the use of color in modern human skin across other trichromatic species or ancestral species with very different skin and hair coloration (Changizi, Zhang & Shimojo, 2006; Jacobs, 2013).

In any case, the hypothesis of color categorization as it applies to foraging has a different implication: instead of the role of color vision being limited to increasing visual contrast to chromatic edges, it may instead serve to categorize the background colors (e.g., the foliage) into a single perceptual group (green), irrespective of its internal luminance edges (again, see Brainard & Maloney, 2011; Carvalho et al., 2017).

In this line, I speculatively propose that color categorization emerged according to the categorical, functional relevance for the perceiver, which was first enabled due to the correlation of these things' spectral properties, influenced by complex optic and material interactions. As postulated above, the category of green may serve to categorize plants, which contain the typically dominant pigment of chlorophyll a, which has a reflectance spectra maximal between 450 and 650 nm within our range of spectral sensitivity, which centers around wavelengths commonly perceived as green. Blue is represented by a relatively wide range of wavelengths, which may correspond to the category of the sky or sea, as a product of Raleigh scattering producing spectra of less than 500 nm (note that blue conveys functional relevance

for detecting changes in weather: Jameson & Hurvich, 1989). Shorter wavelengths of light

provide more selective discriminations, and may be advantageous for categorizing food (e.g.,

with reds and yellow coming from carotenoids or dietary minerals). Accordingly, human color

categories may be biologically tuned towards properties of the environment persistent

throughout the evolution of mammal color vision, leading to some universalities across modern

people in their color categorization systems (Berlin & Kay, 1969; Cook, Kay, & Regier, 2005).

In this view, biology is dominant, but not determinant. The color categories people see

are emergent in development, and fine-tuned later in life, from perceptual experience. For

example, the perception of color (and color categories) may be influenced by the spectral statics

of their environment (Webster & Mollon, 1997; Webster, 2015), the linguistic color terms of

their language, and their learned associations of each color category with other functional

categories. Color perception is taken to reflect high-level cognitive function, i.e., not merely the

sensation from photoreceptors, but the integrated responses from learning neural systems

(Kelber & Osorio, 2010). In light of this view, the finding of high-level perceptual responses with

EEG and frequency-tagging is not surprising.

Chapter 6

References

_____

References

_____

6.1 Introduction and Transitions

Abrams, A. B., Hills, J. M. & Brainard, D. H. (2007). The relation between color discrimination and

color constancy: when is optimal adaptation task dependent? Neural Computation,

19(10), 2610-2637.

Allen, G. (1879). The colour-sense: its origin and development. Mind, 4(15), 415-421.

Anthanasopoulos, P., Dering, B., Wiggett, A., Kuipers, J. R., & Thierry, G. (2010). Perceptual shift

in bilingualism: brain potentials reveal plasticity in pre-attentive colour perception.

Cognition, 116(3), 437-443.

Bae, G. Y., Olkkonen, M., Allred, S. R., & Flombaum, J. I. (2015). Why some colors appear more

memorable than others: A model combining categories and particulars in color working

memory. Journal of Experimental Psychology: General, 144(4), 744-763.

Barlow, H. B. (1982). What causes trichromacy? A theoretical analysis using comb-filtered

spectra. Vision Research, 22(6), 635-643.

Bartels, A. & Zeki, S. (2000). The architecture of the colour centre in the human visual brain: new

results and a review. European Journal of Neuroscience, 12(1), 172-193.

Beauchamp, M. S., Haxby, J. V., Jennings, J. E. & DeYoe, E. A. (1999). An fMRI version of the

Farnsworth-Munsell 100-Hue test reveals multiple color-selective areas in human ventral

occipitotemporal cortex. Cerebral Cortex, 9(3), 257-263.

Beauchamp, M. S., Haxby, J. V., Rosen, A. C. & DeYoe, E. A. (2000). A functional MRI case study

of acquired cerebral dyschromatopsia. Neuropsychologia, 38(8), 1170-1179.

Boehm, A. E., MacLeod, D. I. A., & Bosten, J. M. (2014). Compensation for red-green contrast
    loss in anomalous trichromats. Journal of Vision, 14(13):19, 1-17.

Bornstein, M.H. (1987). Perceptual categories in vision and audition. In S. Harnad (Ed.),
    Categorical perception: The groundwork of cognition (pp. 287-300). Cambridge University
    Press: Cambridge.

Bouvier, S. E. & Engel, S. A. (2006). Behavioral deficits and cortical damage loci in cerebral
    achromatopsia. Cerebral Cortex, 16, 183–191.

Bowmaker, J. K., Thorpe, A. & Douglas, R. H. (1991). Ultraviolet-sensitive cones in the goldfish.
    Vision Research, 31(3), 349-353.

Bowmaker, J. K. & Dartnall, H. J. (1980). Visual pigments of rods and cones in a human retina.
    Journal of Physiology, 298, 501-511.

Boynton, R. M., Fargo, L., Olson, C. X., & Smallman, H. S. (1989). Category effects in color
    memory. Color Research and Application, 14(5), 229-234.

Brainard, D. H. (2015). Color and the cone mosaic. Annual Review of Vision Science, 1:519-546.

Brainard, D. H. & Maloney, L. T. (2011). Surface color perception and equivalent illumination
    models. Journal of Vision, 11(5):1, 1-18.

Brent, P. J., Kennard, C. & Ruddock, K. H. (1994). Residual colour vision in a human heianope:
    spectral responses and colour discrimination. Proceedings of the Royal Society:
    Biological Sciences, 256(1347), 219-225.

Brouwer, G. J. & Heeger, D. J. (2009). Decoding and reconstructing color from responses in
    human visual cortex. Journal of Neuroscience, 29(44), 13992-14003.

Buck, S. L. (2004). Rod-cone interactions. In L. M. Chalupa and J. S. Werner (Eds.), The Visual
    Neurosciences (vol. 2, pp. 863-878). MIT Press: Boston.

Chao, L. L., Haxby, J. V. & Martin, A. (1999). Attribute-based neural substrates in temporal cortex for perceiving and knowing about objects. Nature Neuroscience, 2(10), 913-919.

CIE, 1976. Colorimetry – Part 5. CIE Publication No. 11664-5:2016(E). Central Bureau of the Commission Internationale d'Éclairage, Vienna.

Clifford, A., Holmes, A., Davies, I. R. L. & Franklin, A. (2010). Color categories affect pre-attentive color perception. Biological Psychology, 85(2), 275-282.

Clifford, A., Franklin, A., Holmes, A., Drivonikou, V. G., Ozgen, Em., & Davies, I. R. L. (2012). Neural correlates of acquired color category effects. Brain and Cognition, 80, 126-143.

Collin, S. P. & Trezise, A. E. (2004). The origins of colour vision in vertebrates. Clinical & Experimental Optometry, 87(4-5), 217-223.

Conway, B. R., Moeller, S. & Tsao, D. Y. (2007). Specialized color modules in macaque extrastriate cortex. Neuron, 56(3), 560-573.

Conway, B. R. (2014). Color signals through dorsal and ventral visual pathways. Visual Neuroscience, 31, 197–209.

Crognale, M. A., Duncan, C. S., Shoenhard, H., Peterson, D. J. & Berryhill, M. E. (2013). The locus of color sensation: Cortical color loss and the chromatic visual evoked potential. Journal of Vision, 13(10):15, 1-11.

Cronin, T. W. & Bok, M. J. (2016). Photoreception and vision in the ultraviolet. Journal of Experimental Biology, 219(18), 2790-2801.

Dacey, D. M. (2000). Parallel pathways for spectral coding in primate retina. Annual review of neuroscience, 23(1), 743-775.

Derrington, A. M., Krauskopf, J. & Lennie, P. (1984). Chromatic mechanisms in lateral geniculate nucleus of macaque. Journal of Physiology, 357, 241-265.

De Valois, R. L., Smith, C. J., Karoly, A. J. & Kitai, S. T. (1958). Electrical responses of primate

　　visual system. I. Different layers of macaque lateral geniculate nucleus. Journal of

　　Comparative Physiological Psychology, 51(6), 662-668.

De Valois, R. L., Abramov, I. & Jacobs, G. H. (1996). Analysis of response patterns of LGN cells.

　　Journal of the Optical Society of America, 56(7), 966-977.

Dumoulin, S. O., Harvey, B. M., Fracasso, A., Zuiderbaan, W., Luijten, P. R., Wandell, B. A., &

　　Petridou, N. (2017). In vivo evidence of functional and anatomical stripe-based

　　subdivisions in human V2 and V3. Scientific Reports, 7:733, 1-12.

Emery, K. J., Volbrecht, V. J., Peterzell, D. H., & Webster, M. A. (2017). Variations in normal color

　　vision: VII. Relationships between color naming and hue scaling. Vision Research, 141,

　　66-75.

Engel, S. A. (2005). Adaptation of oriented and unoriented color-selective neurons in human

　　visual areas. Neuron, 34(4), 613-623.

Engel, S. A. & Furmanski, C. S. (2001). Selective adaptation to color contrast in human primary

　　visual cortex. Journal of Neuroscience, 21(11), 3949-3954.

Engel, S. A., Zhang, X. & Wandell, B. (1997). Colour tuning in human visual cortex measured with

　　functional magnetic resonance imaging. Nature, 388(6637), 68-71.

Fonteneau, E. & Davidoff, J. (2007). Neural correlates of colour categories. Cognitive

　　Neuroscience and Neurophysiology, 18(13), 1323-1327.

Forder, L., He, X. & Franlkin, A. (2017). Colour categories are reflected in sensory stages of

　　colour perception when stimulus issues are resolved. PLOS One, 12(5): e0178097.

Foster, D. H. (2011). Color constancy. Vision Research, 51(7), 674-700.

Frome, F. S., Buck, S. L., & Boynton, R. M. (1981). Visibility of borders: separate and combined effects of color differences, luminance contrast, and luminance level. Journal of the Optical Society of America, 71(2), 145-150.

Gegenfurtner, K. R. (2003). Cortical mechanisms of colour vision, Nature Reviews Neuroscience, 4, 563-572.

Gegenfurtner, K. R. & Kiper, D. C. (2003). Annual Review of Neuroscience, 26, 181-206.

Gerth, C., Delahunt, P. B., Crognale, M. A., & Werner, J. S. (2003). Topography of the chromatic pattern-onset VEP. Journal of Vision, 3, 171-182.

Gilbert, A. L., Reiger, T., Kay, P. & Ivry, R. B. (2006). Whorf hypothesis is supported in the right visual field but not the left. PNAS USA, 103(2), 489-494.

Goddard, E., Mannion, D. J., McDonald, J. S., Solomon, S G. & Clifford, C. W. G. (2011). Color responsiveness argues against a dorsal component of human V4. Journal of Vision, 11(4):3, 1-21.

Gouras, P. & Zrenner, E. (1981). Color coding in primate retina. Vision Research, 21(11), 1591-1598.

Hadjikhani, N., Liu, A. K., Dale, A. M., Cavanagh, P. & Tootell, R. B. H. (1998). Retinotopy and color sensitivity in human visual cortical area V8. Nature Neuroscience, 1, 235–241.

Hanley, J. R. (2015). Color categorical perception. Encyclopedia of Color Science and Technology, 1-6. Springer Science+Business Media: New York.

Hardin, C. L. (1992). The Virtues of Illusion, Philosophical Studies, 68(3), 371-82.

Harnad, S. (1987). Categorical perception. Cambridge University Press: Cambridge.

Hatfield, G. (I992). Color perception and neural encoding: does metameric matching entail a loss

    of information? Proceedings of the Biennial Meeting of the Philosophy of Science

    Association, 1, 492-504.

He, X., Witzel, C., Forder, L., Clifford, A. & Franklin, A. (2014). Color categories only affect pot-

    perceptual processes when same- and different-category colors are equally

    discriminable. Journal of the Optical Society of America A, 31(4), A322-331.

Hering, E. (1920). Grundzüge der Lehre vom Lichtsinn. Berlin: Springer. (English version: Outlines

    of a Theory of the Light Sense. 1964. Translated by L.M. Hurvich and D. Jameson.

    Cambridge, MA: Harvard University Press).

Horiguchi, H., Winawer, J., Dougherty, R. F. & Wandell, B. A. (2012). Human trichromacy

    revisited. PNAS USA, 110(3), E260-269.

Jacobs, G. H. (1996). Primate photopigments and primate color vision. PNAS USA, 93(2), 577-

    581.

Jacobs, G. H. (2009). Evolution of colour vision in mammals. Philosophical Transactions of the

    Royal Society B, 364, 2957-2967.

Jacobs, G. H. (2013). Losses of functional opsin genes, short-wavelength cone photopigments,

    and color vision –a significant trend in the evolution of mammalian vision. Visual

    Neuroscience, 30(1-2), 39-52.

Jaeger, W., Krastel, H., & Braun, S. (1988). Cerebral achromatopsia (symptoms, course,

    differential diagnosis and strategy of the study). I. Klinische Monatsblatter fur

    Augenheilkunde, 193(6), 627–634.

Jameson, K. A. & D'Andrade, R. G. (1997). It's not really red, green, yellow, blue : an inquiry into perceptual color space. In C. L. Hardin & L. Maffi (Eds.), Color Categories in Thought and Language, (pp. 295-319). Cambridge University Press: New York.

Johnson, E. N. & Mullen, K. T. (2016). Color in the Cortex. In Human Color Vision (pp. 189-217). Springer International Publishing.

Jones, C. D., Osorio, D. & Baddeley, R. J. (2001). Colour categorization by domestic chicks. Philosophical Transactions of the Royal Society B, 268, 2077-2084.

Jonson, E. N. & Mullen, K. T. (2016). Color in the Cortex. In J. Kremers et al. (Eds.), Human Color Vision, Springer: Zurich.

Jordan, G. & Mollon, J. D. (1993). A study of women heterozygous for colour deficiencies. Vision Research, 33(11), 1495-1508.

Jordan, G., Deeb, S. S., Bosten, J. M., & Mollon, J. D. (2010). The dimensionality of color vision in carriers of anomalous trichromacy. Journal of Vision, 10(8):12, 1-19.

Kelber, A. & Osorio, D. (2010). From spectral information to animal colour vision: experiments and concepts. Philosophical Transactions of the Royal Society B, 277, 1617-1625.

Lafer-Sousa, R., Conway, B. R. & Kanwisher, N. G. (2016). Color-biased regions of the ventral visual pathway lie between face- and place-selective regions in humans, as in macaques. Journal of Neuroscience, 36(5), 1682-1697.

Land, E . H. (1977). The retinex theory of color vision. Scientific American, 237(6), 108-128.

Lee, B. B. (2008). The evolution of concepts of color vision. Neurociencias, 4(4), 209-224.

Lee, B. B. (2014). Color coding in the primate visual pathway: a historical view. Journal of the Optical Society of America A, 31(4), A103-A112.

Liu, J. & Wandell, B. A. (2005). Specializations for chromatic and temporal signals in human visual cortex. Journal of Neuroscience, 25, 3459–3468.

Lucas, R. J. (2013). Mammalian inner retinal photoreception. Current Biology, 23(3), R125-133.

Lueck, C. J., Zeki, S., Friston, K. J., Deiber, M. P., Cope, P., Cunningham, V. J., et al. (1989). The colour centre in the cerebral cortex of man. Nature, 340, 386–389.

MacLeod, D. I. & Boynton, R. M. (1979). Chromaticity diagram showing cone excitation by stimuli of equal luminance. Journal of the Optical Society of America, 69(8), 1183-1186.

Marr, D. 1982 . Vision. Freeman: New York.

Marshall, J. & Arikawa, K. (2014). Unconventional colour vision. Current Biology, 24(24), R1150-R1154.

Martin, A., Haxby, J. V., Lalonde, F. M., Wiggs, C. L., & Ungerleider, L. G. (1995). Discrete cortical regions associated with knowledge of color and knowledge of action. Science, 270(5233), 102-105.

McCann, J. J. & Benton, J. L. (1969). Interaction of the long-wave cones and the rods to produce color sensations. Journal of the Optical Society of America, 59(1), 103-107.

McKeefry, D. J. & Zeki, S. (1997). The position and topography of the human colour centre as revealed by functional magnetic resonance imaging. Brain, 120(12), 2229-2242.

Meadows, J. C. (1974). Disturbed perception of colours associated with localized cereberal lesions. Brain, 97, 615–632.

Menzel, R. & Backhaus, W. (1991). Colour vision in insects. In: P. Gouras (Ed.), Vision and Visual Dysfunction. The perception of Colour (pp. 262-288). MacMillan: London.

Mo, L., Xu, G., Kay, P. & Tan, L. H. (2011). Electrophysiological evidence for the left-lateralized

    effect of language on preattentive categorical perception of color. PNAS USA, 108(34),

    14026-14030.

Mullen, K. T., Chang, D. H. F. & Hess, R. F. (2015). The selectivity of responses to red-green

    colour and achromatic contrast in the human visual cortex: an fMRI adaptation study.

    European Journal of Neuroscience, 42, 2923-2933.

Mullen, K. T., Dumoulin, S. O., McMahon, K. L., de Zubicaray, G. I., & Hess, R. F. (2007).

    Selectivity of human retinotopic visual cortex to S-cone-opponent, L/M-cone-opponent

    and achromatic stimulation. European Journal of Neuroscience, 25, 491–502.

Murphey, D. K., Yoshor, D. & Beauchamp, M. S. (2008). Perception matches selectivity in the

    human anterior color center. Current Biology, 18(3), 216-220.

Naka, K. I. & Rushton, W. A. (1966). An attempt to analyse colour reception by

    electrophysiology, 185(3), 556-586.

Nasr, S., Polimeni, J. R., & Tootell, R. B. (2016). Interdigitated color- and disparity-selective

    columns within human visual cortical areas V2 and V3. Journal of Neuroscience, 36(6),

    1841-1857.

Nassau, K. (1983). The Physics and Chemistry of Color. John Wiley & Sons: New York.

Nathans, J. , Thomas, D., & Hogness, D. S. (1986). Molecular genetics of human color vision: the

    genes encoding blue, green, and red pigments. Science, 232, 193-202.

Neitz, J. & Neitz, M. (2011). The genetics of normal and defective color vision. Vision Research,

    51(7), 633-651.

Neitz, J. & Jacobs, G. H. (1986). Polymorphism of the long-wavelength cone in normal human

    colour vision. Nature, 323(6089), 623-625.

Persichetti, A. S., Thomposon-Schill, S. L., Butt, O. H., Brainard, D. H., & Aguirre, G. K. (2015). Functional magnetic resonance imaging adaptation reveals a noncategorical representation of hue in early visual cortex. Journal of Vision, 15(6):18, 1–19.

Pilling, M., Wiggett, A., Ozgen, E. & Davies, I. R. L. (2003). Is color "categorical perception" really perceptual? Memory and Cognition, 31(4), 538-551.

Poralla, J. & Neumeyer, C. (2006). Generalization and categorization of spectral color in goldfish. II. Experiments with two and six training wavelengths. Journal of Comparative Physiology A, 192(5), 469-179.

Rabin, J., Switkes, E., Crognale, M. A., Schneck, M. E. & Adams, A. J. (1994). Visual evoked potentials in three-dimensional color space: Correlates of spatio-chromatic processing. Vision Research, 34, 2657–2671.

Regan D. (1966). Some characteristics of average steady-state and transient responses evoked by modulated light. Electroencephalography and Clinical Neurophysiology, 20 (3), 238–248.

Retter, T. L. & Rossion, B. (2016). Uncovering the neural magnitude and spatio-temporal dynamics of natural image categorization in a fast visual stream. Neuropsychologia, 91, 9-28.

Riggs, L. A. & Sternheim, C. E. (1968). Human retinal and occipital potentials evoked by changes of the wavelength of the stimulation light. Journal of the Optical Society of America, 59(5), 635-640.

Roberson, D., Pak, H. & Hanley, J. R. (2008). Categorical perception of colour in the left and right visual field is berbally mediated: evidence from Korean. Cognition, 107(2), 752-762.

Rodieck, R. W. (1998). The first steps in seeing. Sinauer Associates: Sunderland, MA.

Sabesan, R., Schmidt, B. P., Tuten, W. S., & Roorda, A. (2016). The elementary representation of spatial and color vision in the human retinal. Science Advances, 2, e1600797.

Schnapf, J. L., Kraft, T. W. & Baylor, D. A. (1987). Spectral sensitivity of human cone photoreceptors. Nature, 325(6103), 439-441.

Schragom C. G. & Russo, C. A. (2003). Timing the origin of New World Monkeys. Molecular Biology and Evolution, 20(10), 1620-1625.

Shapley, R. (2019). Physiology of color vision in primates. Oxford Research Encyclopedia of Neuroscience. 1-34.

Shapley, R. & Hawken, M. J. (2011). Color in the cortex: single- and double-opponent cells. Vision Research, 51(7), 701-717.

Shapley, R. M., Hawken, M. J. & Johnson, E. B. (2014). Color in primary visual cortex. In J. S. Werner & L. M. Chalupa (Eds.) The New Visual Neurosciences (pp. 569-586), MIT Press: Cambridge.

Simmons, W., Ramjee, V., Beauchamp, M. S., McRae, K., Martin, A., & Barsalou, L. W. (2007). A common substrate for perceiving and knowing about color. Neuropsychologia, 45(12), 2802-2810.

Slotnick, S. D. (2009). Memory for color reactivates color processing region. Cognitive Neuroscience and Neurophysiology, 20, 1568-1571.

Smith, R. C. & Baker, K. S. (1981). Optical properties of the clearest natural waters (200-800 nm). Applied Optics, 20(2), 177-184.

Smith, V. C. & Pokorny, J. (1977). Large-field trichromacy in protanopes and deuteranopes. Journal of the Optical Society of America, 67(2), 213-220.

Solomon, S. G. & Lennie, P. (2007) The machinery of colour vision. Nature Reviews
    Neuroscience, 8, 276-286.

Stoerig, P. & Cowey, A. (1989). Wavelength sensitivity in blindsight. Nature, 342(6252), 916-918.

Stockman, A. & Sharpe, L. T. (2000). The spectral sensitivities of the middle- and long-
    wavelength-sensitive cones derived from measurements in observers of known
    genotype. Vision Research, 40(13), 1711-1737.

Sumner, P., Anderson, E. J., Sylvester, R., Haynes, J. D. & Rees, G. (2008). Combined orientation
    and colour information in human V1 for both L-M and S-cone chromatic axes.
    NeuroImage, 39(2), 814-824.

Thierry, G., Athanasopoulos, P., Wiggett, A., Dering, B. & Kuipers, J.-R. (2009). Unconscious
    effects of language-specific terminology on preattentive color perception. Proceedings
    of the National Academy of Sciences, 106(11), 4567-4570.

Thompson, E. (1995). Colour vision, evolution, and perceptual content. Synthese, 104, 1-32.

Thompson, E., Palacios, A. & Varela, F. J. (1992). Ways of coloring : Comparative color vision as a
    case study for cognitive sciences. In F. J. Newmeyer (Ed.), Language Form and Language
    Function, pp. 351-418. MIT Press: Boston.

Tootell, R. B., Silverman, M. S., De Valois, R. L. & Jacobs, G. H. (1983). Functional organization of
    the second cortical visual area in primates. Science, 220(4598), 737-739.

Tootell, R. B., Nelissen, K., Vanduffel, W. & Orban, G. A. (2004). Search for color 'center(s)' in
    macaque visual cortex. Cerebral Cortex, 14(4), 353-363.

Ts'o, D. Y. & Gilbert, C. D. (1988). The Organization of Chromatic and Spatial Interactions in the
    Primate Striate Cortex. The Journal of Neuroscience, 8(5), 1712-l 727.

Uchikawa, K., & Shinoda, H. (1996). Influence of basic color categories on color memory

   discrimination. Color Research and Applications, 21(6), 430-439.

Verrey, D. (1888). Hemiachromatopsie droite absolute. Archives de Ophthalimologie (Paris), 8,

   289-300.

von Helmholtz, H. (1867). Handbuch der Physiologischen Optik, Vol. II, published by Leopold

   Voss: Leipzig. In J.P.C. Southall (Ed.), Translation (Helmoltz's Treatise on Physiological

   Optics, 1909), Optical Society of America: Washington, D.C., 1924, pp. 286-287.

Wade, A. R., Brewer, A. A., Rieger, J. W., & Wandell, B. B. (2002). Functional measurements of

   human ventral occipital cortex: retinotopy and colour. Philosophical Transaction of the

   Royal Society of London B, 357, 963–973.

Wade, A. R., Augath, M., Logothesis, N., & Wandell, B. A. (2008). fMRI measurements of color in

   macaque and human. Journal of Vision, 8(10), 1-6.

Wandell, B. A., Dumoulin, S. O. & Brewer, A. A. (2007). Visual field maps in human cortex.

   Neuron, 56(2), 366-383.

Wassle, H. (2004). Parallel processing in the mammalian retina. Nature Reviews Neuroscience,

   5(10), 747-757.

Webster, M. A. (2015). Color Vision. In J. T. Wixted & J. Serences (Eds.) Stevens' Handbook of

   Experimental Psychology and Cognitive Neuroscience, Fourth Edition, Vol. 2. (pp. 343-

   384). Wiley.

Webster, M. A. & Kay, P. (2012). Color categories and color appearance. Cognition, 122(3), 375-

   392.

Webster, M. A. Juricevic, I. & McDermott, K. C. (2010). Simulations of adaptation and color appearance in observers with varying spectral sensitivity. Opthalmic & Physiological Optics, 30(5), 302-610.

Webster, M. A., Miyahara, E., Malkoc, G. & Raker, V. E. (2000). Variations in normal color vision. I. Cone-opponent axes. Journal of the Optical Society of America A, 17(9), 1535-1544.

Winawer, J., Witthoft, N., Frank, M. C., Wu, L., Wade, A R. & Broditsky, L. (2007). Russian blues reveal effects of language on color discrimination. PNAS USA, 104(19), 7780-7785.

Winawer, J., Horiguchi, H., Sayres, R. A., Amano, K. & Wandell, B. A. (2010). Mapping hV4 and ventral occipital cortex: The venous eclipse. Journal of Vision, 10(5), 1-33.

Winawer, J. & Witthoft, N. (2015). Human V4 and ventral occipital retinotopic maps. Visual Neuroscience, 32:E020, 1-27.

Winkler, A., Spillmann, L., Werner, J. S. & Webster, M. A. (2015). Asymmetries in blue-yellow color perception and in the color of "the dress". Current Biology, 25(13), R547-R548.

Witzel, C. & Gegenfurtner, K. R. (2015). Categorical facilitation with equally discriminable colors. Journal of Vision, 15(8):22.

Wright, A. A. & Cumming, W. W. (1971). Color-naming functions for the pigeon. Journal of the Experimental Analysis of Behavior, 15(1), 7-17.

Xiao, M., Wang, Y. & Fellman, D. (2003). A spatially organized representation of colour in macaque cortical area V2. Nature, 421(6922), 535-539.

Yang, J., Kanazawa, S., Yamaguchi, M. K. & Kuriki, I. (2016). Cortical response to categorical color perception in infants investigated by near-infrared spectroscopy. PNAS, 113(9), 2370-2375.

Yokoyama, S. & Yokoyama, R. (1989). Molecular evolution of human visual pigment genes.

Molecular Biology & Evolution, 6(2), 186-197.

Young, T. (1802). II. The Bakerian Lecture. On the theory of light and colours. Philosophical

Transactions of the Royal Society, 92, 12--49.

Zeki, S. M. (1973). Colour coding in rhesus monkey prestriate cortex. Brain Research, 53, 422-

427.

Zeki S. (1990). A century of cerebral achromatopsia. Brain, 113, 1721–1777.

Zeki, S. & Bartels, A. (1999). The clinical and functional measurement of cortical (in)activity in

the visual brain, with special reference to the two subdivisions (V4 and V4α) of the

human colour centre. Philosophical Transactions of the Royal Society of London B, 354,

1371-1382.

Zeki, S. & Marini, L. Three cortical stages of color processing in the human brain. Brain, 121, 166-

1685.

Zeki, S., Watson, J. D. G., Lueck, C. J., Friston, K. J., Kennard, C. & Frackowiak, R. S. J. (1991). A

direct demonstration of functional specialization in human visual-cortex. Journal of

Neuroscience, 11, 641–649.

6.2 Study 1: Neural correlates of perceptual color inferences as revealed by #thedress

Ales, J. M. & Norcia, A. M. (2009). Assessing direction-specific adaptation using the steady-state

visual evoked potential: Results from EEG source imaging. Journal of Vision, 9(7):8, 1–13.

Allison, T., Begleiter, A., McCarthy, G., Roessler, E. Nobre, A. C. & Spencer, D. D. (1993).

Electrophsyiological studies of color processing in human visual cortex.

Electroencephalography and Clinical Neurophysiology, 88(5), 343-355.

Anllo-Vento, L., Luck, S. J. & Hillyard, S. A. (1998). Spatio-temporal dynamics of attention to

    color: evidence from human electrophysiology. Human Brain Mapping, 6(4), 216-238.

Arend, L. & Reeves, A. (1986). Simultaneous color constancy. Journal of the Optical Society of

    America A, 3, 1743-1751.

Beauchamp, M. S., Haxby, J. V., Jennings, J. E. & DeYoe, E. A. (1999). An fMRI version of the

    Farnsworth-Munsell 100-Hue test reveals multiple color-selective areas in human ventral

    occipitotemporal cortex. Cerebral Cortex, 9(3), 257-263.

Berens, P. (2009). CircStat: A MATLAB toolbox for circular statistics. Journal of Statistical

    Software, 31, 1–21.

Bouvier, S. E. & Engel, S. A. (2006). Behavioral deficits and cortical damage loci in cerebral

    achromatopsia. Cerebral Cortex, 16, 183–191.

Brainard, D. H. & Wandell, B. A. (1992). Asymmetric color matching: How color appearance

    depends on the illuminant. Journal of the Optical Society of America A, 9, 1433-1448.

Brainard, D. H. & Hurlbert, A. C. (2015). Colour vision: Understanding #TheDress. Current

    Biology, 25, R551–R554.

Brouwer, G. J. & Heeger, D. J. (2009). Decoding and reconstructing color from responses in

    human visual cortex. Journal of Neuroscience, 29(44), 13992-14003.

Chetverikov, A. & Ivanchei, I. (2016). Seeing "the dress" in the right light: perceived colors and

    inferred light sources. Perception, 45(8), 910-930.

Churma, M.E. (1994). Blue shadows: physical, physiological, and psychological causes. Applied

    Optics, 33, 4719–4722.

Coggan, D. C., Liu, W., Baker, D. H. & Andrews, T. J. (2016). Category-selective patterns of neural response in the ventral visual pathway in the absence of categorical information. NeuroImage, 135, 107-114.

Coia, A. J., Jones, C., Duncan, C. S. & Crognale, M. A. (2014). Physiological correlates of watercolor effect. Journal of the Optical Society of America A, 31(4), A15-A22.

Conway, B. R. (2009). Color vision, cones, and color-coding in the cortex. Neuroscientist, 15(3), 274-290.

Conway, B. R. & Tsao, D. Y. (2009). Color-tuned neurons are spatially clustered according to color preference within alert macaque posterior inferior temporal cortex. Proceedings of the National Academy of Sciences, 106(42), 18034-18039.

Conway, B. R., Chatterjee, S., Field, G. D., Horwitz, G. D., Johnson, E. N., Koida, K. & Mancuso, K. (2010). Advances in color science: from retina to behavior. Journal of Neuroscience, 30(45), 14955-14963.

Conway, B. R. (2014). Color signals through dorsal and ventral visual pathways. Visual Neuroscience, 31, 197–209.

Corbetta, M., Miezin, F. M., Dobmeyer, S., Shulman, G. L. & Petersen, S. E. (1990). Attentional modulation of eural processing of shape, color, and velocity in humans. Science, 248(4962), 1556-1559.

Corbetta, M., Miezin, F. M., Dobmeyer, S., Shulman, G. L. & Petersen, S. E. (1991). Selective and divided attention during visual discriminations of shape, color, and speed: functional anatomy by positron emission tomography. Journal of Neuroscience, 11(8), 2383-2402.

Crognale, M. A., Duncan, C. S., Shoenhard, H., Peterson, D. J. & Berryhill, M. E. (2013). The locus of color sensation: Cortical color loss and the chromatic visual evoked potential. Journal of Vision, 13(10):15, 1-11.

Dacey, D. M. (2000). Parallel pathways for spectral coding in primate retina. Annual review of neuroscience, 23(1), 743-775.

Dacey, D. M., Crook, J. D. & Packer, O. S. (2014). Distinct synaptic mechanisms create parallel S-ON and S-OFF color opponent pathways in the primate retina. Visual Neuroscience, 31(2), 139-151.

Derrington AM, Krauskopf J, Lennie P. Chromatic mechanisms in lateral geniculate nucleus of macaque. The Journal of physiology. 1984 Dec 1;357(1):241-65.

Dixon, E. L. & Shapiro, A. G. (2017). Spatial filtering, color constancy, and the color-changing dress. Journal of Vision, 17(3):7.

Dzhelyova, M. & Rossion, B. (2014). The effect of parametric stimulus size variation on individual face discrimination indexed by fast periodic visual stimuliation. BMC Neuroscience, 15:87, 1-12.

D'Zmura, M., & Lennie, P. (1986). Mechanisms of color constancy. JOSA A, 3(10), 1662-1672.

Engel, S., Zhang, X. & Wandell, B. (1997). Colour tuning in human visual cortex measured with functional magnetic resonance imaging. Nature, 388(6637), 68-71.

Forder, L., Bosten, J., He, X. & Franklin, A. (2017). A neural signature of the unique hues. Scientific Reports, 7:42364, 1-8.

Foster, D. H. (2011). Color constancy. Vision Research, 51(7), 674-700.

Foster, D. H., Craven, B. J. & Sale, E. R. H. (1992). Immediate colour constancy. Opthalmic & Physiological Optics. 12(2), 157-160.

Gegenfurtner, K. R. (2003). Cortical mechanisms of colour vision, Nature Reviews Neuroscience, 4, 563-572.

Gegenfurtner, K. R., Bloj, M., & Toscani, M. (2015). The many colours of 'the dress.' Current Biology, 25, R543–R544.

Goddard, E., Mannion, D. J., McDonald, J. S., Solomon, S G. & Clifford, C. W. G. (2011). Color responsiveness argues against a dorsal component of human V4. Journal of Vision, 11(4):3, 1-21.

Goffaux, V., Jacques, C., Mouraux, A., Oliva, A., Schyns, P. G., Rossion, B. (2005). Diagnostic Colors Contribute to the Early Stages of Scenes Categorization: Behavioral and Neurophysiological Evidence. Visual Cognition, 12, 878-892.

Granrud, C., Yonas, A. & Opland, E. (1985) Infants' sensitivity to the depth cue of shading. Perception and Psychophysics, 37(5), 415–419.

Hadjikhani, N., Liu, A. K., Dale, A. M., Cavanagh, P. & Tootell, R. B. H. (1998). Retinotopy and color sensitivity in human visual cortical area V8. Nature Neuroscience, 1, 235–241.

Hesslinger, V. M. & Carbon, C. C. (2016). #TheDress: The role of illumination information and individual differences in the psychophysics of perceiving white-blue ambiguities. I-perception, 7(2):2041669516645592, 1-10.

Hurlbert, A. C. (1998). Computational models of color constancy. In Walsh, V. Kulikowski, J. (Eds.), Perceptual Constancy: Why Things Look As They Do (pp. 283–322). Cambridge: Cambridge University Press.

Jacques, C.*, Retter, T.L.*, Rossion, B. (2016). A single glance at a face generates larger and qualitatively different category-selective spatio-temporal signatures than other ecologically-relevant categories in the human brain. *NeuroImage*, 137, 21-33.

Jaeger, W., Krastel, H., & Braun, S. (1988). Cerebral achromatopsia (symptoms, course,

differential diagnosis and strategy of the study). I. Klinische Monatsblatter fur

Augenheilkunde, 193(6), 627–634.

Johnson, E. N. & Mullen, K. T. (2016). Color in the Cortex. In Human Color Vision (pp. 189-217).

Springer International Publishing.

Keysers, C., Xiao, D. K., Foldiak, P. & Perrett, D. I. (2001). The speed of sight. Journal of Cognitive

Neuroscience, 13(1), 90-101.

Kulikowski, J. J., Walsh, V., McKeefry, D., Butler, S. R. & Carden, D. (1994). The

electrophysiological basis of colour processing in macaques with V4 lesions. Behavioral

Brain Research, 60, 73-78.

Krauskopf, J., Williams, D. R. & Heeley, D. W. (1982). Cardinal directions of color space. Vision

Research, 22, 1123–1131.

Kuriki, I., Nakamura, S., Sun, P., Ueno, K., Matsumiya, K. et al. (2011). Decoding color responses

in human visual cortex. IEICE Transactions on Fundamentals of Electronics,

Communications, and Computer Sciences, E94.A(2), 473-479.

Lafer-Sousa, R., Hermann, K. L. & Conway, B. R. (2015). Striking individual differences in color

perception uncovered by 'the dress' photograph. Current Biology, 25, R545–R546.

Lafer-Sousa, R., Conway, B. R. & Kanwisher, N. G. (2016). Color-biased regions of the ventral

visual pathway lie between face- and place-selective regions in humans, as in macaques.

Journal of Neuroscience, 36(5), 1682-1697.

Lafer-Sousa, R. & Conway, B. R. (2017). #TheDress: Categorical perception of an ambiguous color

image. Journal of Vision, 17(12):25, 1-30.

Land, E. H. & McCann, J. J. (1971). Lightness and retinex theory. Journal of the Optical Society of America, 61(1), 1-11.

Lee, B. B. (2004). Paths to colour in the retina. Clinical and Experimental Optometry, 87(4-5), 239-248.

Liu, J. & Wandell, B. A. (2005). Specializations for chromatic and temporal signals in human visual cortex. Journal of Neuroscience, 25, 3459–3468.

Lotto, R. B., & Purves, D. (2002). The empirical basis of color perception. Consciousness and Cognition, 11, 609–629.

Luck, S. J. An introduction to the event-related potential technique (2005). Cambridge, MA: MIT Press.

Lueck, C. J., Zeki, S., Friston, K. J., Deiber, M. P., Cope, P., Cunningham, V. J., et al. (1989). The colour centre in the cerebral cortex of man. Nature, 340, 386–389.

Mahroo, O. A., Williams, K. M., Hossain, I T., Yonova-Doing, E., Kozareva, D. et al. (2017). Do twins share the same dress code? Quantifying relative genetic and environmental contributions to subjective perceptions of "the dress" in a classical twin study. Journal of Vision, 17(1):29, 1-7.

McCarthy, G. & Wood, C. C. (1985). Scalp distributions of event-related potentials: an ambiguity associated with analysis of variance models. Electroencephalography and Clinical Neurophysiology, 62(3), 203-208.

McDermott, K. C., Malkoc, G., Mulligan, J. B., & Webster, M. A. (2010). Adaptation and visual salience. Journal of vision, 10(13), 17-17.

Meadows, J. C. (1974). Disturbed perception of colours associated with localized cereberal lesions. Brain, 97, 615–632.

Mullen, K. T., Dumoulin, S. O., McMahon, K. L., de Zubicaray, G. I., & Hess, R. F. (2007). Selectivity of human retinotopic visual cortex to S-cone-opponent, L/M-cone-opponent and achromatic stimulation. European Journal of Neuroscience, 25, 491–502.

Murphey, D. K., Yoshor, D. & Beauchamp, M. S. (2008). Perception matches selectivity in the human anterior color center. Current Biology, 18(3), 216-220.

Norcia, A. M., Appelbaum, L. G., Ales, J. M., Cottereau, B. R. & Rossion, B. (2015). The stead-state visual evoked potential in vision research: A review. Journal of Vision, 15(6):4, 1-46.

Oostenveld, R. & Praamstra, P. (2001). The five percent electrode system for high-resolution EEG and ERP measurements. Clinical Neurophysiology,112(4), 713-719.

Parkes, L. M., Marsman, J. B., Oxley, D. C., Goulemas, J. Y. & Wuerger, S. M. (2009). Multivoxel fMRI analysis of color tuning in human primary visual cortex. Journal of Vision, 9(1):1, 1-13.

Pearce, B., Crichton, S., Mackiewicz, M., Finlayson, G.D. & Hurlbert, A. (2014). Chromatic illumination discrimination ability reveals that human colour constancy is optimised for blue daylight illuminations. PLoS One, 9, e87989.

Poldrack, R. A., Halchenko, Y. O., Hanson, S. J. (2009). Decoding the large-scale structure of brain function by classifying mental states across individuals. Psychological Science, 20, 1364–1372.

Potter, M.C., Wyble, B., Hagmann, C.E., & McCourt, E.S. (2014). Detecting meaning in RSVP at 13 ms per picture. Attention, Perception, & Psychophysics, 76(2), 270-279.

Rabin, J., Switkes, E., Crognale, M. A., Schneck, M. E. & Adams, A. J. (1994). Visual evoked potentials in three-dimensional color space: Correlates of spatio-chromatic processing. Vision Research, 34, 2657–2671.

Rabin, J., Houser, B., Talbert, C. & Patel, R. (2016). Blue-black or white-gold? Early stage

processing and the color of 'the dress'. PLOS One, 11(8), e0161090.

Regan D. (1966). Some characteristics of average steady-state and transient responses evoked

by modulated light. Electroencephalography and Clinical Neurophysiology, 20 (3), 238–

248.

Retter, T. L. & Rossion, B. (2016a). Visual adaptation provides objective electrophysiological

evidence of facial identity discrimination. Cortex, 80, 35-50.

Retter, T. L. & Rossion, B. (2016b). Uncovering the neural magnitude and spatio-temporal

dynamics of natural image categorization in a fast visual stream. Neuropsychologia, 91, 9-

28.

Retter, T. L. & Rossion, B. (2017). Visual adaptation reveals an objective electrophysiological

measure of high-level individual face discrimination. Scientific Reports, 7:3269, 1-10.

Roman Originals (2018). #The Dress that broke the internet. Available at:

https://www.romanoriginals.co.uk/thedress [Accessed January 20, 2018].

Rossion, B., Prieto, E. A., Boremanse, A., Kuefner, D. & Van Belle, G. (2012). A steady-state visual

evoked potential approach to individual face perception: effect of inversion, contrast-

reversal and temporal dynamics. NeuroImage, 63, 1585–1600.

Rossion, B. (2014a). Understanding individual face discrimination by means of fast periodic

visual stimulation. Experimental Brain Research, 232, 1599-1621.

Rossion, B. (2014b). Understanding face perception by means of human electrophysiology.

Trends in Cognitive Sciences, 18, 310-318.

Rossion, B., Torfs, K., Jacques, C. & Liu-Shuang, J. (2015). Fast periodic presentation of natural face images reveals a robust face-selective electrophysiological response in the human brain. Journal of Vision, 15(1):18, 1-.

Sakai, K., Watanabe, E., Onodera, Y., Uchida, I., Kato, H. et al. (1995). Functional mapping of the human colour centre with echo-planar magnetic resonance imaging. Proceedings of the Royal Society of London B, 261, 89-98.

Sato, K., Kanazawa, S. & Yamaguchi, M. K. (2016). Infants' discrimination of shapes from shading and cast shadows. Attention, Perception and Psychophysics, 78(5), 1453-1459.

Schalk, G., Kapeller, C., Guger, C., Ogawa, H., Hiroshima, S. et al. (2017). Facephenes and rainbows: Causal evidence for functional and anatomical specificity of face and color processing in the human brain. Proceedings of the National Academy of Sciences, 114(46), 12285-12290.Schlaffke, L., et al. (2015). The brain's dress code: How The Dress allows to decode the neuronal pathway of an optical illusion, Cortex, 73, 271–275.

Shapley, R. & Hawken, M. J. (2011). Color in the cortex: single- and double-opponent cells. Vision Research, 51(7), 701-717.

Shevell, S. K. & Kingdom, F. A. (2008). Color in complex scenes. Annu. Rev. Psychol., 59, 143-166.

Smithson, H. E. (2005). Sensory, computational and cognitive components of human colour constancy. Philosophical Transactions of the Royal Society of London B, 360, 1329-1346.

Solomon, S. G. & Lennie, P. (2007) The machinery of colour vision. Nature Reviews Neuroscience, 8, 276-286.

Srinivasan, R., Russell, D. P., Edelman, G. M. & Tononi, G. (1999). Increased synchronization of neuromagnetic responses during conscious perception. Journal of Neuroscience, 19, 5435-5448.

Swiked (2015). guys-please-help-me-is-this-dress-white-and. Available

at: http://swiked.tumblr.com/post/112073818575/guys-please-help-me-is-this-dress-

white-and [Accessed January 20, 2018].

Tailby, C., Solomon, S. G. & Lennie, P. (2008). Functional asymmetries in visual pathways

carrying S-cone signals in macaque. Journal of Neuroscience, 28(15), 4078-4087.

Thierry, G., Athanasopoulos, P., Wiggett, A., Dering, B. & Kuipers, J.-R. (2009). Unconscious

effects of language-specific terminology on preattentive color perception. Proceedings of

the National Academy of Sciences, 106(11), 4567-4570.

Toscani, M., Gegenfurtner, K. R., & Doerschner, K. (2017). Differences in illumination estimation

in #thedress. Journal of Vision, 17 (1): 22, 1–14

Tyler, C. W. & Kaitz, M. (1977). Movement adaptation in the visual evoked response.

Experimental Brain Research, 27, 209–209.

van den Brink, R. (2014). *circ_htest.m* (Version 1.0.0.0) [Source code]. Available from

https://www.mathworks.com/matlabcentral/fileexchange/46349-circ_htest-m

Vemuri, K., Bisla, K., Mulpuru, S. & Varadharajan, S. (2016). Do normal pupil diameter

differences in the population underlie the color selection of #the dress? J Opt Soc Am, 1,

37–42.

Verrey, D. (1888). Hemiachromatopsie droite absolute. Archives de Ophthalimologie (Paris), 8,

289-300.

Wallisch, P. (2017). Illumination assumptions account for individual differences in the perceptual

interpretation of a profoundly ambiguous stimulus in the color domain: "The

dress". Journal of Vision, 17(4):5, 1-14.

Walsh, V. (1999). How does the cortex construct color? Proceedings of the National Academy of Sciences, 96(24), 13594-13596.

Wandell, B. A., Baseler, H., Poirson, A. B., Boynton, G. M. & Engel, S. E. (2000). Computational neuroimaging: Color tuning in two human cortical areas measured using fMRI. Eds. K. Gegenfurtner & L. T. Sharpe, Cambridge University Press (Cambridge): Colour vision: From genes to perception (pp. 269–282).

Wang, Q., Richters, D. P. & Eskew Jr., R. T. (2014). Noise masking of S-cone increments and decrements. Journal of Vision, 14(13):8, 1-17.

Winkler, A., Spillmann, L., Werner, J. S. & Webster, M. A. (2015). Asymmetries in blue-yellow color perception and in the color of "the dress". Current Biology, 25(13), R547-R548.

Witzel, C. (2015). The Dress: Why do different observers see extremely different colours in the same photo? Retrieved August 2015, from http://lpp.psycho.univ-paris5.fr/feel/?page_id=929.

Witzel, C., Racey, C. & O'Regan, K. (2017). The most reasonable explanation of "the dress": Implicit assumptions about illumination. Journal of Vision, 17(2):1, 1-19.

Wool, L. E., Komban, S. J., Kremkow, J., Jansen, M., Li, X. et al. (2015). Salience of unique hues and implications for color theory. Journal of Vision, 15(2):10, 1–11.

Zeki S. (1990). A century of cerebral achromatopsia. Brain, 113, 1721–1777.

Zeki, S., Watson, J. D. G., Lueck, C. J., Friston, K. J., Kennard, C. & Frackowiak, R. S. J. (1991). A direct demonstration of functional specialization in human visual-cortex. Journal of Neuroscience, 11, 641–649.

Zhu, W., Drewes, J. & Gegenfurtner, K. R. (2013). Animal detection in natural images: effects of color and image database. Public Library of Science One, 8(10): e75816, 1-14.

6.3. Study 2: Differential cortical responses to color depart from cone-opponent mechanisms

Anllo-Vento, L., Luck, S. J. & Hillyard, S. A. (1998). Spatio-temporal dynamics of attention to color: evidence from human electrophysiology. Human Brain Mapping, 6(4), 216-238.

Barbur, J. L., Harlow, A. J., & Plant, G. T. (1994). Insights into the different exploits of colour in the visual cortex. Proceedings: Biological Science, 258(1353), 327-334.

Beauchamp, M. S., Haxby, J. V., Jennings, J. E. & DeYoe, E. A. (1999). An fMRI version of the Farnsworth-Munsell 100-Hue test reveals multiple color-selective areas in human ventral occipitotemporal cortex. Cerebral Cortex, 9(3), 257-263.

Brouwer, G. J. & Heeger, D. J. (2009). Decoding and reconstructing color from responses in human visual cortex. Journal of Neuroscience, 29(44), 13992-14003.

Conway, B. R. (2014). Color signals through dorsal and ventral visual pathways. Visual Neuroscience, 31, 197–209.

Conway, B. R. & Tsao, D. Y. (2009). Color-tuned neurons are spatially clustered according to color preference within alert macaque posterior inferior temporal cortex. PNAS, 106(42): 18034-18039.

Corbetta, M., Miezin, F. M., Dobmeyer, S., Shulman, G. L. & Petersen, S. E. (1990). Attentional modulation of eural processing of shape, color, and velocity in humans. Science, 248(4962), 1556-1559.

Corbetta, M., Miezin, F. M., Dobmeyer, S., Shulman, G. L. & Petersen, S. E. (1991). Selective and divided attention during visual discriminations of shape, color, and speed: functional anatomy by positron emission tomography. Journal of Neuroscience, 11(8), 2383-2402.

Dacey, D. M. (2000). Parallel pathways for spectral coding in primate retina. Annual review of

    neuroscience, 23(1), 743-775.

Dzhelyova, M. & Rossion, B. (2014). The effect of parametric stimulus size variation on individual

    face discrimination indexed by fast periodic visual stimuliation. BMC Neuroscience,

    15:87, 1-12.

Emery, K. J., Volbrecht, V. J., Peterzell, D. H., & Webster, M. A. (2017a). Variations in normal

    color vision: VII. Relationships between color naming and hue scaling. Vision Research,

    141, 66-75.

Emery, K. J., Volbrecht, V. J., Peterzell, D. H., & Webster, M. A. (2017b). Variations in normal

    color vision: VI. Factors underlying individual differences in hue scaling and their

    implications for models of color appearance. Vision Research, 141, 51-65.

Engel, S., Zhang, X. & Wandell, B. (1997). Colour tuning in human visual cortex measured with

    functional magnetic resonance imaging. Nature, 388(6637), 68-71.

Forder, L., Bosten, J., He, X. & Franklin, A. (2017). A neural signature of the unique hues.

    Scientific Reports, 7:42364, 1-8.

Gegenfurtner, K. R. (2003). Cortical mechanisms of colour vision, Nature Reviews Neuroscience,

    4, 563-572.

Gerth, C., Delahunt, P. B., Crognale, M. A., & Werner, J. S. (2003). Topography of the chromatic

    pattern-onset VEP. Journal of Vision, 3, 171-182.

Goddard, E., Mannion, D. J., McDonald, J. S., Solomon, S G. & Clifford, C. W. G. (2011). Color

    responsiveness argues against a dorsal component of human V4. Journal of Vision,

    11(4):3, 1-21.

Hadjikhani, N., Liu, A. K., Dale, A. M., Cavanagh, P. & Tootell, R. B. H. (1998). Retinotopy and color sensitivity in human visual cortical area V8. Nature Neuroscience, 1, 235–241.

Jacques, C.*, Retter, T.L.*, Rossion, B. (2016). A single glance at a face generates larger and qualitatively different category-selective spatio-temporal signatures than other ecologically-relevant categories in the human brain. *NeuroImage*, 137, 21-33.

Johnson, E. N. & Mullen, K. T. (2016). Color in the Cortex. In Human Color Vision (pp. 189-217). Springer International Publishing.

Keysers, C. & Perrett, D. I. (2002). Visual masking and RSVP reveal neural competition. *Trends in Cognitive Science*, 6, 120–125.

Komatsu, H., Ideura, Y., Kaji, S., & Yamane, S. (1992). Color selectivity of neurons in the inferior temporal cortex of the awake macaque monkey. Journal of Neuroscience, 12(2), 408-424.

Kulikowski, J. J., Robson, A. G., & McKeefry, D. J. (1996). Specificity and selectivity of chromatic visual evoked potentials. Vision Research, 36, 3397-3401.

Kuriki, I., Nakamura, S., Sun, P., Ueno, K., Matsumiya, K. et al. (2011). Decoding color responses in human visual cortex. IEICE Transactions on Fundamentals of Electronics, Communications, and Computer Sciences, E94.A(2), 473-479.

Kuriki, I., Sun, P., Ueno, K., Tanaka, K., & Cheng, K. (2015). Hue selectivity in human visual cortex revealed by functional magnetic resonance imaging. Cerebral Cortex, 25(12), 4869-4884.

Lafer-Sousa, R., Conway, B. R. & Kanwisher, N. G. (2016). Color-biased regions of the ventral visual pathway lie between face- and place-selective regions in humans, as in macaques. Journal of Neuroscience, 36(5), 1682-1697.

Lee, R. J., Mollon, J. D., Zaidi, Q., & Smithson, H. E. (2009). Latency characteristics of the short-wavelength-sensitive cones and their associated pathways. Journal of Vision, 9(12):5, 1-17.

Lee, B. B. (2004). Paths to colour in the retina. Clinical and Experimental Optometry, 87(4-5), 239-248.

Liu, J. & Wandell, B. A. (2005). Specializations for chromatic and temporal signals in human visual cortex. Journal of Neuroscience, 25, 3459–3468.

Lueck, C. J., Zeki, S., Friston, K. J., Deiber, M. P., Cope, P., Cunningham, V. J., et al. (1989). The colour centre in the cerebral cortex of man. Nature, 340, 386–389.

Martin, A., Haxby, J. V., Lalonde, F. M., Wiggs, C. L., & Ungerleider, L. G. (1995). Discrete cortical regions associated with knowledge of color and knowledge of action. *Science,* 270(5233), 102-105.

Mullen, K. T., Dumoulin, S. O., McMahon, K. L., de Zubicaray, G. I., & Hess, R. F. (2007). Selectivity of human retinotopic visual cortex to S-cone-opponent, L/M-cone-opponent and achromatic stimulation. European Journal of Neuroscience, 25, 491–502.

Murphey, D. K., Yoshor, D. & Beauchamp, M. S. (2008). Perception matches selectivity in the human anterior color center. Current Biology, 18(3), 216-220.

Nasr, S., Polimeni, J. R., & Tootell, R. B. (2016). Interdigitated color- and disparity-selective columns within human visual cortical areas V2 and V3. Journal of Neuroscience, 36(6), 1841-1857.

Oostenveld, R. & Praamstra, P. (2001). The five percent electrode system for high-resolution EEG and ERP measurements. Clinical Neurophysiology,112(4), 713-719.

Or, C.-C., Retter, T. L., & Rossion, B. (2019). The contribution of color information to rapid face

    categorization in natural scenes. Journal of Vision, 19(5):20, 1-20.

Parkes, L. M., Marsman, J. B., Oxley, D. C., Goulemas, J. Y. & Wuerger, S. M. (2009). Multivoxel

    fMRI analysis of color tuning in human primary visual cortex. Journal of Vision, 9(1):1, 1-

    13.

Quek, G. & Rossion, B. (2017). Category-selective human brain processes elicited in fast periodic

    visual stimulation streams are immune to temporal predictability. *Neuropsychologia*,

    104, 182-200.

Rabin, J., Switkes, E., Crognale, M. A., Schneck, M. E. & Adams, A. J. (1994). Visual evoked

    potentials in three-dimensional color space: Correlates of spatio-chromatic processing.

    Vision Research, 34, 2657–2671.

Rasheed, S. & Marini, D. (2015). Classification of EEG signals produced by RGB colour stimuli.

    Journal of Biomedical Engineering and Medical Imaging, 2:5, 1-15.

Regan D. (1966). Some characteristics of average steady-state and transient responses evoked

    by modulated light. Electroencephalography and Clinical Neurophysiology, 20 (3), 238–

    248.

Regan, B., Reffin, J., & Mollon, J. (1994). Luminance noise and the rapid determination of

    discrimination ellipses in colour deficiency. Vision Research, 34(10). 1279-1299.

Retter, T. L., Gwinn, O. S., O'Neil, S., Jiang, F., & Webster, M. A. (2017). Electrophysiological

    correlates of perceptual blue-yellow asymmetries with #thedress. Journal of Vision,

    17(10), 128.

Retter, T. L. & Rossion, B. (2016). Uncovering the neural magnitude and spatio-temporal

    dynamics of natural image categorization in a fast visual stream. *Neuropsychologia*, 91,

    9-28.

Riggs, L. A. & Sternheim, C. E. (1968). Human retinal and occipital potentials evoked by changes

    of the wavelength of the stimulation light. Journal of the Optical Society of America,

    59(5), 635-640.

Robson, A. G. & Kulikowski, J. J. (1998). Objective specification of tritanopic confusion lines using

    visual eboked potentials. Vision Research, 38, 3241-3245.

Rossion, B., Torfs, K., Jacques, C. & Liu-Shuang, J. (2015). Fast periodic presentation of natural

    face images reveals a robust face-selective electrophysiological response in the human

    brain. Journal of Vision, 15(1):18, 1-18.

Shapley, R. (2019). Physiology of color vision in primates. Oxford Research Encyclopedia of

    Neuroscience. 1-34.

Simmons, W., Ramjee, V., Beauchamp, M. S., McRae, K., Martin, A., & Barsalou, L. W. (2007). A

    common substrate for perceiving and knowing about color. Neuropsychologia, 45(12),

    2802-2810.

Solomon, S. G. & Lennie, P. (2007) The machinery of colour vision. Nature Reviews

    Neuroscience, 8, 276-286.

Thierry, G., Athanasopoulos, P., Wiggett, A., Dering, B. & Kuipers, J.-R. (2009). Unconscious

    effects of language-specific terminology on preattentive color perception. Proceedings

    of the National Academy of Sciences, 106(11), 4567-4570.

Thorpe, S. J., Fize, D. & Marlot, C. (1996). Speed of processing in the human visual system.

    Nature, 381(6582), 520-522.

Wade, A. R., Augath, M., Logothesis, N., & Wandell, B. A. (2008). fMRI measurements of color in macaque and human. Journal of Vision, 8(10), 1-6.

Webster, M. A., Miyahara, E., Malkoc, G. & Raker, V. E. (2000). Variations in normal color vision. I. Cone-opponent axes. Journal of the Optical Society of America A, 17(9), 1535-1544.

Yang, L. & Leung, H. (2013). An online BCI game based on the decoding of users' attention to color stimulus. Conference Proceedings: Annual International Conference of the IEEE Engineering in Medicine and Biology Society. 5267-5270.

Zeki, S., Watson, J. D. G., Lueck, C. J., Friston, K. J., Kennard, C. & Frackowiak, R. S. J. (1991). A direct demonstration of functional specialization in human visual-cortex. Journal of Neuroscience, 11, 641–649.

6.4. Study 3: Early and automatic activation of color memory in visual object recognition

Allen, G. (1879). The colour-sense: its origin and development. Mind, 4(15), 415-421.

Allison, T., Begleiter, A., McCarthy, G., Roessler, E. Nobre, A. C. & Spencer, D. D. (1993). Electrophsyiological studies of color processing in human visual cortex. Electroencephalography and Clinical Neurophysiology, 88(5), 343-355.

Anllo-Vento, L., Luck, S. J. & Hillyard, S. A. (1998). Spatio-temporal dynamics of attention to color: evidence from human electrophysiology. Human Brain Mapping, 6(4), 216-238.

Bae, G. Y., Olkkonen, M., Allred, S. R., & Flombaum, J. I. (2015). Why some colors appear more memorable than others: A model combining categories and particulars in color working memory. Journal of Experimental Psychology: General, 144(4), 744-763.

Bannert, M. M. & Bartels, A. (2013). Decoding the yellow of a gray banana. Current Biology, 23, 2268-2272.

Bartleson, C. J. (1960). Memory colors of familiar objects. Journal of the Optical Society of America, 50(1), 73-77.

Bentin, S., Allison, T., Puce, A., Perez, E., & McCarthy, G. (1996). Electrophysiological studies of face perception in humans. Journal of Cognitive Neuroscience, 8(6), 551–565.

Biedermann, I. (1987). Recognition-by-components: a theory of human image understanding. Psychological Review, 94(2), 115-147.

Biederman, I. & Ju, G. (1988). Surface versus edge-based determinants of visual recognition. Cognitive Psychology, 21(1), 38-64.

Boynton, R. M., Fargo, L., Olson, C. X., & Smallman, H. S. (1989). Category effects in color memory. Color Research and Application, 14(5), 229-234.

Bramao, I., Reis, A., Petersson, K. M., & Faisca, L. (2011). The role of color information on object recognition: A review and meta-analysis. Acta Psychologica, 138, 244-253.

Bramao, I., Faisca, L., Magnus, K., & Reis, A. (2012a). The contribution of color to object recognition. In Ed. I. Kypraios, Advances in Object Recognition Systems, Oxford University Press: Oxford.

Bramao, I., Francisco, A., Inácio, F., Faísca, L., Reis, A., & Petersson, K. M. (2012b). Electrophysiological evidence for colour effects on the naming of colour diagnostic and noncolour diagnostic objects. Visual Cognition, 20(10), 1164-1185.

Bruner, J. S. & Postman, L. (1949). On the perception of incongruity : a paradigm. Journal of Personality, 18, 206-223.

Callaghan, T. C. (1984). Dimensional interaction of hue and brightness in preattentive field segregation. Perception & Psychophysics, 36, 25-34.

Cavanagh, P. (1987). Reconstructing the third dimension: Interactions between color, texture, motion, binocular disparity, and shape. Computer vision, Graphics & Image Processing, 37, 171-195.

De Valois, K. K. & Switkes, E. (1983). Simultaneous masking interactiosn between chromatic and luminance gratings. Journal of the Optical Society of America, 73(1), 11-18.

Delk, J. L. & Fillenbaum, S. (1965). Differences in perceived color as a function of characteristic color. American Journal of Psychology, 78(2), 290-293.

Duncker, K. (1939). The influence of past experience upon perceptual properties. The American Journal of Psychology, 52(2), 255-265.

Dzhelyova, M. & Rossion, B. (2014). The effect of parametric stimulus size variation on individual face discrimination indexed by fast periodic visual stimuliation. BMC Neuroscience, 15:87, 1-12.

Elsner, A. (1978). Hue difference contours can be used in processing orientation information. Perception & Psychophysics, 24(5), 451-456.

Frome, F. S., Buck, S. L., & Boynton, R. M. (1981). Visibility of borders: separate and combined effects of color differences, luminance contrast, and luminance level. Journal of the Optical Society of America, 71(2), 145-150.

Gegenfurtner, K. R. & Rieger, J. (2000). Sensory and cognitive contributions of color to the recognition of natural scenes. Current Biology, 10, 805-808.

Gerth, C., Delahunt, P. B., Crognale, M. A., & Werner, J. S. (2003). Topography of the chromatic pattern-onset VEP. Journal of Vision, 3, 171-182.

Grossberg, S. & Mingolla, E. (1985). Neural dynamics of perceptual grouping: Textures, boundaries, and emergent segmentations. Perception & Psychophysics, 38, 141-171.

Hagmann, C. E. & Potter, M. C. (2016). Ultrafast scene detection and recognition with limited

    visual information. Visual Cognition, 24(1), 2-14.

Hagen, S. Vuong, Q. C., Scott, L. S., Curran, T., & Tanaka, J. W. (2014). The role of color in expert

    object recognition. Journal of Vision, 14(9):9, 1-13.

Hansen, T., Olkkonen, M., Walter, S. & Gegenfurtner, K. R. (2006). Memory modulates color

    appearance. Nature Neuroscience, 9(11), 1367-1368.

Harper, R. S. (1953). The perceptual modification of colored figures. The American Journal of

    Psychology, 66(1), 86-89.

Hering, E. (1920). Grundzüge der Lehre vom Lichtsinn. Berlin: Springer. (English version: Outlines

    of a Theory of the Light Sense. 1964. Translated by L.M. Hurvich and D. Jameson.

    Cambridge, MA: Harvard University Press).

Humphrey, G. K., Goodale, M. A., Jakobson, L. S. & Servos, P. (1994). The role of surface

    information in object recognition: studies of a visual form agnosic and normal subjects.

    Perception, 23(12), 1457-1481.

Jacques, C.*, Retter, T.L.*, Rossion, B. (2016). A single glance at a face generates larger and

    qualitatively different category-selective spatio-temporal signatures than other

    ecologically-relevant categories in the human brain. NeuroImage, 137, 21-33.

Kilmer, J. M. & Lemon, R. N. (2013). What we know currently about mirror neurons. Current

    Biology, 23(23), R1057-62.

Lee, R. J. & Mather, G. (2019). Chromatic adaptation from achromatic stimuli with implied color.

    Attention, Perception & Psychophysics. https://doi.org/10.3758/s13414-019-01716-5

Lee, R. J., Mollon, J. D., Zaidi, Q., & Smithson, H. E. (2009). Latency characteristics of the short-wavelength-sensitive cones and their associated pathways. Journal of Vision, 9(12):5, 1-17.

Lloyd-Jones, T. J., Roberts, M. V., Leek, E. C., Foquet, N. C., & Truchanowicz, E. G. (2012). The time course of activation of object shape and shape+colour representations during memory retrieval. PLOS One, 7(11), e48550.

Lu, A., Xu, G., Jin, H., Mo, L., Zhang, J., & Zhang, J. X. (2010). Electrophsyiological evidence for effects of color knowledge in object recognition. Neuroscience Letters, 469, 405-410.

Lupyan, G. (2015). Object knowledge changes visual appearance: Semantic effects on color afterimages. Acta Psychologica, 161, 117-130.

Markoff, J. L. (1972). Target recognition performance with chromatic and achromatic displays (Research Rep. No. SRM-148). Honeywell: Minneapolis, MN.

Marr, D. & Nishihara, H. K. (1978). Representation and recognition of the spatial organization of three-dimensional shapes. Proceedings of the Royal Society B, 200(1140).

Martin, A., Haxby, J. V., Lalonde, F. M., Wiggs, C. L., & Ungerleider, L. G. (1995). Discrete cortical regions associated with knowledge of color and knowledge of action. Science, 270(5233), 102-105.

Matkovic, K., Neumann, L., Neumann, A., Psik, T. & Purgathofer, W. (2005). Global contrast factor – a new approach to image contrast. Computational Aesthetics in Graphics, Visualization and Imaging, 159-167. code: https://gist.github.com/zabela/8539136

Mitterer, H. & de Ruiter, J. P. (2008). Recalibrating color categories using world knowledge. Psychological Science, 19(7), 629-634.

Nagai, J., & Yokosawa, K. (2003). What regulates the surface color effect tin object recognition: Color diagnosticity or category? Technical Report on Attention and Cognition, 28, 1-4.

Naor-Raz, G., Tarr, M. J., & Kerseten, D. (2003). Is color an intrinsic property of object representation? Perception, 32, 667-680.

Norcia, A. M., Appelbaum, L. G., Ales, J. M., Cottereau, B. R. & Rossion, B. (2015). The stead-state visual evoked potential in vision research: A review. Journal of Vision, 15(6):4, 1-46.

Olkkonen, M., Hansen, T. & Gegenfurtner, K. R. (2008). Color appearance of familiar objects: Effects of object shape, texture, and illumination changes. Journal of Vision, 8(5):13, 1-16.

Oliva, A. & Torralba, A. (2001). Modeling the shape of the scene: a holistic representation of the spatial envelope. International Journal of Computer Vision, 42(3), 145-175. code: https://github.com/fly2leoo/matlab-gist

Oostenveld, R. & Praamstra, P. (2001). The five percent electrode system for high-resolution EEG and ERP measurements. Clinical Neurophysiology,112(4), 713-719.

Price, C. J. & Humphreys, G. W. (1987). The effects of surface detail on object categorization and naming. The Quarterly Journal of Experimental Psychology, 41A(4), 797-828.

Proverbio, A. M., Burco, F., del Zotto, M., & Zani, A. (2004). Blue piglets? Electophysiological evidence for the primacy of shape over color in object recognition. Cognitive Brain Research, 18, 288-300.

Quek, G. L. & Rossion, B. (2017). Category-selective human brain processes elicited in fast periodic visual stimulation streams are immune to temporal predictability. Neuropsychologia, 104, 182-200.

Rabin, J., Switkes, E., Crognale, M. A., Schneck, M. E. & Adams, A. J. (1994). Visual evoked

potentials in three-dimensional color space: Correlates of spatio-chromatic processing.

Vision Research, 34, 2657–2671.

Regan D. (1966). Some characteristics of average steady-state and transient responses evoked

by modulated light. Electroencephalography and Clinical Neurophysiology, 20 (3), 238–

248.

Retter, T. L. & Rossion, B. (2016). Uncovering the neural magnitude and spatio-temporal

dynamics of natural image categorization in a fast visual stream. Neuropsychologia, 91, 9-

28.

Retter, T. L., Gwinn, O. S., O'Neil, S., Jiang, F., & Webster, M. A. (2017). Electrophysiological

correlates of perceptual blue-yellow asymmetries with #thedress. Journal of Vision,

17(10), 128.

Riggs, L. A. & Sternheim, C. E. (1968). Human retinal and occipital potentials evoked by changes

of the wavelength of the stimulation light. Journal of the Optical Society of America, 59(5),

635-640.

Robson, A. G. & Kulikowski, J. J. (1998). Objective specification of tritanopic confusion lines using

visual eboked potentials. Vision Research, 38, 3241-3245.

Rossion, B. & Pourtois, G. (2004). Revisiting Snodgrass and Vanderwart's object pictorial set: The

role of surface detail in basic-level object recognition. Perception, 33, 217-236.

Rossion, B., Prieto, E. A., Boremanse, A., Kuefner, D. & Van Belle, G. (2012). A steady-state visual

evoked potential approach to individual face perception: effect of inversion, contrast-

reversal and temporal dynamics. NeuroImage, 63, 1585–1600.

Rossion, B., Torfs, K., Jacques, C. & Liu-Shuang, J. (2015). Fast periodic presentation of natural face images reveals a robust face-selective electrophysiological response in the human brain. Journal of Vision, 15(1):18, 1-18.

Slotnick, S. D. (2009). Memory for color reactivates color processing region. Cognitive Neuroscience and Neurophysiology, 20, 1568-1571.

Tanaka, J. W. & Presnell, L. M. (1999). Color diagnosticity in object recognition. Perception & Psychophysics. 61(6), 1140-1153.

Tanaka, J. Weiskopf, D. & Williams, P. (2001). The role of color in high-level vision. Trends in Cognitive Science. 5(5), 211-215.

Therriault, D. J., Yaxley, R. H., & Zwaan, R. A. (2009). The role of color diagnosticity in object recognition and representation. Cognitive Processing, 10(4), 335-342.

Tiechmann, L., Grootswagers, T., Carlson, T., & Rich, A. N. (2018). Seeing versus knowing: the temporal dynamics of real and implied colour processing in the human brain. BioX archive.

Tiechmann, L., Quek, G. L., Robinson, A., Grootswagers, T., Carlson, T., & Rich, A. N. (2019). Yellow strawberries and red bananas: The influence of object-colour knowledge on emerging object representations in the human brain. BioX archive.

Trosianko, T. & Harris, J. P. (1988). Phase discrimination in compound chromatic gratings. Vision Research, 28, 1041-1049.

Uchikawa, K., & Shinoda, H. (1996). Influence of basic color categories on color memory discrimination. Color Research and Applications, 21(6), 430-439.

Van Gulick, A., & Tarr, M. (2010). Is object color memory categorical? Journal of Vision, 10(7):407, 407a.

Vandenbroucke, A. R. E., Fahrenfort, J. J., Meuwese, J. D. I., Scholte, H. S., & Lamme, V. A. F.

(2016). Prior knowledge about objects determines neural color representation in human

visual cortex. Cerebral Cortex, 26, 1401-1408.

von Helmholtz, H. (1867). Handbuch der Physiologischen Optik, Vol. II, published by Leopold

Voss: Leipzig. In J.P.C. Southall (Ed.), Translation (Helmoltz's Treatise on Physiological

Optics, 1909), Optical Society of America: Washington, D.C., 1924, pp. 286-287.

Walls, G. L. (1942). The vertebrate eye and its adaptive radiation. Cranbook Instittue of Science:

Bloomfields Hills, MI.

Winkler, A., Spillmann, L., Werner, J. S. & Webster, M. A. (2015). Asymmetries in blue-yellow

color perception and in the color of "the dress". Current Biology, 25(13), R547-R548.

Witzel, C., Valkova, H., Hansen, T., & Gegenfurtner, K. R. (2011). Object knowledge modulates

colour appearance. i-Perception, 2, 13-50. dx.doi.org/10.1068/i0396

Wurm, L. H., Legge, G. E., Isenberg, L. M., & Luebker, A. (1993). Color improves object

recognition in normal and low vision. Journal of Experimental Psychology: Human

Perception and Performance, 19(4), 899-911.

6.5. Discussion

Abrams, A. B., Hills, J. M. & Brainard, D. H. (2007). The relation between color discrimination and

color constancy: when is optimal adaptation task dependent? Neural Computation,

19(10), 2610-2637.

Allison, T., Begleiter, A., McCarthy, G., Roessler, E. Nobre, A. C. & Spencer, D. D. (1993).

Electrophsyiological studies of color processing in human visual cortex.

Electroencephalography and Clinical Neurophysiology, 88(5), 343-355.

Anllo-Vento, L., Luck, S. J. & Hillyard, S. A. (1998). Spatio-temporal dynamics of attention to
color: evidence from human electrophysiology. Human Brain Mapping, 6(4), 216-238.

Anthanasopoulos, P., Dering, B., Wiggett, A., Kuipers, J. R., & Thierry, G. (2010). Perceptual shift
in bilingualism: brain potentials reveal plasticity in pre-attentive colour perception.
Cognition, 116(3), 437-443.

Bannert, M. M. & Bartels, A. (2013). Decoding the yellow of a gray banana. Current Biology, 23,
2268-2272.

Bartels, A. & Zeki, S. (2000). The architecture of the colour centre in the human visual brain: new
results and a review. European Journal of Neuroscience, 12(1), 172-193.

Berlin, B. & Kay, P. (1969). Basic Color Terms: Their Universality and Evolution. University of
California Press: Berkeley.

Bird, C., Berens, S. C., Horner, A. J. & Franklin, A. (2014). Categorical encoding of color in the
brain. PNAS USA, 111(12), 4590-4595.

Boehm, A. E., MacLeod, D. I. A., & Bosten, J. M. (2014). Compensation for red-green contrast
loss in anomalous trichromats. Journal of Vision, 14(13):19, 1-17.

Bouvier, S. E. & Engel, S. A. (2006). Behavioral deficits and cortical damage loci in cerebral
achromatopsia. Cerebral Cortex, 16, 183–191.

Brent, P. J., Kennard, C. & Ruddock, K. H. (1994). Residual colour vision in a human heianope:
spectral responses and colour discrimination. Proceedings of the Royal Society:
Biological Sciences, 256(1347), 219-225.

Brainard, D. H. (2015). Color and the cone mosaic. Annual Review of Vision Science, 1:519-546.

Brainard, D. H. & Maloney, L. T. (2011). Surface color perception and equivalent illumination
models. Journal of Vision, 11(5):1, 1-18.

Brouwer, G. J. & Heeger, D. J. (2009). Decoding and reconstructing color from responses in

human visual cortex. Journal of Neuroscience, 29(44), 13992-14003.

Caine, N. G., Osorio, D. & Mundy, N. I. (2010). A foraging advantage for dichromatic marmosets

(Callithrix geoffroyi) at low light intensity. Biology Letters, 6(1), 36-38.

Carvalho, L. S., Pessoa, D. M. A., Mountford, J. K., Davies, W. I. L. & Hunt, D M. (2017). The

genetic and evolutionary drives behind primate color vision. Frontiers in Ecology and

Evolution, 5:34.

Changizi, Zhang & Shimojo, 2006

Clifford, A., Holmes, A., Davies, I. R. L. & Franklin, A. (2010). Color categories affect pre-attentive

color perception. Biological Psychology, 85(2), 275-282.

Clifford, A., Franklin, A., Holmes, A., Drivonikou, V. G., Ozgen, Em., & Davies, I. R. L. (2012).

Neural correlates of acquired color category effects. Brain and Cognition, 80, 126-143.

Conway, B. R. (2009). Color vision, cones, and color-coding in the cortex. Neuroscientist, 15(3),

274-290.

Conway, B. R. (2014). Color signals through dorsal and ventral visual pathways. Visual

Neuroscience, 31, 197–209.

Cook, R. S., Kay, P. & Regier, T. (2005). The World Color Survey Database. In H. Cohen & C.

Lefebvre (Esd.) Handbook of Categorization in Cognitive Science (pp. 224-240). Elsevier:

London.

Crognale, M. A., Duncan, C. S., Shoenhard, H., Peterson, D. J. & Berryhill, M. E. (2013). The locus

of color sensation: Cortical color loss and the chromatic visual evoked potential. Journal of

Vision, 13(10):15, 1-11.

Dean, P. (1979.). Visual cortex ablation and thresholds for successively presented stimuli in rhesus monkeys: II. Hue. Experimental Brain Research, 35(1), 69-83.

Derrington, A. M., Krauskopf, J. & Lennie, P. (1984). Chromatic mechanisms in lateral geniculate nucleus of macaque. Journal of Physiology, 357, 241-265.

De Valois, R. L., Smith, C. J., Karoly, A. J. & Kitai, S. T. (1958). Electrical responses of primate visual system. I. Different layers of macaque lateral geniculate nucleus. Journal of Comparative Physiological Psychology, 51(6), 662-668.

Dominy, N. J. & Lucas, P. W. (2001). Ecological importance of trichromatic vision to primates. Nature, 410, 363-3663

Dumoulin, S. O., Harvey, B. M., Fracasso, A., Zuiderbaan, W., Luijten, P. R., Wandell, B. A., & Petridou, N. (2017). In vivo evidence of functional and anatomical stripe-based subdivisions in human V2 and V3. Scientific Reports, 7:733, 1-12.

Engel, S. A. & Furmanski, C. S. (2001). Selective adaptation to color contrast in human primary visual cortex. Journal of Neuroscience, 21(11), 3949-3954.

Engel, S. A., Zhang, X. & Wandell, B. (1997). Colour tuning in human visual cortex measured with functional magnetic resonance imaging. Nature, 388(6637), 68-71.

Fonteneau, E. & Davidoff, J. (2007). Neural correlates of colour categories. Cognitive Neuroscience and Neurophysiology, 18(13), 1323-1327.

Forder, L., He, X. & Franlkin, A. (2017). Colour categories are reflected in sensory stages of colour perception when stimulus issues are resolved. PLOS One, 12(5): e0178097.

Foster, D. H. (2011). Color constancy. Vision Research, 51(7), 674-700.

Gegenfurtner, K. R. (2003). Cortical mechanisms of colour vision, Nature Reviews Neuroscience, 4, 563-572.

Gegenfurtner, K. R. & Kiper, D. C. (2003). Annual Review of Neuroscience, 26, 181-206.

Gouras, P. & Zrenner, E. (1981). Color coding in primate retina. Vision Research, 21(11), 1591-1598.

Hadjikhani, N., Liu, A. K., Dale, A. M., Cavanagh, P. & Tootell, R. B. H. (1998). Retinotopy and color sensitivity in human visual cortical area V8. Nature Neuroscience, 1, 235–241.

Hardin, C. L. (1992). The Virtues of Illusion, Philosophical Studies, 68(3), 371-82.

Hatfield, G. (I992). Color perception and neural encoding: does metameric matching entail a loss of information? Proceedings of the Biennial Meeting of the Philosophy of Science Association, 1, 492-504.

He, X., Witzel, C., Forder, L., Clifford, A. & Franklin, A. (2014). Color categories only affect pot-perceptual processes when same- and different-category colors are equally discriminable. Journal of the Optical Society of America A, 31(4), A322-331.

Hiramatsu, C., Melin, A. D., Aureli, F., Scaffner, C. M., Vorobyev, M. Matsumoto, Y, et a. (2008). Importance of achromatic contrast in short-range fruit foraging of primates. PLoS ONE, 3:e3356.

Hubel, D. H. & Livingstone, M. S. (1985). Complex-unoriented cells in a subregion of primate area 18. Nature, 315(3017), 325-327.

Jacobs, G. H. (2009). Evolution of colour vision in mammals. Philosophical Transactions of the Royal Society B, 364, 2957-2967.

Jacobs, G. H. (2013). Losses of functional opsin genes, short-wavelength cone photopigments, and color vision –a significant trend in the evolution of mammalian vision. Visual Neuroscience, 30(1-2), 39-52.

Jaeger, W., Krastel, H., & Braun, S. (1988). Cerebral achromatopsia (symptoms, course, differential diagnosis and strategy of the study). I. Klinische Monatsblatter fur Augenheilkunde, 193(6), 627–634.

Jameson, K. A. & D'Andrade, R. G. (1997). It's not really red, green, yellow, blue : an inquiry into perceptual color space. In C. L. Hardin & L. Maffi (Eds.), Color Categories in Thought and Language, (pp. 295-319). Cambridge University Press: New York.

Jameson, D. & Hurvich, L. M. (1989). Essay concerning color constancy. Annual Review of Psychology, 40, 1-22.

Johnson, E. N. & Mullen, K. T. (2016). Color in the Cortex. In Human Color Vision (pp. 189-217). Springer International Publishing.

Jordan, G., Deeb, S. S., Bosten, J. M., & Mollon, J. D. (2010). The dimensionality of color vision in carriers of anomalous trichromacy. Journal of Vision, 10(8):12, 1-19.

Kelber, A. & Osorio, D. (2010). From spectral information to animal colour vision: experiments and concepts. Philosophical Transactions of the Royal Society B, 277, 1617-1625.

Kiper, D. C., Fenstemaker, S. B. & Gegenfurtner, K. R. (1997). Chromatic properties of neurons in macaque area V2. Visual Nerusocience, 14(6), 1061-1072.

Koida, K. & Komatsu, H. (2007). Effects of task demands on the responses of color-selective neurons in the inferior temporal cortex. Nature Neuroscience, 10(1), 108-116.

Komatsu, H., Ideura, Y., Kaji, S. & Yamane, S. (1992). Color selectivity of neurons in the inferior temporal cortex of the awake macaque monkey. Journal of Neuroscience. 12, 408–424

Kremers, J., Scholl, H. P., Knau, H. Berendschott, T. T. Usui, T. & Sharpe, L. T. (2000). L/M cone ratios in human trichromats assessed by psychophysics, electroretinography, and retinal densitometry. Journal of the Optical Society of America A, 17(3), 517-526.

Kulikowski, J. J., Walsh, V., McKeefry, D., Butler, S. R. & Carden, D. (1994). The
    electrophysiological basis of colour processing in macaques with V4 lesions. Behavioral
    Brain Research, 60, 73-78.

Land, E . H. (1977). The retinex theory of color vision. Scientific American, 237(6), 108-128.

Liu, J. & Wandell, B. A. (2005). Specializations for chromatic and temporal signals in human
    visual cortex. Journal of Neuroscience, 25, 3459–3468.

Luck, S. J. An introduction to the event-related potential technique (2005). Cambridge, MA: MIT
    Press.

Lueck, C. J., Zeki, S., Friston, K. J., Deiber, M. P., Cope, P., Cunningham, V. J., et al. (1989). The
    colour centre in the cerebral cortex of man. Nature, 340, 386–389.

MacLeod, D. I. & Boynton, R. M. (1979). Chromaticity diagram showing cone excitation by
    stimuli of equal luminance. Journal of the Optical Society of America, 69(8), 1183-1186.

Marr, D. 1982 . Vision. Freeman: New York.

Marshall, J. & Arikawa, K. (2014). Unconventional colour vision. Current Biology, 24(24), R1150-
    R1154.

Martin, A., Haxby, J. V., Lalonde, F. M., Wiggs, C. L., & Ungerleider, L. G. (1995). Discrete cortical
    regions associated with knowledge of color and knowledge of action. Science, 270(5233),
    102-105.

Meadows, J. C. (1974). Disturbed perception of colours associated with localized cereberal
    lesions. Brain, 97, 615–632.

Mo, L., Xu, G., Kay, P. & Tan, L. H. (2011). Electrophysiological evidence for the left-lateralized
    effect of language on preattentive categorical perception of color. PNAS USA, 108(34),
    14026-14030.

Mollon, J. D. (1989). " Tho' she kneel'd in that place where they grew…": The uses and originals of primate colour vision. Journal of Experimental Biology, 146, 21-38.

Moutoussis, K. & Zeki, S. (2002). The relationship between cortical activation and perception investigated with invisible stimuli. PNAS USA, 99(14), 9527-9532.

Mullen, K. T., Chang, D. H. F. & Hess, R. F. (2015). The selectivity of responses to red-green colour and achromatic contrast in the human visual cortex: an fMRI adaptation study. European Journal of Neuroscience, 42, 2923-2933.

Mullen, K. T., Dumoulin, S. O., McMahon, K. L., de Zubicaray, G. I., & Hess, R. F. (2007). Selectivity of human retinotopic visual cortex to S-cone-opponent, L/M-cone-opponent and achromatic stimulation. European Journal of Neuroscience, 25, 491–502.

Murphey, D. K., Yoshor, D. & Beauchamp, M. S. (2008). Perception matches selectivity in the human anterior color center. Current Biology, 18(3), 216-220.

Nasr, S., Polimeni, J. R., & Tootell, R. B. (2016). Interdigitated color- and disparity-selective columns within human visual cortical areas V2 and V3. Journal of Neuroscience, 36(6), 1841-1857.

Nathans, J. , Thomas, D., & Hogness, D. S. (1986). Molecular genetics of human color vision: the genes encoding blue, green, and red pigments. Science, 232, 193-202.

Neitz, J. & Neitz, M. (2011). The genetics of normal and defective color vision. Vision Research, 51(7), 633-651.

Neitz, J., Neitz, M. & Jacobs, G. H., (1993). More than three different cone pigments among people with normal color vision. Vision Research, 33(1), 117-122.

Neitz, J. & Jacobs, G. H. (1986). Polymorphism of the long-wavelength cone in normal human colour vision. Nature, 323(6089), 623-625.

Persichetti, A. S., Thomposon-Schill, S. L., Butt, O. H., Brainard, D. H., & Aguirre, G. K. (2015). Functional magnetic resonance imaging adaptation reveals a noncategorical representation of hue in early visual cortex. Journal of Vision, 15(6):18, 1–19.

Polyak, S. L. (1957). The Vertebrate Visual System. University of Chicago Press: Chicago.

Riggs, L. A. & Sternheim, C. E. (1968). Human retinal and occipital potentials evoked by changes of the wavelength of the stimulation light. Journal of the Optical Society of America, 59(5), 635-640.

Roorda, A. & Williams, D. R. (1999). The arrangement of the three cone classes in the living human eye. Nature, 397(6719), 520-522.

Sakai, K., Watanabe, E., Onodera, Y., Uchida, I., Kato, H. et al. (1995). Functional mapping of the human colour centre with echo-planar magnetic resonance imaging. Proceedings of the Royal Society of London B, 261, 89-98.

Shapley, R. & Hawken, M. J. (2011). Color in the cortex: single- and double-opponent cells. Vision Research, 51(7), 701-717.

Shapley, R. M., Hawken, M. J. & Johnson, E. B. (2014). Color in primary visual cortex. In J. S. Werner & L. M. Chalupa (Eds.) The New Visual Neurosciences (pp. 569-586), MIT Press: Cambridge.

Simmons, W., Ramjee, V., Beauchamp, M. S., McRae, K., Martin, A., & Barsalou, L. W. (2007). A common substrate for perceiving and knowing about color. Neuropsychologia, 45(12), 2802-2810.

Solomon, S. G. & Lennie, P. (2007) The machinery of colour vision. Nature Reviews Neuroscience, 8, 276-286.

Stoerig, P. & Cowey, A. (1989). Wavelength sensitivity in blindsight. Nature, 342(6252), 916-918.

Sumner, P. & Mollon, J.D. (2000). Catarrhine photopigments are optimized for detecting targets against a foliage background. Journal of Experimental Biology. 203, 1963–1986.

Thierry, G., Athanasopoulos, P., Wiggett, A., Dering, B. & Kuipers, J.-R. (2009). Unconscious effects of language-specific terminology on preattentive color perception. Proceedings of the National Academy of Sciences, 106(11), 4567-4570.

Thompson, E. (1995). Colour vision, evolution, and perceptual content. Synthese, 104, 1-32.

Tootell, R. B., Nelissen, K., Vanduffel, W. & Orban, G. A. (2004). Search for color 'center(s)' in macaque visual cortex. Cerebral Cortex, 14(4), 353-363.

Ts'o, D. Y. & Gilbert, C. D. (1988). The Organization of Chromatic and Spatial Interactions in the Primate Striate Cortex. The Journal of Neuroscience, 8(5), 1712-l 727.

Vandenbroucke, A. R. E., Fahrenfort, J. J., Meuwese, J. D. I., Scholte, H. S., & Lamme, V. A. F. (2016). Prior knowledge about objects determines neural color representation in human visual cortex. Cerebral Cortex, 26, 1401-1408.

Verrey, D. (1888). Hemiachromatopsie droite absolute. Archives de Ophthalimologie (Paris), 8, 289-300.

von Helmholtz, H. (1867). Handbuch der Physiologischen Optik, Vol. II, published by Leopold Voss: Leipzig. In J.P.C. Southall (Ed.), Translation (Helmoltz's Treatise on Physiological Optics, 1909), Optical Society of America: Washington, D.C., 1924, pp. 286-287.

Wade, A. R., Brewer, A. A., Rieger, J. W., & Wandell, B. B. (2002). Functional measurements of human ventral occipital cortex: retinotopy and colour. Philosophical Transaction of the Royal Society of London B, 357, 963–973.

Wade, A. R., Augath, M., Logothesis, N., & Wandell, B. A. (2008). fMRI measurements of color in macaque and human. Journal of Vision, 8(10), 1-6.

Wassle, H. (2004). Parallel processing in the mammalian retina. Nature Reviews Neuroscience, 5(10), 747-757.

Webster, M. A. (2015). Color Vision. In J. T. Wixted & J. Serences (Eds.) Stevens' Handbook of Experimental Psychology and Cognitive Neuroscience, Fourth Edition, Vol. 2. (pp. 343-384). Wiley.

Webster, M. A. Juricevic, I. & McDermott, K. C. (2010). Simulations of adaptation and color appearance in observers with varying spectral sensitivity. Opthalmic & Physiological Optics, 30(5), 302-610.

Webster M. A. & Mollon, J. D. (1997). Adaptation and the color statistics of natural images. Vision Research, 37(23), 3283-3298.

Wu, Y., Wang, H., Wang, H. & Hadly, E. A. (2017). Rethinking the origins of primates by reconstructing their diel activity patterns using genetics and morphology. Scientific Reports, 7:11837.

Yokoyama, S. & Yokoyama, R. (1989). Molecular evolution of human visual pigment genes. Molecular Biology & Evolution, 6(2), 186-197.

Young, T. (1802). II. The Bakerian Lecture. On the theory of light and colours. Philosophical Transactions of the Royal Society, 92, 1--38.

Zeki, S. M. (1973). Colour coding in rhesus monkey prestriate cortex. Brain Research, 53, 422-427.

Zeki, S. (1983). Colour coding in the cerebral cortex: the responses of wavelength-selective and colour-coded cells in monkey visual cortex to changes in wavelength composition. Neuroscience, 9(4), 767-781.

Zeki S. (1990). A century of cerebral achromatopsia. Brain, 113, 1721–1777.

Zeki, S. & Bartels, A. (1999). The clinical and functional measurement of cortical (in)activity in

the visual brain, with special reference to the two subdivisions (V4 and V4α) of the

human colour centre. Philosophical Transactions of the Royal Society of London B, 354,

1371-1382.

Zeki, S., Watson, J. D. G., Lueck, C. J., Friston, K. J., Kennard, C. & Frackowiak, R. S. J. (1991). A

direct demonstration of functional specialization in human visual-cortex. Journal of

Neuroscience, 11, 641–649.